

**SUCCESSFUL DEVELOPMENT OF A FLOW CYTOMETRIC ASSAY TO ANALYZE  
CYTOKINE-INDUCED PHOSPHORYLATION PATHWAYS [CIPP] WITHIN  
PERIPHERAL BLOOD LEUKOCYTES**

by

David T. Montag Jr.

B.S., Case Western Reserve University, 2003

Submitted to the Graduate Faculty of  
the School of Engineering in partial fulfillment  
of the requirements for the degree of  
Master of Science

University of Pittsburgh

2006

UNIVERSITY OF PITTSBURGH

SCHOOL OF ENGINEERING

This thesis was presented

by

David T. Montag, Jr.

It was defended on

July 6, 2006

and approved by

Partha Roy, Ph.D., Department of Bioengineering

Albert D. Donnenberg, Ph.D., Department of Medicine

Thesis Advisor: Michael T. Lotze, M.D., Departments of Surgery and Bioengineering

**SUCCESSFUL DEVELOPMENT OF A FLOW CYTOMETRIC ASSAY TO ANALYZE  
CYTOKINE-INDUCED PHOSPHORYLATION PATHWAYS [CIPP] WITHIN  
PERIPHERAL BLOOD LEUKOCYTES**

David T. Montag, Jr., M.S.

University of Pittsburgh, 2006

Current strategies designed to assess cells in the peripheral blood are limited to evaluation of phenotype or delayed measurement [ $>6$  hours] of function, usually quantifying cytokine production, cytolytic activity, or response to antigens. Furthermore, these assays often do not assess the individual cell types comprising peripheral blood, instead providing a bulk-readout for the total population. We reasoned that functional abnormalities in distinct peripheral blood cells, which act as immune sentinels capable of rapidly reacting to various injurious agents while circulating throughout the body, could serve as migratory biomarkers, reflecting pathological environs that cells experience in the setting of inflammatory states, including cancer. Two major pathways regulating immune responses are the JAK/STAT and MAPK pathways. These pathways are initiated by ligand-receptor binding, and are rapidly propagated by subsequent protein phosphorylation cascades. Additionally, these pathways are often abnormally activated within cancer cells themselves. We applied flow cytometric strategies, evaluating the brief application of cytokines *in vitro* to interrogate the early phosphorylation events of these signaling

pathways in normal peripheral blood mononuclear cells (PBMC). Individual cytokine doses and time intervals of treatment were assessed to identify conditions useful in a clinical laboratory and as an initial goal, to induce maximal phosphorylation. Surprisingly, all of the STAT proteins assessed and ERK1/2 are maximally phosphorylated within 15 minutes in human PBMC, simply following addition of cytokines alone. Within two hours, cells typically return to their basal phosphorylation states. Confirmation of these results was achieved by Western blotting. Increased phosphorylation usually correlated with increased concentrations of individual cytokines. Furthermore, we developed conditions to enable simultaneous staining of cell surface proteins, identifiable with distinct PBMC subpopulations: CD4, CD8, CD14, CD19, and CD56, together with intracellular phosphorylated proteins. Of the permeabilizing conditions tested, 75% methanol enabled superior simultaneous detection of both cell surface and intracellular epitopes. Using this technique, we were able to identify differential responsiveness between individual cell types. These strategies will enable robust development of simple blood analyses to identify normal activation as well as impairments in STAT and MAPK signaling pathways associated with various human disease states including acute and chronic inflammatory conditions throughout clinical immunology.

## TABLE OF CONTENTS

ACKNOWLEDGEMENTS.....	xiii
1.0 INTRODUCTION.....	1
2.0 LITERATURE REVIEW.....	5
2.1 FLOW CYTOMETRY.....	5
2.2 CYTOMETRIC FUNCTIONAL ASSAYS.....	7
2.3 ASSAYS TO ASSESS PROTEIN PHOSPHORYLATION.....	9
2.3.1 Phosphorylation state-specific antibodies (PSSAs).....	10
2.3.2 Western blotting.....	11
2.3.3 Protein microarrays.....	14
2.3.4 Flow cytometric method.....	16
2.3.5 Imaging cytometry.....	19
2.3.6 Comparison of phospho-epitope detection methods.....	23
2.4 IMPORTANT PHOSPHO-SIGNALING PATHWAYS.....	27
2.4.1 The JAK/STAT pathway.....	27
2.4.1.1 Alternative methods of JAK/STAT activation.....	30
2.4.1.2 Negative regulators of JAK/STAT signaling.....	31
2.4.1.3 Gene ablation studies of JAK/STAT family members.....	32
2.4.2 The MAP kinase pathway.....	33

2.4.2.1	Mechanisms of p38 activation.....	35
2.4.2.2	Mechanisms of ERK1/2 activation.....	36
2.4.2.3	Negative regulators of MAP kinase signaling.....	37
2.4.2.4	Roles of MAP kinase signaling in cellular function.....	38
2.5	ABERRANT PBMC SIGNALING IN THE SETTING OF CANCER.....	39
2.5.1	Dysfunctional JAK/STAT and MAP kinase signaling in leukemic cells.....	39
2.5.2	Altered cytokine expression in tumor microenvironments.....	41
2.5.3	Signaling defects within “normal” PBMC in the setting of cancer.....	43
3.0	SPECIFIC AIMS OF THESIS.....	46
3.1	SPECIFIC AIM 1.....	47
3.2	SPECIFIC AIM 2.....	48
4.0	FLOW CYTOMETRIC CHARACTERIZATION OF PROTEIN PHOSPHORYLATION PATHWAYS IN HUMAN PBMC.....	49
4.1	ABSTRACT.....	49
4.2	INTRODUCTION.....	50
4.3	MATERIALS AND METHODS.....	53
4.3.1	Reagents.....	53
4.3.2	Isolation of PBMC.....	54
4.3.3	Preparation of PBMC for flow cytometry.....	54
4.3.4	Western blotting of total and phospho-STAT.....	55
4.3.5	Flow cytometric analysis of phospho-proteins.....	56

4.4 RESULTS.....	57
4.4.1 Dose and time-dependent responsiveness of STAT1 phosphorylation in cytokine stimulated PBMC.....	57
4.4.2 Dose and time-dependent responsiveness of STAT3 phosphorylation in cytokine stimulated PBMC.....	59
4.4.3 Dose and time-dependent responsiveness of STAT5 phosphorylation in cytokine stimulated PBMC.....	62
4.4.4 Dose and time-dependent responsiveness of STAT6 phosphorylation in cytokine stimulated PBMC.....	67
4.4.5 Dose and time-dependent responsiveness of p38 MAPK and ERK1/2 phosphorylation in cytokine stimulated PBMC.....	69
4.5 DISCUSSION.....	72
5.0 SIMULTANEOUS MEASUREMENT OF CELL SURFACE AND INTRACELLULAR PHOSPHORYLATED PROTEINS IN HUMAN PBMC.....	77
5.1 ABSTRACT.....	77
5.2 INTRODUCTION.....	78
5.3 MATERIALS AND METHODS.....	80
5.3.1 Antibodies, cytokines, and fixation and permeabilization reagents.....	80
5.3.2 Isolation of PBMC.....	81
5.3.3 PBMC stimulation and phospho-protein staining.....	81
5.3.4 Western blotting of total and phospho-STAT.....	82
5.3.5 Flow cytometric analysis of phospho-proteins.....	84
5.4 RESULTS.....	84
5.4.1 Effects of saponin and 90% methanol permeabilization on intracellular and cell surface labeling.....	84
5.4.2 Use of a panel of different permeabilizing agents to enhance concurrent intracellular and cell surface detection.....	87

5.4.3 Varying methanol concentrations to improve simultaneous cell surface and intracellular labeling.....	89
5.4.4 Characterization of differential responses in protein phosphorylation in PBMC subtypes following cytokine stimulation.....	91
5.4.5 Inter- and intra-individual variability in STAT phosphorylation.....	96
5.5 DISCUSSION.....	102
6.0 SUMMARY AND FUTURE DIRECTIONS.....	105
APPENDIX.....	110
BIBLIOGRAPHY.....	112



## LIST OF TABLES

Table 1. Comparison of phospho-epitope detection strategies. Flow cytometry is more appropriate for complex cell populations and single cell analysis.....	26
Table 2. Multiple donor variability in STAT phosphorylation. Variability in STAT3 and STAT5 phosphorylation in unstimulated and stimulated cells from three different donors is limited.....	98
Table 3. Single donor variability in STAT phosphorylation. Variability in STAT1 and STAT3 phosphorylation in unstimulated and stimulated cells isolated from a single individual at different time points is low.....	101

## LIST OF FIGURES

Figure 1. Typical setup for a three-color cytometer with two scatter detectors.....	6
Figure 2. Relative kinetics of cell activation following stimulus. Phosphorylation is one of the earliest events to occur.....	8
Figure 3. Generic Western blotting procedure utilizing a colorimetric detection method. This technique is applicable for phospho-protein analysis.....	12
Figure 4. Schematic illustrating image processing algorithms used by imaging cytometry to define cellular localization. This technique is useful for signaling assays involving nuclear translocation.....	21
Figure 5. Schematic illustrating a general and simplified pathway of STAT activation. Activated STATs are phosphorylated, form dimers, and translocate to the nucleus.....	29
Figure 6. A schematic illustrating major modules of the MAP kinase signaling pathway. ERK1/2 and p38 are important downstream proteins activated by phosphorylation.....	34
Figure 7. Interferons ( $\alpha$ and $\gamma$ ) induce rapid phosphorylation of STAT1 in PBMC, primarily in monocytes, in a dose-dependent manner.....	58
Figure 8. Following cytokine treatment (IL-10, IFN $\alpha$ , and IL-6) phosphorylation of STAT3 is transiently induced in a dose-dependent manner.....	61
Figure 9. IL-3 and IL-7 induce phosphorylation of STAT5 in different PBMC populations. IL-3 activates monocytes alone, while IL-7 activates lymphocytes.....	63
Figure 10. Differential responsiveness of STAT5 to IL-2 in lymphocytes and monocytes is verified via Western blot and flow cytometry. Western blot flow cytometry provide qualitatively comparable data.....	65

Figure 11. TH2 cytokines IL-4 and IL-13 induce phosphorylation of STAT6 in a dose-dependent manner. IL-13 activates monocytes alone, while IL-4 activates lymphocytes and monocytes.....	68
Figure 12. Prolonged phosphorylation of p38 MAPK by PMA within monocytes. Unlike other proteins analyzed, p38 did not decrease in phosphorylation after two hours of treatment.....	70
Figure 13. Global phosphorylation of ERK1/2 in both monocytes and lymphocytes. Monocytes and lymphocytes display different kinetics of phosphorylation.....	71
Figure 14. Methanol is superior to saponin permeabilization for simultaneous staining of intracellular and cell surface proteins. Saponin is not capable of providing accessibility to phospho-epitopes.....	86
Figure 15. Marked differences in intracellular and cell surface staining of proteins are noted using a panel of permeabilizing agents. Methanol appears to be best for combined surface and intracellular labeling.....	88
Figure 16. 75% methanol enables simultaneous intracellular and cell surface labeling. Compared to other methanol concentrations, 75% is superior for dual surface and intracellular phospho-staining.....	90
Figure 17. Remarkable differences in individual phospho-proteins are detected in monocytes. Triplicate samples confirm previous protein phosphorylation results in monocytes following stimulation.....	92
Figure 18. Phospho-protein analysis reveals differential responsiveness of CD19 <sup>+</sup> , CD4 <sup>+</sup> , CD8 <sup>+</sup> , and CD56 <sup>+</sup> cells to individual cytokines. Overall, CD19 <sup>+</sup> cells appear to be least responsive to cytokines in terms of phosphorylation.....	94
Figure 19. Western blot confirms differential protein phosphorylation in distinct cell types. Only lymphocytes, not monocytes, display STAT5 phosphorylation following IL-2 stimulation, as previously shown by flow cytometry.....	95
Figure 20. Modest inter-individual variability in protein phosphorylation. STAT3 and STAT5 phosphorylation within monocytes, CD4 <sup>+</sup> , CD8 <sup>+</sup> , CD19 <sup>+</sup> , and CD56 <sup>+</sup> lymphocytes from three different individuals displays little variability.....	97

Figure 21. Limited intra-individual variability in protein phosphorylation. STAT1 and STAT3 phosphorylation within monocytes, CD4 <sup>+</sup> , CD8 <sup>+</sup> , CD19 <sup>+</sup> , and CD56 <sup>+</sup> lymphocytes isolated from a single individual at different times displays limited variability.....	100
Figure 22. Flow cytometry and Western blot provide similar results for IL-2 dose-dependent STAT5 phosphorylation.....	110
Figure 23. Flow cytometry and Western blot provide similar results for IL-2 time-dependent STAT5 phosphorylation.....	111

## ACKNOWLEDGEMENTS

O humble graduate student, how thy toils make thee weary! For not thy family, friends, and teachers, thou wouldst surely perish. These are not wise words of yore, passed down through the ages, but a testament of my gratitude to everyone that has supported me throughout graduate school. The wonderful people that have helped make it a pleasurable experience are numerous, but there are several key players that I would like to thank explicitly in this rather limited space.

First of all, I would like to thank my advisor and mentor, Dr. Michael T. Lotze, for his expert guidance throughout my studies. Not only did you allow me to freely explore ideas and present my findings at national/international conferences, which helped me grow as a scientist, but were always willing to set aside time to discuss science with me, as well as future goals and how to achieve them. Additionally, through your invaluable help with countless manuscript revisions, I learned the long, arduous process of authoring and submitting manuscripts to scientific journals (not without a gentle push every now and then). From arriving in your lab as a student with no immunology experience and no familiarity with flow cytometry, I gratefully attribute my newly acquired knowledge and skills to your leadership and dedication. In addition, I would like to thank Drs. Partha Roy and Albert Donnenberg for being members of my thesis committee. Through your helpful feedback during the development of my thesis, you have greatly contributed to its completion. My thanks also go to all past and present members of the Lotze lab that I have had the pleasure of working with, especially Richard DeMarco, a great

friend and gifted scientist with a contagious enthusiasm for science, who was single-handedly responsible for providing me with hands-on experience with flow cytometry and other laboratory techniques.

At this point, I'd like to thank all of my friends for the fun and good times over the years because work without play and humor would be terribly dull. I am particularly grateful for my friendship with Joe Candiello and Alicia DeFail, fellow bioengineering graduate students, who have made graduate school a more enjoyable experience from the outset. Good luck to both of you with your PhDs!!

Most importantly, without the constant support of my family, I never would have gotten very far. You always manage to believe in my abilities even at times when I do not. Throughout the years you have always been there to celebrate my accomplishments, but more significantly to show your compassion and understanding in times of difficulty. For all of this, I express my thanks and love.

To my best friend and fiancée, Sarah, I owe immeasurable thanks. Your ever-optimistic attitude and sharp sense of humor never fail to quickly extinguish any of my worries or frustrations. I count myself lucky to have found such a caring, like-minded companion. I love you beyond imagination. I'd also like to thank each member of your family, who has always treated me like one of their own.

## 1.0 INTRODUCTION

*“The engineer is the key figure in the material progress of the world. It is his engineering that makes a reality of the potential value of science by translating scientific knowledge into tools, resources, energy, and labor to bring them into the service of man ... To make contributions of this kind the engineer requires the imagination to visualize the needs of society and to appreciate what is possible as well as the technological and broad social age understanding to bring his vision to reality.” – Sir Eric Ashby (1958)*

In the setting of most diseases, including infection [1-4], autoimmunity [5, 6], and cancer [7-11], analysis of cellular function within the peripheral blood provides clinicians and scientists with important insights into pathobiology. Most functional assays applied to peripheral blood mononuclear cells (PBMC), however, are tedious, require long culturing periods and separation of cellular subsets, which could introduce artifacts, falsely representing native, *in vivo* function [12, 13]. Functional assays developed for clinical application should be designed to be robust and rapid to quickly screen patient samples, thus reducing the time interval during which cells are manipulated. Some of the earliest events identified during complex biologic responses are those associated with proximal signaling events, whereby individual cellular pathways are activated by protein phosphorylation cascades that dictate distal events including cytokine production, oxidative burst, and cytolytic activity [14]. Thus, an assay to detect these rapid changes in cellular function following a specific stimulus may prove useful in the clinical setting.

By utilizing recently developed reagents, phosphorylation state specific antibodies (PSSAs), it is possible to distinguish between phosphorylated and unphosphorylated proteins

belonging to important signaling pathways. Such antibodies have previously been employed in a variety of applications, including more conventional biochemical assays such as Western blotting, and in more recent assays, including flow and imaging cytometry, as well as protein microarrays [15-20]. Of these applications, only flow and imaging cytometry are capable of analyzing individual cells, particularly in complex mixtures. However, imaging cytometry analyzes cells at a somewhat slower rate than conventional flow cytometry, requires the capability of managing large data files with multiple detailed images acquired, and is best suited for adherent cells. In contrast to cytometry, Western blots and protein microarrays provide an average result spanning an entire population of cells, perhaps best applied with relatively homogenous cell populations. As a result, we evaluated flow cytometric strategies as a platform for our analysis of phosphorylated proteins within PBMC, a complex population of largely non-adherent cells.

Two major signaling pathways, the JAK/STAT and MAP kinase pathways, are central to the regulation of many vital cellular processes and controlled by protein phosphorylation cascades [21-26]. Furthermore, abnormal activation, or phosphorylation, of many proteins belonging to these pathways within cancerous cells, including malignancies associated with PBMC, is extensively documented in the scientific literature [27-35]. Interestingly, the main stimuli activating the aforementioned pathways are cytokines, growth factors, and cellular stress, which are often abnormally expressed or elevated within the serum in the setting of cancer [36-43] or other inflammatory disorders. As a result, we reasoned to believe that evaluation of non-malignant PBMC residing in patients with a variety of acute and chronic inflammatory conditions will display altered signaling pathways, providing scientists and clinicians with a useful and rapidly available diagnostic tool.



Because the application of flow cytometry to phosphorylated signaling proteins is a relatively novel strategy, we first characterized the phosphorylation of several important members of the JAK/STAT and MAP kinase signaling pathways: STAT1, STAT3, STAT5b, STAT6, p38 MAPK, and ERK1/2, following the brief application of appropriate stimuli in a dose and time-dependent manner. By taking advantage of the fact that monocytes and lymphocytes typically have different light scattering properties, we were able to analyze results within each of these populations separately without the use of additional reagents. Once suitable stimulation conditions were established, we successfully developed methodology to simultaneously label intracellular phospho-epitopes and cell surface proteins used to identify subpopulations of cells within the PBMC: CD4<sup>+</sup> or CD8<sup>+</sup> T cells, CD14<sup>+</sup> monocytes, CD19<sup>+</sup> B cells, and CD56<sup>+</sup> NK cells. This strategy allowed us to examine differential signaling within individual PBMC subsets following activation with various stimuli. The methods developed in this thesis provide an excellent stepping-stone for more in-depth studies regarding cell activation and its involvement in various diseases.

With regard to the organization of this thesis, the layout is as follows. The introductory chapter summarizes the essential aspects of flow cytometry, various assays used to study protein phosphorylation, including Western blotting, protein microarrays, flow cytometry, and imaging cytometry, the JAK/STAT and MAP kinase signaling pathways, signaling abnormalities within hematological malignancies, alterations in cytokine expression associated with tumors, and defects in “normal” PBMC within the setting of cancer. Chapter three outlines the two specific aims of this thesis, including our hypotheses for each of them individually. In chapters four and five, we introduce our reasoning for pursuing specific aims one and two respectively, followed

by materials and methods used to accomplish each and the ensuing results and discussion sections. In conclusion, a summary of the results from each of the aims is provided, in addition to implications of these findings and directions proposed for future investigation.

## **2.0 LITERATURE REVIEW**

### **2.1 FLOW CYTOMETRY**

Flow cytometry is an invaluable technique used to rapidly analyze large numbers of cells from a wide variety of sources. Provided the original sample is a single-particle suspension, cytometers can detect particles ranging from one centimeter to ten angstroms in size (i.e., single-cell organisms to individual molecules) [44]. Due to its usefulness and broad utility, flow cytometry is applicable in a wide range of fields such as clinical medicine, pharmacology, toxicology, bacteriology, virology, environmental sciences, and bioprocess monitoring [45]. In contrast to traditional methods that provide an average measurement for an entire population, flow cytometric data enables resolution of individual particles resident within a population. Naturally, this is desirable when analyzing complex, heterogeneous samples, such as peripheral blood, where information from rare subpopulations would be lost if a population-based average was obtained.

In principle, a flow cytometer is designed to acquire light-scatter and fluorescence measurements that are associated with components or characteristics of individual cells. To achieve these measurements, a flow cytometer employs lasers, fluidics, optics, detectors, measuring circuits, and computer electronics. Briefly, a single cell suspension is injected into a flow cell, where a surrounding stream of sheath fluid hydrodynamically focuses it into the central most region of a laser beam oriented orthogonal to the direction of flow, allowing cells to

pass through one at a time. When the laser makes contact with a cell, the incident light is scattered. Detectors are arranged to collect forward scattered and right-angle side scattered light. Forward scatter relates to the size of the cells passing through the laser while side scatter relates to their granularity and internal complexity. Using these scatter parameters alone, individual populations of cells may be identified within complex mixtures. If the cells are labeled with fluorescent dyes or antibodies conjugated to fluorophores, particular components of the cells may also be detected. Dyes or fluorophores excited by the laser will emit fluorescence, which can be captured by additional optical detectors in combination with optical filters to select for specific wavelengths. Following contact with the optical detectors, photons are converted to an electronic signal, which is then digitized by measuring circuits, and sent to a computer for data analysis. The optical components of a typical three-color flow cytometer are illustrated in Figure 1 [44]. As one may imagine, current cytometers have the capability of simultaneously measuring

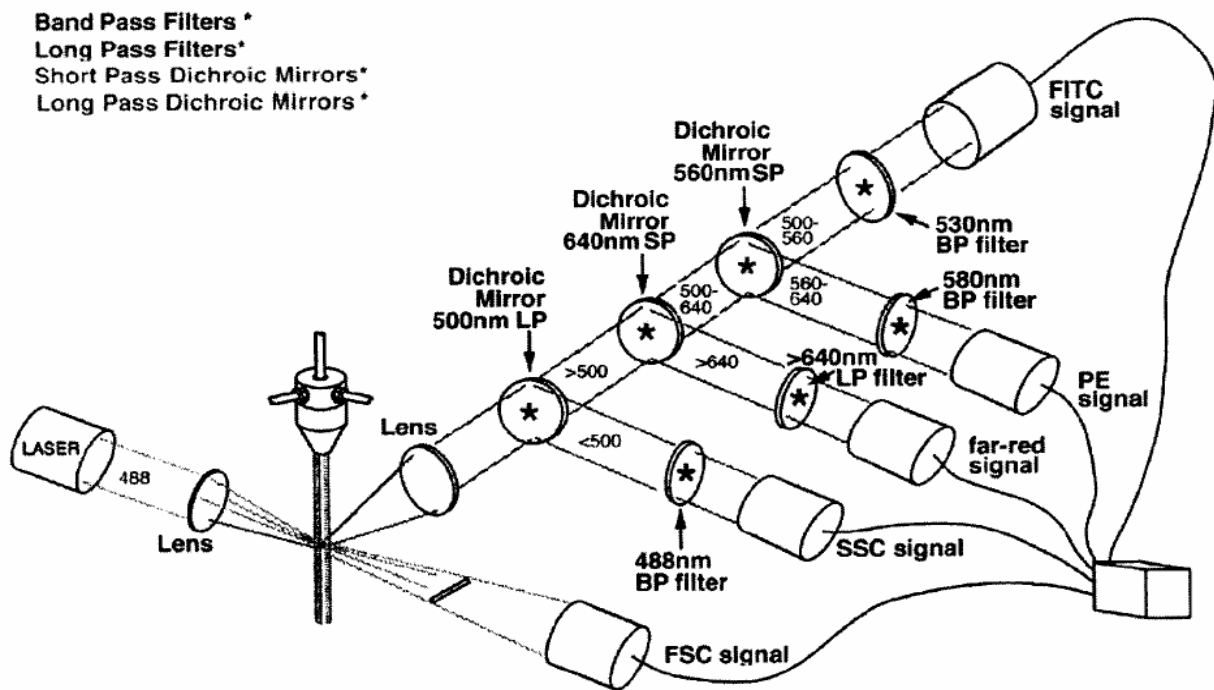


**Figure 1.** Typical setup for a three-color cytometer with two scatter detectors [44].

more than just three fluorescent parameters by utilizing a combination of different fluorophores, applying highly evolved hardware and software. Some high-end, recently developed cytometers are capable of measuring up to 17 different fluorescent parameters and two scatter parameters [46]. As a starting point, the number of simultaneous parameters is limited by the availability of fluorophores with appropriate characteristics. In general, these fluorophores should be biologically inert (unable to bind to cellular elements or affect cells), have high cell-associated fluorescence intensities, exhibit little spectral overlap with one another, and should be easily conjugated to antibodies [47].

The use of flow cytometry in biological and medical research, as well as in clinical medicine, underscores the versatility of this technology. Most notably, cytometry is utilized for the characterization of hematologic malignancies based on immunophenotypic analysis of cells in the bloodstream. However, cytometry also affords the opportunity to combine cell enumeration and immunophenotyping with measures of cell function, which provides clinicians and researchers with a richer set of information.

## **2.2 CYTOMETRIC FUNCTIONAL ASSAYS**

A key component to identifying and understanding clinical disorders and host responses to stimuli is the ability to evaluate cellular function. Compared to conventional biochemical functional assays, flow cytometry allows individual cells to be assessed without the need for a priori separation, which is especially important when dealing with complex cell populations such as peripheral blood mononuclear cells (PBMC). Furthermore, the additional manipulation of

cells incurred by separation may alter a cell's native function [12, 13]. Not only does flow cytometry allow one to examine individual cells without separation, but it also requires shorter protocol times, provides a larger dynamic range of data collection, dispenses of the need to radioactively label materials, and affords the ability to analyze rare subsets [48] and multiple epitopes within a single cell [49].

There are a large number of functional assays suitable for flow cytometric analysis, including phagocytosis, gene expression, apoptosis, redox reactions, cytokine production, cell proliferation, cytotoxicity, and cell signaling [15, 50-55]. Although flow cytometry significantly decreases the protocol time compared to traditional methods, for many of these assays, incubation times may be anywhere from several hours up to several days. Figure 2 illustrates the stages of T cell activation in response to a stimulus [14]. Early responses are defined as those

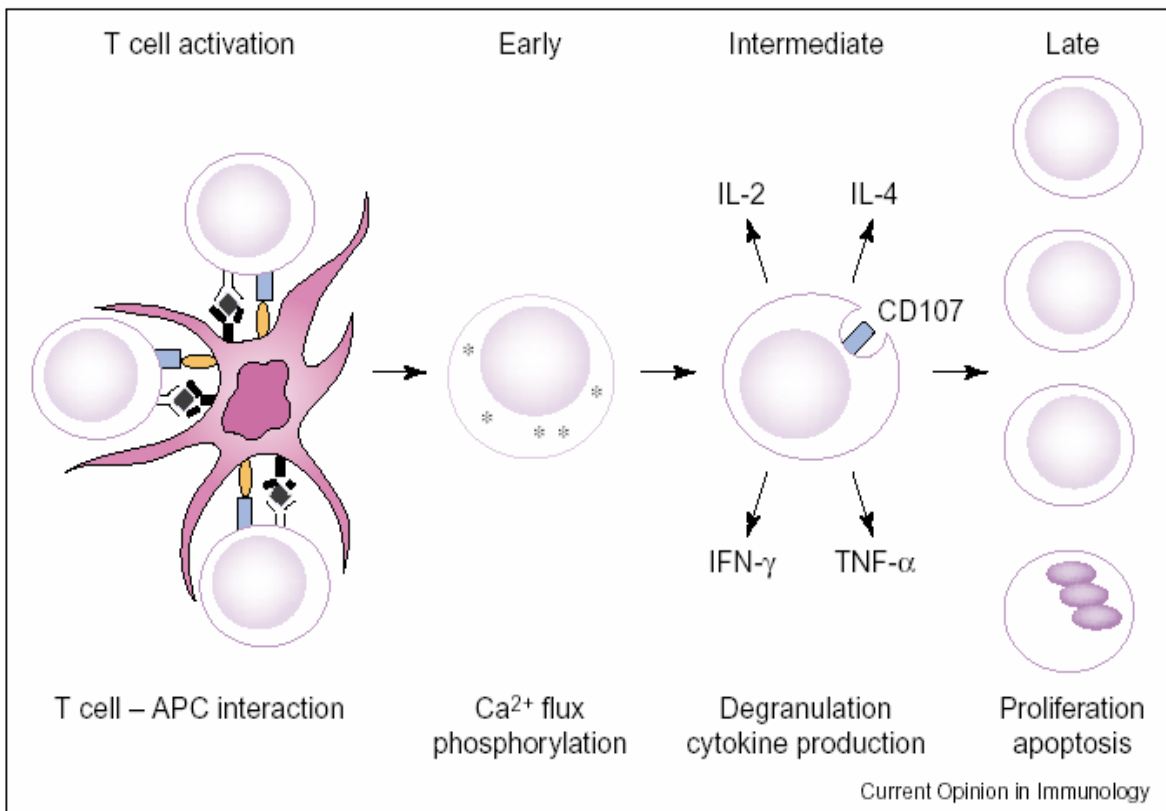


**Figure 2.** Relative kinetics of cell activation following stimulus [14].

that occur within seconds to minutes, intermediate responses occur within several hours, and late events after several days. Assays developed as clinical diagnostics should be designed to be robust and rapid to quickly screen patient samples, thus reducing the interval that the cells are manipulated (i.e. culture, incubation, storage), which could introduce artifactual responses. Of the functional assays listed, the early events in cell signaling, such as phosphorylation and calcium influx, occur most rapidly. However, of these, only phosphorylation yields specific information concerning distinct signaling pathways within the cell. Accordingly, we plan to focus our studies on the upstream phosphorylation of proteins belonging to important signaling networks that control immune regulation.

### **2.3 ASSAYS TO ASSESS PROTEIN PHOSPHORYLATION**

Since the transcriptome, reflecting gene expression, does not always correlate directly with the amount of protein expressed [56, 57] and does not account for post-translational modification including phosphorylation, which is integral to protein function, it is important to directly analyze proteins. Proteins drive much of cell biology, such as structural aspects of cellular integrity, signaling molecules, entry and exit from the cell cycle, mediating many of these functions especially when phosphorylated. As Philip Cohen mused, “the reversible phosphorylation of proteins regulates nearly every aspect of cell life [58].” As many as 30% of all human proteins are capable of being phosphorylated. Taken altogether, it is clear that protein phosphorylation is a major regulatory component necessary for full understanding of cellular function.

Indeed, there are many approaches available to analyze phosphorylated proteins within cells. As with every technique, each of these brings its own advantages and disadvantages to the table, depending on the experimental objectives. A description and comparison of currently employed phospho-protein detection methods from conventional biochemical assays, such as Western blotting, to more recent advancements: protein microarrays, flow cytometry, and imaging cytometry, will shed light on the relative merits of each system. One common element connecting these methods is the requisite use of antibodies with specificity for phosphorylated proteins.

### **2.3.1 Phosphorylation state-specific antibodies (PSSAs)**

The first phosphorylation state-specific antibodies (PSSAs), both monoclonal and polyclonal, were developed in the 1980s against phosphotyrosine and to a lesser degree phosphothreonine. Unfortunately, these antibodies did not have specificity for any single protein; rather they provided information regarding pan-proteome phosphorylation. PSSA technology advanced in the early 1990s when monoclonal and polyclonal sequence-specific PSSAs were developed [59]. These antibodies were generated by injecting animals with enzymatically phosphorylated peptides and screening the resultant hybridomas for phospho-specificity (for monoclonals) or affinity-purifying phospho-specific antibodies from the sera (for polyclonals). Today, more efficient chemical techniques that do not rely on enzymes are available to phosphorylate peptides used to generate PSSAs.

Once a sequence-specific PSSA has been produced, it must be validated for its specificity. Typically, this is first accomplished by Western blotting. In a Western blot, the PSSA should demonstrate a single band at the appropriate molecular weight, unless other cross-



reactive proteins, degradation products, splice variants, or allelic variants share a linear confirmation similar to the primary amino acid sequence of the peptide used to generate the PSSA. Secondly, the PSSA should reveal phosphorylation of cultured cells in response to known activating stimuli. Another method of probing specificity is to preincubate the PSSA with an excess of the immunizing antigen to determine if it abrogates its immunoreactivity. Critical confirmation could also use strategies where one substitutes the amino acid at the phosphorylation site of the individual target protein within a cell of interest thereby disabling phosphorylation and proving specificity of the PSSA. Since their initial description, PSSAs have found their way into many applications useful for detecting changes in phospho-protein expression.

### **2.3.2 Western blotting**

One traditional, yet powerful, method of detecting specific proteins within complex mixtures, such as cell lysates, is referred to as immunoblotting or Western blotting. Developed in 1979 by Harry Towbin, it was originally designed to detect ribosomal proteins [60], but has been applied to an enormous number of proteins including post-translational modifications such as phosphorylation. In short, the method consists of four basic steps: separating proteins by size via gel electrophoresis, transferring resolved proteins to a membrane, incubating the membrane with antibodies to a specific protein, and detecting the bound antibody. A generic Western blot procedure, utilizing a colorimetric method of detection, is illustrated in Figure 3 [61].

After an initial period of culture, during which cells may be treated with an agent of interest, the cells are lysed, typically in the presence of protease inhibitors to prevent protein degradation. Additionally, when detecting phosphorylated proteins, it is important to include

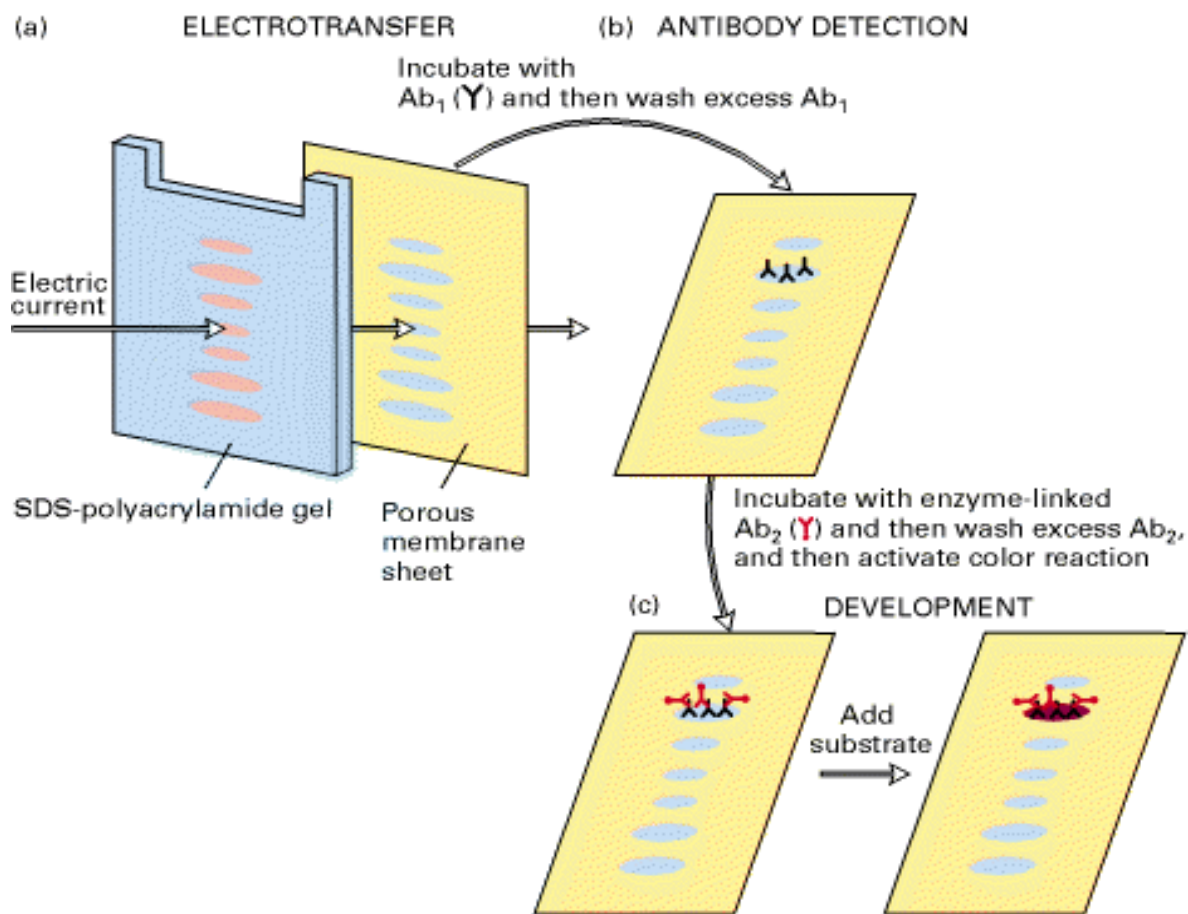


**Figure 3.** Generic Western blotting procedure utilizing a colorimetric detection method [61].

phosphatase inhibitors during this step. To quantify differences in protein levels between different treatment groups, protein concentrations should be approximately equal. This can be achieved by performing an assay to measure the total amount of protein present in cell lysates, such as the colorimetric bicinchoninic acid (BCA) assay, then performing appropriate dilutions. If this step is ignored, differences may still be roughly quantified by normalizing the apparent amount of protein to another protein with relatively constant levels of expression, such as  $\beta$ -actin.

Separation of proteins from the complex mixture in cell lysates is accomplished by gel electrophoresis, which exploits differences in protein molecular weight. In short, a voltage is applied across a gel, typically polyacrylamide, which drives smaller proteins to migrate through the gel at a faster rate than larger proteins. Molecular weights are determined by running a “ladder” through the gel to create markers of known molecular weight. Since proteins exist in various conformations, i.e. some proteins with higher molecular weight may be more compact, thus able to migrate through the gel faster, it is necessary to denature them and reduce any disulfide bonds prior to electrophoresis. In many cases, boiling the proteins in the presence of  $\beta$ -mercaptoethanol is sufficient to reduce disulfide bonds and denature proteins. Additionally, the proteins’ native charges must be masked by incorporating sodium dodecyl sulfate (SDS), which adds negative charge and also contributes to protein denaturation.

Once the voltage has been applied and the proteins have been separated, the proteins may be transferred to a membrane. In this step, the gel is placed on a membrane capable of binding any protein, such as nitrocellulose or polyvinylidene fluoride (PVDF), and another voltage is applied through a buffer to transfer all of the separated proteins from the gel to the membrane, creating a replica pattern. Before antibodies can be used to detect proteins of interest, the

membrane must be blocked to prevent non-specific antibody binding. Often, non-fat dry milk is used for this purpose, however BSA is the blocking agent of choice for phospho-protein detection when using pan-phosphotyrosine, -serine, or -threonine antibodies, as milk contains many phosphorylated proteins. After blocking, a primary antibody targeted against a protein of interest, such as a PSSA, should be incubated with the membrane. After several washes with mild detergent to remove non-specific binding, a secondary antibody containing a detection method should be incubated with the membrane. Protein visualization can be accomplished by colorimetric, fluorescent, chemiluminescent, or radioactive detection [62]. Of these, the highest sensitivity without using radioactivity is achieved with chemiluminescence, where luminol is oxidized to produce light, which is detected on x-ray film. With the noted minor procedural modifications, Western blotting is applicable for the detection of phosphorylated proteins. This is especially useful when a relatively homogenous cellular population is used.

### **2.3.3 Protein microarrays**

Another, more recently developed technique, capable of analyzing post-translational modifications of proteins, like phosphorylation, is the protein microarray, which was built upon the success of earlier gene arrays. In principle, microarrays are miniaturized bait-and-capture assays. Several different formats have been developed over the years relying on different bait molecules, such as aptamers, antibodies, cell lysates, phage or recombinant protein/peptide, nucleic acids, or tissue, immobilized into hundreds of spots on a substrate [63]. In most cases, the capture component is a complex biological mixture of proteins, such as cell lysates and serum. In order to visualize proteins bound to the array, various detection strategies have been devised. In general, they are classified as label-free and labeled probe. Label-free detection

methods include mass spectrometry, surface plasmon resonance, and atomic force microscopy, while labeled probe methods, which differ based on the immobilized bait molecule, incorporate fluorescent, chemiluminescent, chromogenic, or radioactive detection methods[63]. Due to their high sensitivity and resolution, ease of use and clean up, fluorescent strategies have become the method of choice for microarray analysis [64]. In forward phase or antibody array formats, many antibodies against specific proteins are spotted; then a mixture of directly labeled proteins from lysates or serum is applied to the array. Spots containing proteins of interest will produce a signal proportional to the amount of protein bound to the array. Similarly, phosphorylated proteins may be analyzed by spotting various PSSAs onto the array. Additionally, sandwich assays, analogous to ELISA, have been applied to microarrays, where proteins are captured by immobilized antibodies and subsequently detected by directly labeled antibodies. In a direct capture format, also referred to as reverse phase protein microarrays, complex mixtures of proteins, such as lysates from various biopsies or cell cultures, are immobilized onto an array to be detected by directly labeled antibodies. In the same way, phospho-proteins may be analyzed by applying labeled PSSAs. Using forward phase, one can analyze a large number of protein targets within a single specimen simultaneously. Conversely, with reverse phase, one analyzes a single protein target across many samples.

Because of the high-throughput nature of this technique, protein microarrays have proven useful for detecting differences in protein expression levels between healthy individuals and those with various disorders [16, 65]. For example, protein expression levels in the clinical disorder, spinal muscular atrophy, highlights the importance of analyzing phosphorylation events, as it provides evidence that the amount of a protein does not necessarily correlate with the amount of phosphorylated protein. Specifically, total JNK1 levels were lower in the setting

of apparent disease, whereas phospho-JNK1 levels were higher [16]. Thus, protein microarrays are a promising technology that can be easily adapted to study the phospho-proteome and provide insights into disease mechanisms.

#### **2.3.4 Flow cytometric method**

With the advent of flow cytometry, a powerful new method of analyzing multiple parameters within single cells became available. The premise on which the technology is based is the ability to identify cells due to light scatter properties, while cellular elements are detected by measuring fluorescence from fluorophore-conjugated antibodies directed against components of interest. These may be detected on the cell surface, which is a relatively straightforward labeling procedure, or within the cell, as is the case for phosphorylated proteins. In the latter case, the method of staining is more complex and requires protocol optimization for individual targets.

In general, the flow cytometric detection of phosphorylated proteins involves stimulating cells, followed by fixing, permeabilizing, and application of fluorophore-conjugated PSSAs. When developing a protocol based on these steps, it is important to keep in mind the following technical considerations: antigen accessibility, cellular localization, stability of the phospho-epitope, antibody and fluorophore selection, and maintenance of surface staining and scatter properties [18]. After cells are stimulated to induce phosphorylation of a protein of interest, they should be fixed to maintain the stability of the phospho-epitope. The concentration and choice of fixative, as well as time of fixation, are important, as these will affect antigen accessibility, stability of the phospho-epitope, autofluorescence, and scatter properties. If a fixative is too strong, concentrated, or applied too long, it may fix proteins to such a degree that phospho-epitopes are no longer available to bind an individual antibody. Conversely, if the fixative is

insufficient, the stability of the phospho-epitope may be in jeopardy, as phosphatases may still be active. Some fixatives, such as glutaraldehyde, increase the autofluorescence of individual cells, including monocytes, which can mask the signal obtained from some fluorophores.

Additionally, some fixatives may alter scatter properties, which may be troublesome when defining specific cells within complex mixtures.

Once a fixation method has been optimized, a permeabilization strategy must be developed to allow PSSAs access to the interior of the cell. As with fixation, permeabilization affects phospho-epitope detection in a number of ways. Antigen accessibility is a major issue, as many phospho-epitopes are buried by protein-protein interactions, such as within SH2 domains. Furthermore, most PSSAs are generated to a linearized phospho-peptide, which requires denaturing the native protein structure. Therefore, permeabilizers, such as alcohols, that not only solubilize components of the cell membrane, but also induce denaturation, are often required. Additionally, cellular localization of the protein of interest, whether it is nuclear or cytoplasmic, must be considered when choosing a permeabilization method. If one is interested in combining surface staining with phospho-protein detection to phenotype cells, it is important to use a permeabilizer that will not be detrimental to plasma membrane-bound epitopes. Like fixation, different permeabilization agents also have the ability to alter cell scatter properties. Before cells are labeled with PSSAs, it is important to block any potential non-specific binding by incubating the cells with an 'Fc-blocking agent', such as nonimmune, normal polyclonal IgG of the same species as the specific PSSA [66].

In the next essential step, the phosphorylated protein is labeled with a fluorophore-conjugated PSSA. As already noted, the PSSA must be validated for its specificity to only the phosphorylated form of the protein, but applying it to fixed and permeabilized cells requires

further validation, as certain clones of monoclonal antibodies provide more intense and specific staining of intracellular antigens [67]. Another point of consideration is the choice of fluorophore attached to the PSSA; a larger one, such as APC or PE, may impede the antibodies ability to travel freely within the cell. Furthermore, since phospho-proteins are normally expressed at low levels, it is important to choose a fluorophore that is “bright.” To limit the amount of non-specific labeling, the antibody should be titrated and incubated with the cells for an appropriate length of time.

In any flow cytometric experiment, it is important to include several types of controls, including a positive control with a stimulus known to induce protein phosphorylation, detected with a validated PSSA. Additionally, a negative control should be employed. Many groups have utilized isotype controls, which are nominally non-specific antibodies of the same type as the PSSA. However, the use of isotype controls is generally of little value because each antibody and conjugate has different characteristics in terms of “stickiness” and background staining characteristics [47]. Likewise, if there were a discrepancy between the FTP ratios of the isotype and PSSA (the number of fluorophores conjugated per antibody), it would be difficult to draw firm conclusions. As a more appropriate control, it is recommended to treat stimulated and unstimulated cells with the same PSSA. Although this will not offer a measure of basal phosphorylation, it will provide a means of detecting specific phosphorylation following stimulation. If cells are simultaneously stained for multiple targets, surface proteins and phospho-epitopes or multiple phospho-epitopes, it may be necessary to include compensation controls. This is necessary when the fluorophores employed have a sufficient degree of spectral



overlap, which will cause a fluorophore to contribute signal to several individual detectors. To remedy this, compensation is applied, which mathematically limits the contribution of fluorophores in detectors to which they are not assigned.

Several groups have successfully analyzed phosphorylated proteins, such as pSTAT1, pSTAT4, pSTAT5, pSTAT6 and pERK via flow cytometry and obtained qualitatively similar results with Western blotting [15, 19, 20, 68, 69]. However, most of these studies were performed on homogeneous cell populations or did not combine cell surface staining to subset populations from complex mixtures. In spite of these caveats, flow cytometry is indeed a promising technique for evaluating protein phosphorylation with several advantages over other available technologies.

### **2.3.5 Imaging cytometry**

Like flow cytometry, imaging cytometry has been utilized for a large number of biological applications including cell cycle analysis, cell signaling (mainly translocation from the cytoplasm to the nucleus), cell-cell interactions, cell motility, receptor internalization, and assessing cell death pathways. Imaging cytometry combines molecular, morphologic, and phenotypic information at the single-cell level, providing substantial detail [70]. The inclusion of morphological parameters is one of the main differentiating aspects from flow cytometry. At present, there are a variety of imaging cytometers commercially available, each employing similar principles, but individual methods of fluorophore excitation and detection. Most of the previously discussed technical considerations and sample preparation techniques associated with flow cytometry are also applicable to imaging cytometry.

In general, imaging cytometry integrates fluorescent cell-based assays, automated high-resolution microscopy, image processing algorithms, and informatics software used to archive and organize many images and quantitative results [71]. By obtaining images of intact cells and applying image processing algorithms, this technology affords the ability to perform spatio-temporal measurements of fluorescence within various cellular compartments [72]. Once cells are prepared in culture plates and stained with fluorescent dyes or fluorescent-labeled antibodies, they must be excited to detect the components of interest. Imaging cytometers employ a number of illumination sources including lasers, arc lamps, and light-emitting diodes (LEDs). Furthermore, various microscopy systems are utilized such as confocal, multiphoton confocal, digital, and conventional inverted fluorescence microscopy [73]. Additionally, photomultiplier tubes (PMTs), such as those used in flow cytometers, and CCD cameras have found use in imaging cytometers to detect emitted photons. To enable measurement of multiple parameters, these systems typically have multiple band pass emission and excitation filters. Overall, the laser-scanning-PMT imaging cytometers are more sensitive than the arc lamp-CCD camera systems, but are considerably more expensive. Additionally, these laser-PMT systems are slower during image acquisition than less sensitive imaging cytometers. However, both of these are slower at acquiring events than conventional flow cytometers [73]. Most imaging cytometers are completely or semi-automated, which includes automatic measurement of exposure times, autofocusing, and automatic plate scanning. Because of this automation and the ability to multiplex, they are widely used in high-throughput screening strategies employed in drug screening programs.

Another common feature of imaging cytometers is the use of image processing algorithms to identify distinct cellular compartments. To accomplish this, a particular region of

the cell or organelle, usually the nucleus, is labeled with a fluorescent marker from which a primary object is created in the software, as shown in Figure 4 [71]. This primary object is used to identify individual cells and subcellular regions. Typically, the primary faux object created is a circle to identify the nucleus, which is eroded slightly and dilated outward as a ring within the boundaries of the cell to identify a region as the cytoplasm. Within each of these regions, aggregates of higher pixel intensity are also capable of being identified by the algorithm. This particular algorithm demonstrated is an application called “compartmental analysis” designed by

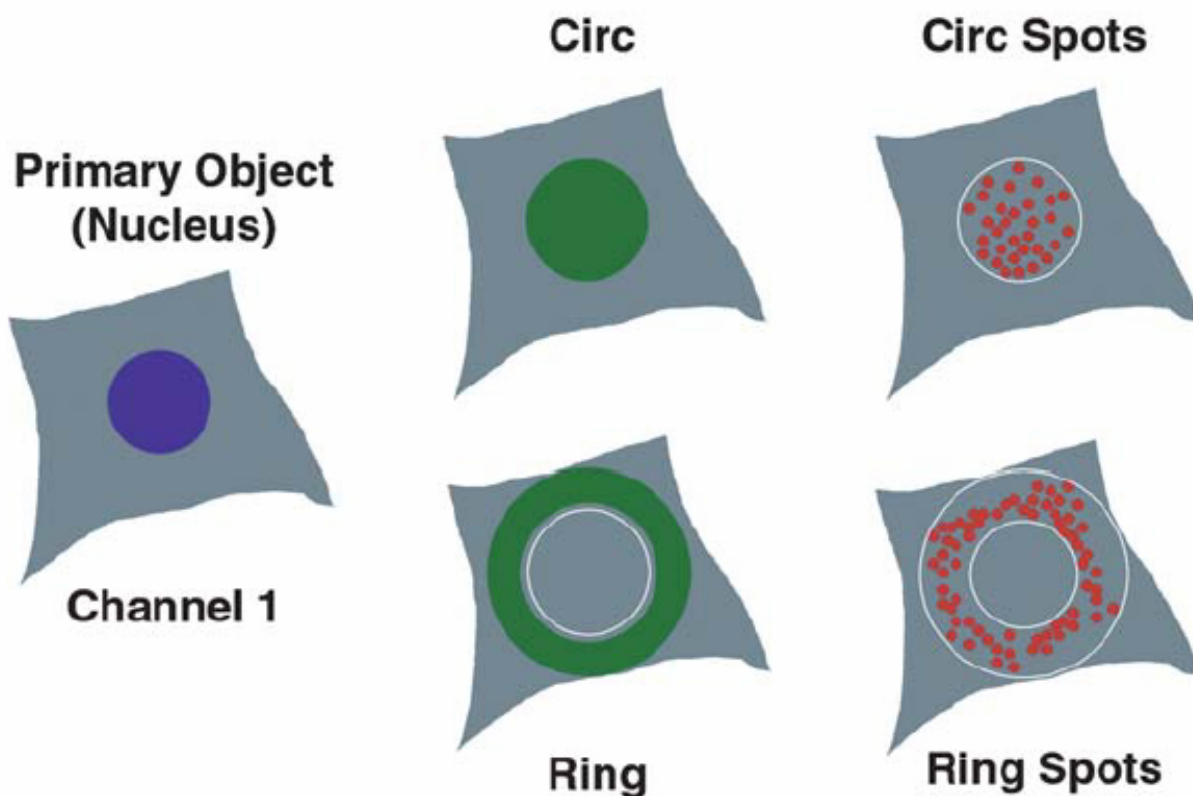


**Figure 4.** Schematic illustrating image processing algorithms used by imaging cytometry to define cellular localization [71].

Cellomics, Inc. Fluorescence intensities can be measured in these defined areas as well as intensity ratios, intensity differences, spot numbers, and spot areas. Obviously, morphological parameters, such as cell size, nuclear area and shape are also included in the measurements [71].

With regards to cell signaling, cells may be stimulated, fixed, and permeabilized, keeping in mind the same considerations outlined for flow cytometry, and then labeled with fluorophore-conjugated antibodies towards specific intracellular proteins of interest, including phosphorylated proteins to identify activated signaling pathways. In this manner, it is possible to pinpoint the cellular localization of phosphorylated proteins, as images of the cells are acquired. Accordingly, the use of PSSAs is permitted, however they are not required to detect activation of signaling pathways. Many signaling proteins, upon phosphorylation, form dimers that translocate to the nucleus to regulate gene transcription. As a result, it is possible to label proteins with antibodies toward unphosphorylated epitopes since imaging cytometry provides the capability of measuring nuclear and cytoplasmic fluorescence intensities separately. Additionally, this compartmental analysis gives a sense for the amount of protein that is activated. As a result of its ability to measure nuclear translocation events in single cells, imaging cytometry has been utilized to study a number of signaling pathways including NF $\kappa$ B [72, 74], p38 MAPK [72], and ERK [71]. Because of the ability to multiplex and obtain images of intact cells, this technology is also capable of analyzing heterogeneous cell populations and cell-cell interactions. Individual cell lineages and subpopulations are readily identifiable by including fluorophore-conjugated antibodies towards cell-specific proteins. Due to its high-throughput nature and unique advantages, such as morphological assessment, and compartmental analysis, automated imaging cytometry is a powerful technique for scientists studying cellular function.

### **2.3.6 Comparison of phospho-epitope detection methods**

Although each of the technologies discussed possesses the ability to measure phosphorylated proteins, there are advantages and disadvantages associated with each. The objectives of an experiment, for instance studying rare cells, heterogeneous populations or localization of components within cells, will determine which technique is most appropriate. A direct comparison of the capabilities and limitations of these methods will help to elucidate their value.

Compared to the other methods discussed, the primary advantage of flow cytometry is the ability to measure events in single cells, as opposed to bulk analysis methods, where it is rivaled only by microscopy and imaging cytometry. Unlike microscopy, flow cytometry is not limited by the number of cells that can be analyzed in a short period of time. The problem with microscopy is overcome in automated imaging cytometry, but these systems still acquire events slower than conventional flow cytometers, especially those capable of automatically acquiring 96-well plate formats for sampling individual cell populations, such as the BD FACSArray. It should also be noted, that imaging cytometry is best suited for adherent or semi-adherent cells. When cells are in suspension, rather than spread-out on a surface, it is much more difficult to create a region for the cytoplasm within the image processing software because the cell/nucleus diameter ratio is markedly lower. Another disadvantage with imaging cytometry is the requirement of dealing with huge data files due to the large number of images acquired.

Whereas flow and imaging cytometry measure events on a cell-by-cell basis, bulk analysis methods obtain a signal that is an average for an entire population of cells. Bulk analysis methods would be unable to distinguish heterogeneity in responsiveness within a population, such as bimodal cell populations and all-or-none responses. Western blotting and protein microarrays necessitate the use of homogeneous cell populations, whereas cytometry is

suitable for complex mixtures of cells due to the ability to immunophenotype and distinguish cells based on light scatter. Imaging cytometers are only capable of providing light scatter information if a laser is used as the illumination source [75]. To study individual cell types from complex mixtures, such as PBMC, via non-cytometric based techniques, requires cell sorting or magnetic separation, which is time consuming and may introduce artifacts. Another result of cytometry's ability to analyze many cells on a single cell basis is rare event analysis, which is not feasible with the other methods discussed. Cytometry is rich in statistical information because so many cells are analyzed individually within each experiment. If the amount of sample is limiting, cytometry also offers an advantage because it requires fewer cells for analysis than Western blotting or protein microarrays. Because flow cytometry affords the ability to stain multiple parameters simultaneously (currently up to 19), this also decreases the amount of sample needed for an experiment. Imaging cytometers currently do not have the ability to measure as many parameters simultaneously. At the same time, many more parameters, limited only by the number of available PSSAs spotted on a chip, can be analyzed by protein microarrays, whereas only one protein may be detected at a time on a Western blot.

All of the advantages aside, flow cytometry does have limitations compared to other technologies. Western blotting offers some unique advantages not attainable by flow cytometry or protein microarrays, such as determination of protein size, which can be used to verify proper labeling. If cells are fractionated into nuclear and cytoplasmic components, microarrays and Western blotting can be used to determine cellular localization of proteins. Even without fractionation, imaging cytometers are capable of measuring the localization of cellular components within intact cells. With regards to sensitivity, the signal-to-noise ratio is typically higher with microarrays and Western blots because there is no noise contribution of

autofluorescent cells or problems with antigen accessibility, as with fixed and permeabilized cells. Furthermore, as a result of enzymatic amplification, the signal obtained by Western blotting can be magnified. Proteins with very low expression levels may be below the limits of detection by cytometry. By design, Western blotting incorporates denaturing conditions, which exposes hidden phospho-epitopes. If this is not addressed in microarray or cytometry experiments, it is expected that one would obtain false negatives, as the PSSAs generated against linearized peptides will not be able to recognize phospho-epitopes in a protein's native state. Table 1 summarizes some of the primary differences between each of the methods described. No one technology should be considered the "best" without evaluating each of them contextually, keeping in mind the desired experimental objectives. Because the aim of this study is to analyze early signaling events regulating immune function in peripheral blood mononuclear cells (PBMC), which are non-adherent cells, we have chosen to develop a flow cytometric-based method, which allowed us to study individual cells within this complex population.

**Table 1.** Comparison of phospho-epitope detection strategies.

	<b>Western Blot</b>	<b>Protein Microarray</b>	<b>Flow Cytometry</b>	<b>Imaging Cytometry</b>
Bulk or Single Cell Analysis	Bulk	Bulk	Single cell	Single cell
Suitable Sample Type	Homogeneous	Homogeneous	Heterogeneous	Heterogeneous
Ability to Study Rare Events	No	No	Yes	Yes
Sample Size Needed	Large ( $\sim 10^6$ )	Large ( $\sim 10^6$ )	Small ( $\sim 10^5$ )	Small ( $\sim 10^4$ )
Multiple Parameters	No	Yes	Yes	Yes
Size Determination	Yes	No	No	No
Intracellular Localization Determination	Yes (if cells are fractionated)	Yes (if cells are fractionated)	No	Yes
Signal-to-Noise Ratio	No autofluorescence or antigen accessibility issues	No autofluorescence or antigen accessibility issues	Decreased by autofluorescence and antigen accessibility	Decreased by autofluorescence and antigen accessibility



## 2.4 IMPORTANT PHOSPHO-SIGNALING PATHWAYS

Cells often respond to environmental stimuli, such as factors released from cells, damage, and stress conditions, via rapid and sequential protein phosphorylation. Depending on the cell type, stimulus, and context in which it is presented, phosphorylation events are triggered through distinct pathways, two major ones being the JAK/STAT and MAP kinase signaling pathways. The JAK/STAT pathway is important in regulating host defense, cell growth, development, and apoptosis. Similarly, the MAP kinase signaling pathway plays a major role in regulating cell cycle progression, apoptosis, cytokine production, and cell differentiation in response to stress, inflammation, and other stimuli. Due to their many important roles in controlling various aspects of cell life, it is critical to understand how these pathways normally function and how their dysregulation may contribute to abnormalities in immunity and cell growth and death.

### 2.4.1 The JAK/STAT pathway

Originally discovered by James E. Darnell Jr.'s group in 1992, STATs (signal transducers and activators of transcription) are a family of latent proteins that are activated via tyrosine phosphorylation, leading to nuclear translocation and regulation of gene expression. There are seven identified STAT family members: STAT1, STAT2, STAT3, STAT4, STAT5a, STAT5b, and STAT6, ranging in length from 750 to 850 amino acids [26]. STATs share a number of functional domains, including the N-terminal domain, followed by a coiled-coil domain, a DNA-binding domain connected by a linker to an SH2 domain, and a transactivation domain at the C-terminus [76]. In general, extracellular proteins, mainly cytokines and growth hormones, activate STATs after they bind to their cognate receptors. When a ligand binds to its receptor it induces receptor dimerization, as is the case for growth hormone or erythropoietin, or they form

heteromultimers, as is true for many interleukins and interferons [77]. Following this step, protein kinases called Janus kinases (JAKs) that are noncovalently associated with receptors transphosphorylate each other and the receptors to which they are bound. Phosphorylation of the receptor provides a docking site for STAT proteins via their Src-homology-2 (SH2) domain. Upon binding to the receptor, STATs are phosphorylated on a single tyrosine residue between their SH2 and transactivation domains by JAKs. This step leads to the formation of STAT homo- or heterodimers through reciprocal SH2/phosphotyrosine interactions. All STAT family members can form homodimers, while STAT1/STAT3, STAT5a/STAT5b, and STAT1/STAT2/IRF9 can form heterodimers and –trimers, respectively. Monomeric phosphorylated STATs have not been identified. Once the dimers are formed, STATs may enter the nucleus through interactions with importins and their nuclear localization sequence (NLS) to regulate transcription of a variety of genes depending on the nature of the dimer and its interaction with other nuclear proteins. This basic scheme of STAT activation is illustrated in Figure 5 [26].

Within the nucleus, STAT dimers bind directly to consensus sites within promoter or enhancer regions of genes. Gamma activated sequences (GAS) or interferon sensitive response elements (ISRE) are primary examples for STAT1 and STAT2. Because many of these regions are roughly 20 base pairs apart, the STAT dimers often form tetramers through interactions between their N-termini [26]. Additionally, STAT dimers may regulate transcription without direct binding by interacting with other proteins in enhanceosomes through TAD

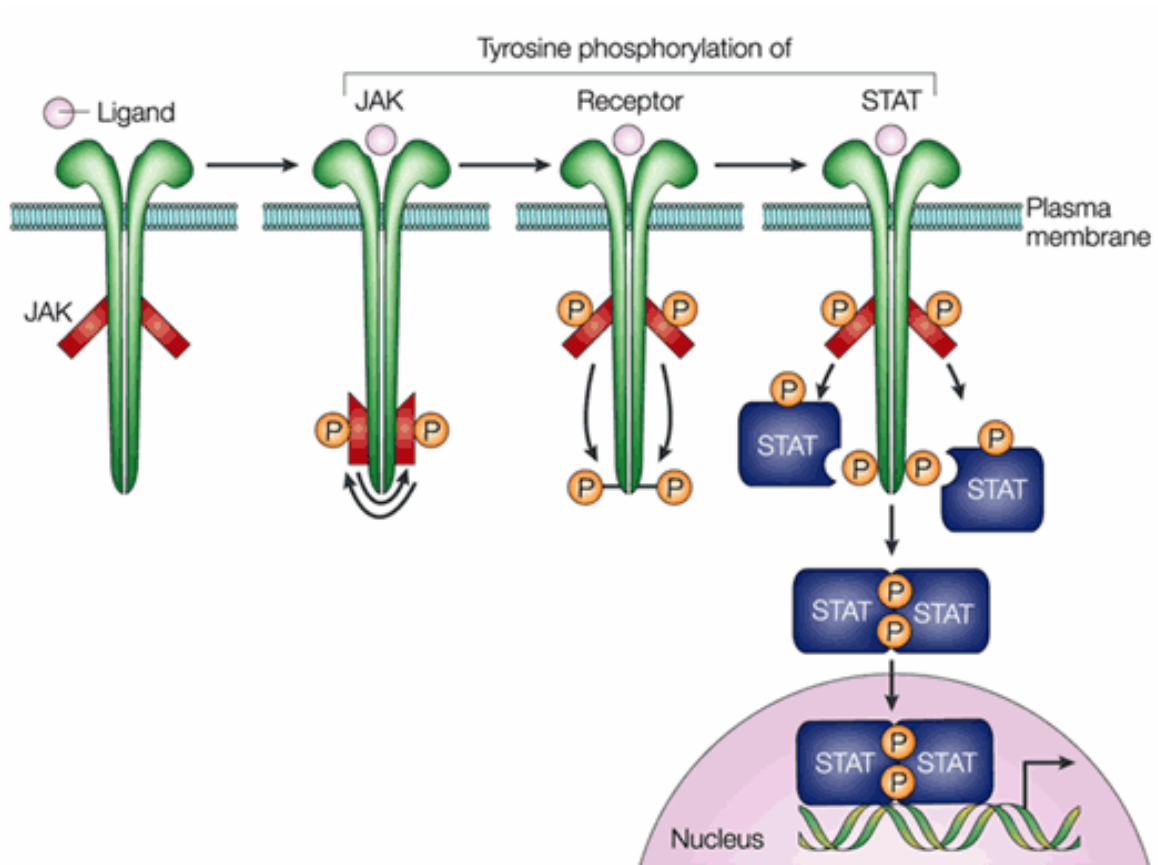


**Figure 5.** Schematic illustrating a general and simplified pathway of STAT activation [26].

interactions. In order to be exported from the nucleus, it is important for STAT proteins to become dephosphorylated by nuclear phosphatases [26]. The total activation-inactivation cycle time for a STAT protein is estimated to be approximately 20 minutes.

**2.4.1.1 Alternative methods of JAK/STAT activation** In contrast to the canonical pathway, in which STATs are tyrosine phosphorylated by JAKs, alternative methods of activation exist. For example, the receptors for many growth factors acting on the JAK/STAT pathway contain intrinsic tyrosine kinase activity, negating the requirement for JAK involvement [22]. It is also proposed that seven transmembrane domains can activate STATs after they bind peptide, presumably through associations with non-receptor tyrosine kinases [26]. Although not necessary for nuclear translocation, STATs are serine phosphorylated in their C-terminal domain in response to bacterial infection, which increases transcriptional potency. This also provides an opportunity for cross-talk between individual pathways, as MAP kinase is implicated in serine phosphorylation of STATs [77]. With regards to the status of unphosphorylated STAT proteins, very little is known. Recently, nonphosphorylated STATs were shown not to exist as monomers. For example, in human Hep3B cells, STAT3 associates as dimers or higher order statesome complexes, often associated with clathrin, implicating a role of endocytosis in STAT signaling [78]. Another group observed nonphosphorylated STAT dimers with two unique crystal structures. In one structure, the dimer is formed by interactions between coiled-coil (CC) and DNA binding domains (DBD) in an antiparallel manner. In the other, the STATs are parallel with their N-termini lodged between them. Mutations to the N-termini, DBD, and CC did not affect tyrosine phosphorylation, but increased resistance to dephosphorylation [79]. Additionally, in MCF-7 breast cancer lines and HeLa cervical cancer lines, nonphosphorylated and tyrosine mutated STAT3 were still capable of forming dimers. However, mutation of a

single lysine residue, which is acetylated, prevented the formation of STAT3 homodimers [80]. The associations of nonphosphorylated STATs are likely to be unique within distinct cell types and additional work is required to understand their importance.

**2.4.1.2 Negative regulators of JAK/STAT signaling** Like most physiologic processes, the JAK/STAT pathway is homeostatically regulated by inhibitory mechanisms. There are three major families of proteins that negatively affect STAT phosphorylation: protein tyrosine phosphatases (PTPs), suppressors of cytokine signaling (SOCS), and protein inhibitors of activated STATs (PIAS) [77]. Of these, only the SOCS family of proteins is inducible following STAT activation; the remainder are constitutively expressed [81]. PTPs are perhaps the simplest class of inhibitory molecules. Some members of this family (SHP1, SHP2, CD45, PTP1B) exert their effects by dephosphorylating JAKs or the phosphorylated docking site on the associated receptor. Additionally, some PTPs have the ability to dephosphorylate STATs on both tyrosine and serine residues within the cytoplasm (SHP2, PTP1B, TCPTP) and nucleus (TCPTP, SHP2) [76]. In a classical negative feedback loop, the SOCS family of proteins of which there are eight members (CIS and SOCS1-7) are upregulated in cells following cytokine stimulation [76]. Individual members of the family mediate inhibition, binding to phosphorylated JAKs to prevent their activity or to phosphorylated receptors to compete for STAT docking sites. Additionally, SOCS proteins can regulate ubiquitin-mediated proteosomal degradation of its targets as another mechanism of inhibition through interactions with ubiquitin ligases [81]. Because these proteins are inducible, they do not affect initiation or strength of STAT activation, only the kinetics of signal termination. There is new evidence to suggest that SOCS family members display cell-specific selectivity in their regulatory actions [82]. Members of the family of negative regulators, PIAS, consisting of four members (PIAS1, PIAS3, PIASX, and PIASY), bind to

activated STAT dimers and prevent them from binding DNA [77]. However, PIAS members have been shown to inhibit STAT activity without affecting their DNA binding capacity, possibly through interaction with histone deacetylases (HDACs) [76]. PIAS also sumolyates STATs, which inhibits their activity in a way that is not fully understood [81]. In normal cells, these three main classes of negative regulators manage to regulate the JAK/STAT pathway.

**2.4.1.3 Gene ablation studies of JAK/STAT family members** Except for STAT3 which is embryonic lethal, most STAT proteins are not necessary for survival or development. Their individual roles have been studied through gene deletions in mice. The slower growth of cells induced by interferon is fully dependent on transcriptionally active STAT1. This molecule mainly promotes apoptosis and growth arrest. Deletion in mice increases susceptibility to viral infection and tumor formation [21]. To date, STAT2 has only been implicated in type I interferon signaling, promoting antiviral responses [25]. STAT3 is associated with dual and opposing roles. In many instances, STAT3 activation induces cell proliferation and anti-apoptosis, but in other cell types and contexts, it plays a role in promoting apoptosis and differentiation [21]. STAT3's role in cancer has been explored heavily because its persistent activation via a mutant protein, where the phosphotyrosine/SH2 interactions are substituted for disulfide bonds, is sufficient for cellular transformation [25]. In other knockout studies, the absence of STAT4 and STAT6 leads to defects in response to cytokines that regulate polarization of naïve T cells into Th1 and Th2 groups, respectively, thus resulting in impaired cell-mediated and humoral immunity [83]. STAT5a and STAT5b, share 96% homology, but perform many non-overlapping functions. For instance, mammary gland development is impaired in STAT5a

deficient mice, but not STAT5b. T cells in STAT5a null mice exhibit decreased proliferative capacity and IL-2R $\alpha$  expression, while STAT5b deficient T cells have a more marked abrogation of proliferation and lower NK cell counts with diminished cytolytic activity [25].

In summary, the STAT family of transcription factors is responsible for controlling a host of important cellular functions, not limited to immunity alone. In all, over 40 polypeptides are known to activate the JAK/STAT pathway [21], which highlights its critical role in controlling many cellular functions. Because this family of proteins is so important in regulating cell proliferation, apoptosis, and immunity, it should not be surprising that its dysregulation is associated with many types of cancer. The involvement of disordered STAT signaling in several important diseases emphasizes the urgency to understand this pathway in normality and clinical disorders.

#### **2.4.2 The MAP kinase pathway**

The mitogen-activated protein (MAP) kinase pathway is responsible for controlling cellular reactions to mitogenic and stress stimuli. Within the MAP kinase pathway are four main modules that have specificity for particular stimuli; these are extracellular signal-related kinases (ERK1/2), Jun amino-terminal kinases (JNK1/2/3), p38 proteins (p38 $\alpha/\beta/\gamma/\delta$ ), and ERK5. Essentially, each module is regulated by three sequential protein phosphorylations, whereby an activated MAP kinase kinase kinase (MAPKKK) phosphorylates a MAP kinase kinase (MAPKK), which in turn phosphorylates a MAP kinase (MAPK) [23]. The distal activated MAPK phosphorylates additional specific effector kinases called MAPK activated

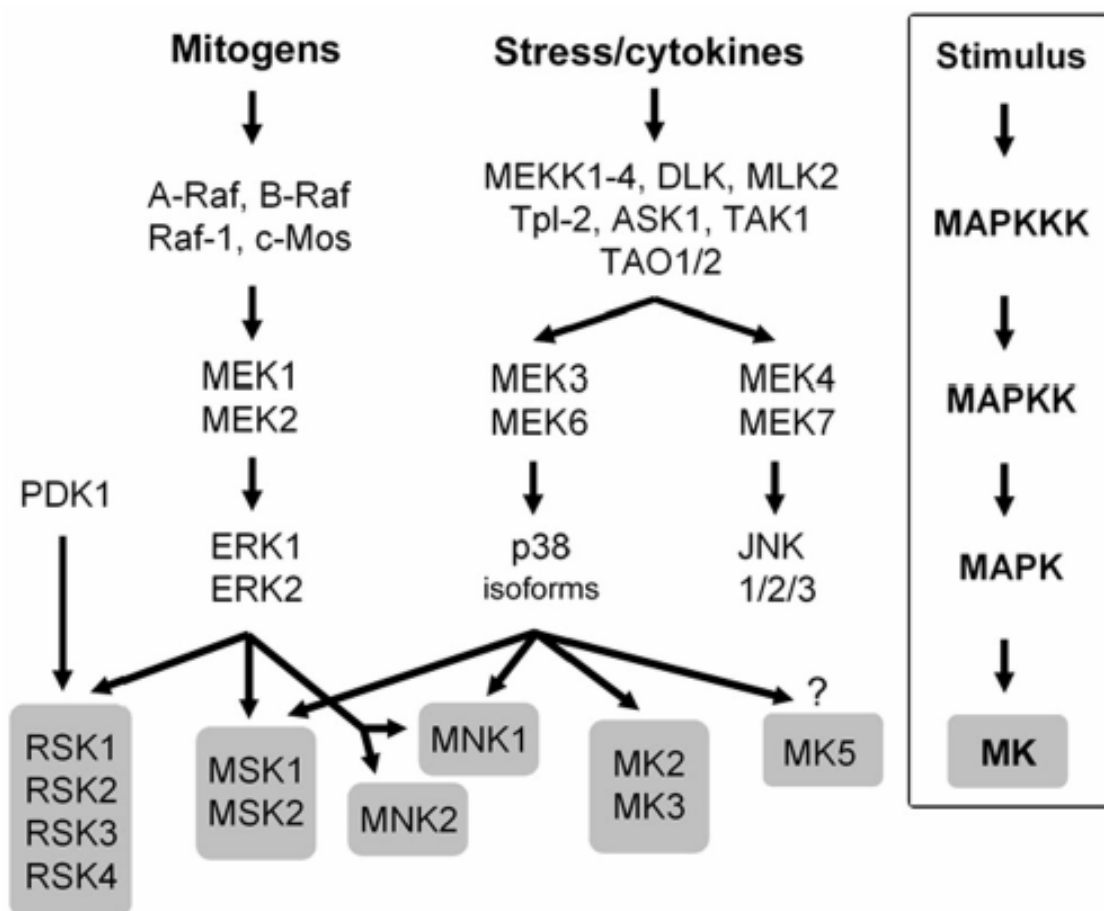


**Figure 6.** A schematic illustrating major modules of the MAP kinase signaling pathway [84].



protein kinases (MKs) or translocates to the nucleus to regulate transcription directly. A basic schematic for these signaling cascades is illustrated in Figure 6 [84]. Built into each of these modules is increasing complexity, as scaffolding proteins are believed to participate in signaling by spatially localizing proteins or even directly activating them [85]. Overall, the MAP kinase signaling pathway is an extremely complex cascade of phosphorylated proteins that arms cells with the ability to respond to environmental stresses and growth cues, making it critical for cell proliferation and survival.

**2.4.2.1 Mechanisms of p38 activation** Activation of p38 proteins is a major pathway by which cells respond to proinflammatory cytokines and environmental stress. First identified in 1994 as a MAPK targeted by endotoxin and hyperosmolarity, p38 exists as four different isoforms:  $\alpha$ ,  $\beta$ ,  $\gamma$ , and  $\delta$ . Of these p38 $\alpha$  is the most extensively studied. In mice, p38 $\alpha$  and  $\beta$  are expressed ubiquitously, while p38 $\gamma$  is mainly associated with muscle and p38 $\delta$  is predominantly localized to kidney and lung [86]. After cells are stimulated by proinflammatory cytokines or stress, such as heat/osmotic shock, oxidation, or UV irradiation, members of the Rho family of small GTPases, including cdc42 and Rac are activated [87]. Because many MAPKKs contain a potential GTPase-binding motif (CRIB), these may lead to their direct activation. Several MAPKKs, such as MEKKs 1-4, MLK2 and 3, DLK, ASK1, Tpl2, and Tak1, have been implicated in p38 signaling [84], which probably depend on the particular stimulus and cell type at hand. Further downstream in the p38 module, MAPKKs activate MAPK via phosphorylations. Two MAPKKs with high specificity for p38 are MEK3 and MEK6; MEK6 activating all p38 isoforms, while MEK3 is selective for  $\alpha$  and  $\beta$ . Another MAPKK, MEK4, is capable of phosphorylating p38, albeit less selectively, as it activates JNK as well [84]. Through these interactions with upstream kinases, p38 is phosphorylated on conserved tyrosine and

threonine residues within its kinase subdomain VIII. Once p38 is activated, it is capable of phosphorylating transcription factor substrates including ATF2, Elk-1, CHOP, MEF2C, and SAP-1 or downstream effector kinases, such as Mnk1, Mnk2, PRAK, and MSK1 [88]. There is cross-talk between p38 and another major signaling pathway, NFκB. As an activator of p38, sodium salicylate, inhibits NFκB [86]. Through these complex interactions with an array of transcription factors, kinases and other signaling pathways, p38 centrally controls gene expression in response to cell stress and inflammatory environments.

**2.4.2.2 Mechanisms of ERK1/2 activation** Another module of the MAPK signaling pathway, ERK1/2, is more responsive to mitogens, rather than stress and inflammation. In the ERK signaling pathway, mitogens commonly activate a small GTPase known as Ras via receptor tyrosine kinases or G-protein-coupled receptors. Membrane-associated Ras is activated by recruitment of SOS, a guanine nucleotide exchange factor, stimulating Ras to exchange GDP for GTP [84]. In turn, Ras activates Raf (A-Raf, B-Raf, and Raf-1), a serine-threonine kinase, which phosphorylates the MAPKKs, MEK1 and MEK2. These kinases are the immediate upstream activators of ERK1 and ERK2, which share 83% homology in amino acid sequence [89]. Once activated by dual phosphorylations on conserved tyrosine and threonine residues in their activation loop, ERK1 and 2 translocate to the nucleus, presumably as dimers, to activate transcription factors responsible for controlling gene expression. Additionally, activated ERK1/2 phosphorylate numerous membrane proteins (CD120a, Syk), nuclear substrates (Elk-1, c-fos, c-myc), cytoskeletal proteins (neurofilaments, paxillin), and other kinases [84]. Similarly to p38, ERK is also regulated by interactions with docking and scaffold proteins, which serve to control its cellular localization [90]. The ERK pathway is able to modulate the effects of growth factors and other mitogens through these coordinate and intricate interactions.

**2.4.2.3 Negative regulators of MAP kinase signaling** A set of proteins exist to inhibit activation of MAP kinase signaling. Numerous phosphatases negatively regulate this pathway, including protein phosphatase 2C (PP2C), protein phosphatase 2A (PP2A), protein tyrosine phosphatases (PTPs), and dual specificity phosphatases (DSPs), which dephosphorylate both tyrosine and threonine residues [91]. Dephosphorylation of either the tyrosine or threonine residue within the MAP kinase activation loop is sufficient for enzymatic inactivation [92]. Protein phosphatases 2C and 2A are two of four major serine/threonine phosphatases that exist in eukaryotes. PP2A has been implicated in ERK inactivation through its ability to dephosphorylate threonine residues [92]. PP2C plays a role in dephosphorylating some of the upstream kinases of p38, MKK4 and MKK6, both *in vitro* and *in vivo* [87]. Additionally, three PTP gene family members, PTP-SL, STEP, and HePTP, are thought to play a role in inactivating ERK [92]. A subclass of PTPs that are referred to as DSPs are inducible depending on the specific stimulus and cell type upon which it acts, designating this as a classic negative feedback mechanism. Evidence suggests that DSPs play a major role in regulating the activation of the MAP kinase signaling pathway, with each DSP displaying specificity for individual kinases. For example, MAP kinase phosphatase 3 (MKP3), a dual specificity phosphatase (DSP), specifically dephosphorylates ERK, but not JNK or p38. On the other hand, MKP5 and M3/6 dephosphorylate JNK and p38, but not ERK. Some DSPs, such as MKP1 and MKP4, dephosphorylate all three major kinases [91]. By no means is this a complete picture of MAPK negative regulation, but it provides an overview of some of the major families of phosphatases involved. By controlling the temporal patterns of MAPK activation, these proteins shape the effects of various stimuli and maintain the transient nature of this pathway in normal cells.

**2.4.2.4 Roles of MAP kinase signaling in cellular function** Although the effects of MAP kinase signaling are both cell type and stimulus dependent, several generalizations have been made concerning its role in cell function. Induced by proinflammatory cytokines, like IL-1 and TNF $\alpha$ , and cell stress, p38 activation is believed to modulate wide-ranging events including cytokine production, platelet aggregation, hepatocyte growth, cytoskeletal organization, apoptosis induction, and cell differentiation [93]. p38 plays an important role in regulating immune function in particular. In mice, p38 activation blocks the differentiation of immature thymocytes, leading to immunodeficient mice. Through studies with p38 inhibitors, p38 activation was also found to be necessary for Th1 polarization of T cells, as well as IFN $\gamma$  production from these cells [88]. On the other hand, p38 activation was not necessary for Th2 polarization, whereas ERK activation was, mainly through regulation of IL-4 receptor function. It should be noted, however, that p38 may mediate opposing roles depending on the cell type, context, and p38 isoform activated [93]. Unlike p38, the ERK module is predominantly activated by growth factors and phorbol esters. In response to these stimuli, ERK primarily serves to influence cell proliferation, differentiation, and survival [90]. ERK is an especially important protein in controlling cell growth, as its persistent activation due to mutations in Ras, an upstream activator, is often associated with increased proliferation of tumor cells [85]. In general, ERK activation is tied to cell survival and proliferation, while p38 activation is associated with pathways that ultimately result in apoptosis [23]. Because dysregulation of ERK and p38 activation, just as JAK/STAT proteins, leads to impairments in cell growth, it is crucial to study their involvement in disorders such as cancer.

## **2.5 ABERRANT PBMC SIGNALING IN THE SETTING OF CANCER**

Blood is routinely drawn in a clinical setting through minimally invasive means, and circulating white blood cells are akin to migrating biosensors, serving as suitable targets for analysis. As their normal function is to act as sentinels and quickly respond to immune challenges and tissue damage, we chose to focus our analysis on signaling within PBMC. Many studies, which will be briefly touched upon, suggest dysfunctional JAK/STAT and MAP kinase signaling within cancerous PBMC. However, some studies also suggest that the presence of tumor affects the signaling and function of normal PBMC. Since the JAK/STAT and MAP kinase pathways are extremely responsive to stress, inflammation, and cytokines, it is not surprising that an altered microenvironment caused by abnormal cytokine secretion from tumors, their surrounding stroma, or infiltrating immune effectors would induce abnormal signaling within PBMC circulating through these regions.

### **2.5.1 Dysfunctional JAK/STAT and MAP kinase signaling in leukemic cells**

Inappropriate activation of JAK/STAT and MAP kinase signaling pathways is a common feature of many leukemias. Overactivation of these pathways is associated with cellular transformation by oncoproteins that are results of genetic mutations, such as chromosomal translocations. In other instances, persistent activation is attributed to autocrine and paracrine signaling via abnormally secreted cytokines. These dysregulated pathways are believed to be causative agents in cancer progression through their effects on target genes responsible for cell proliferation and apoptosis.

An overview of signaling within various types of leukemia highlights the widespread dysregulation of JAK/STAT in the setting of cancer. One type of leukemia, known as chronic

myelogenous leukemia (CML), results from chromosomal translocation, producing a constitutively active tyrosine kinase called BCR/ABL. This chimeric oncogene possesses the ability to induce constitutive activation of the Ras-ERK2 and JAK/STAT pathways. In particular, abnormal phosphorylation of STAT5 and to a lesser extent STAT1 and STAT3 has been observed in human CML cell lines and primary CML cells [30]. In these cells, JAKs were not activated, suggesting BCR/ABL induces STAT phosphorylation directly. Another fusion protein called TEL-PDGFR, is responsible for causing a subgroup of chronic myelomonocytic leukemia (CMML). In several CMML cell lines, TEL-PDGFR is capable of directly inducing constitutive activation of STAT1 and STAT5 without JAK involvement [94]. In primary cells of acute myelogenous leukemia (AML), which is characterized by maturation arrest followed by accumulation of undifferentiated myeloid cells in the bone marrow and peripheral blood, activated STAT1, 3, and 5 has been reported [29, 95]. An activating mutation in FLT3 tyrosine kinase is frequently associated with STAT phosphorylation in many AML patients. Additionally, primary T and B cells from acute lymphocytic leukemia (ALL) patients exhibit highly activated STAT5 and STAT1 to a lesser degree [94]. Another type of leukemia, called adult T cell leukemia (ATL), which is commonly induced by human T lymphotropic virus I (HTLVI), is reported to contain constitutively phosphorylated STAT3 and STAT5 [29].

In addition to the JAK/STAT pathway, dysregulation of the MAP kinase pathway is frequent in leukemic cells. In fact, mutations leading to activated Ras occur in 30% of all cancers, including AML, and juvenile myelomonocytic leukemia [96]. Presumably, these mutations are responsible for constitutive activation of ERK1/2 and its upstream effectors MEK1/2 in primary human AML cells [97]. However, these Ras mutations do not always correlate with abnormal phosphorylation, suggesting that other mechanisms, such as paracrine

and autocrine factors, play a role. Independent of Ras, hairy cell leukemic cells, which are intrinsically activated, mature clonal B cells, contain phosphorylated p38, JNK, and ERK. Though p38 and JNK are activated, they appear to play a role in inducing apoptosis, while ERK counteracts their effects by promoting hairy cell survival [31]. Additionally, ERK and p38, but not JNK, are constitutively phosphorylated in many other primary B cell neoplasms [98]. Likewise, inappropriate activation of the ERK pathway is associated with NK cell leukemia [97]. In summary, within hematological malignancies themselves, aberrant JAK/STAT and MAP kinase signaling is commonly observed, either as a result of genetic mutations or altered environments induced by malignant cells.

### **2.5.2 Altered cytokine expression in tumor microenvironments**

Within the local environment of a tumor, there exists a complex interplay between tumor cells, activated stroma, and infiltrating leukocytes that contribute to a rich milieu of inflammatory cytokines, growth factors, chemokines, and other soluble factors. In addition to these actively secreted factors, tumor cell death via necrosis further contributes to the altered environment by releasing endogenous danger signals. Beyond the immediate tumor microenvironment, some of these factors have been detected at abnormal levels within the sera of individuals bearing tumors. Because the JAK/STAT and MAP kinase pathways are exceptionally sensitive to cytokines, growth factors, and stress/inflammation, it is likely that the presence of tumor and its associated alterations in protein expression will affect these signaling pathways within normal, circulating leukocytes.

Alterations in cytokine expression are exhibited in many types of cancer; either as a result of tumor cell production or surrounding/infiltrating cells, including stromal cells and

inflammatory leukocytes. For instance, patients with advanced stages of breast cancer often have higher than normal serum levels of  $\text{TNF}\alpha$  and  $\text{IL-1}\beta$  [99]. Presumably, these cytokines are often secreted by tumor-associated macrophages (TAMs). Additionally, VEGF expression is markedly increased in breast cancer cells and their reactive stromal cells [100]. In patients with head and neck squamous cell carcinoma (HNSCC), IL-6, IL-8, and VEGF concentrations in the serum of patients are higher when compared with controls [101]. Serum levels of IL-6 are also elevated in patients with colorectal [36], cervical [41], epithelial ovarian [43], and prostate cancer [37], as well as in those with metastatic renal cell [42] and esophageal squamous cell carcinoma [102] and Hodgkin's Disease [103]. In several types of cancer, colorectal [36], metastatic melanoma [38], endometrial [40], and hepatocellular carcinoma [39], IL-8 serum concentrations are also elevated. Another cytokine, IL-7, is elevated in the serum of Hodgkin's Disease patients and correlates with advanced stage [103]. In other instances, endogenous danger signals, such as HMGB1, uric acid, ATP, adenosine, S100 molecules, and heat shock proteins (HSPs), are elevated in cancer patients. These factors are often overexpressed in tumors and are released when they undergo necrotic cell death [104]. Most of these factors, exhibiting unbalanced expression within the setting of cancer, are capable of activating the JAK/STAT and MAP kinase pathways. Therefore, it is likely that analyzing phosphorylation states of proteins within these pathways will become a useful tool in the immunodiagnosis of cancer or in the monitoring of its treatment.



### 2.5.3 Signaling defects within “normal” PBMC in the setting of cancer

Although very few groups have studied the JAK/STAT and MAP kinase signaling pathways within “normal” PBMC in individuals with cancer, there is evidence to suggest that these pathways and others are abnormal. These studies strengthen the hypothesis that the effects of factors released by tumors, their supporting cells, and activated leukocytes extend beyond the tumor microenvironment. One of the most studied defects in circulating PBMC isolated from cancer patients is the loss or reduction of T-cell receptor (TCR) zeta ( $\zeta$ )-chain, which is associated with impaired immune function. The  $\zeta$ -chain is a subunit of the TCR in T cells and CD16 in NK cells, primarily responsible for signal transduction [105]. Compared to normal controls,  $\zeta$ -chain is significantly decreased in CD4 and CD8 T cells, and CD16 NK cells from many HNSCC patients, with the degree of reduction correlating with cancer aggressiveness [106]. Additionally, decreased expression of  $\zeta$ -chain was found in tumor-infiltrating lymphocytes (TIL) and peripheral blood lymphocytes (PBL) from many oral carcinoma patients [107]. Likewise, decreases in  $\zeta$ -chain were observed in peripheral blood T cells from patients with advanced metastatic melanoma [108], advanced gastric cancer [109], breast cancer [110], colorectal cancer, renal cell carcinoma, prostate cancer, hepatic cancer, and Hodgkin’s lymphoma [111]. Similarly, decreases in p56<sup>lck</sup>, a tyrosine kinase associated with CD4, CD8, and IL-2R $\beta$ , are observed in PBMC from patients with various types of cancer [111]. It should be noted, however, that most of these defects in p56<sup>lck</sup> and  $\zeta$ -chain were only detected in patients with very advanced cancer and the mechanisms by which these changes occur are not well understood. By observing high serum levels of 8-isoprostrane, a product of lipid oxidation and marker for oxidative stress, and large numbers of activated granulocytes in the peripheral blood of cancer patients, it is believed that H<sub>2</sub>O<sub>2</sub> production from these cells may be partly responsible

for these effects [112]. Because IL-8 is often elevated in the serum of cancer patients, as previously described, it is possible that this is responsible for granulocyte activation. Though few studies have examined signaling downstream of the  $\zeta$ -chain in cancer patients, it is likely that the MAP kinase pathway will be affected, as it is involved in TCR signaling [113].

Other studies suggest abnormal activation of another major signaling pathway, NF $\kappa$ B, within PBMC from cancer patients. T cells from many renal cell carcinoma patients had abnormal NF $\kappa$ B activation following anti-CD3/ionomycin treatment, characterized by a failure of RelA, p65, to translocate from the cytoplasm to the nucleus [114]. This study also demonstrated that impaired NF $\kappa$ B activation did not correlate with decreased  $\zeta$ -chain expression. In another study, peripheral blood T lymphocytes from breast cancer patients exhibited impaired ability to translocate RelA, p65, following anti-CD3 and IL-2 stimulation despite normal cytoplasmic levels of p65 [110]. T lymphocytes from some of these patients displayed increases in MKP-1, a MAP kinase phosphatase, suggesting impairments in MAP kinase signaling as well. It is also noteworthy that NF $\kappa$ B impairment is induced in healthy T cells by incubating them with supernatants from renal tumor explants [114].

With regard to dysfunctional JAK/STAT signaling within PBMC acquired from cancer patients, very few studies have been performed. In an experiment, where T and B cells were purified from mice with mammary adenocarcinoma, marked decreases in STAT5a and STAT5b, and to a lesser extent, their mRNA, were observed [115]. These lymphocytes were also impaired in their ability to generate antigen-specific cellular and humoral immune responses. In another study, STAT1 phosphorylation was evaluated in PBMC from melanoma patients and healthy donors following in-vitro IFN $\alpha$  treatment. Compared to melanoma patients, healthy donors had higher basal levels of STAT1 phosphorylation in total PBMC, T cells, and NK cells. However,

total STAT1 levels between the cancer patients and volunteers were equivalent. Additionally, there were no differences in pSTAT1 following *in vitro* stimulation with IFN $\alpha$  [116]. These studies suggest that signaling pathways within “normal” PBMC isolated from cancer patients are aberrant, perhaps as a consequence of the altered cytokine milieu. As the previous example indicates, it is possible that factors chronically released in the setting of cancer may lead to the upregulation of negative regulators of signaling. Therefore, analyzing the activation states of signaling pathways, including the JAK/STAT and MAP kinase pathways, may be valuable tools for diagnosing the presence of cancer or other inflammatory conditions, as well as monitoring the progress of treatment regimens.

### **3.0 SPECIFIC AIMS OF THESIS**

Although the enumeration and phenotyping of peripheral blood cells has proven successful for the diagnosis and evaluation of many clinical conditions, its value is limited. Combining measurements of cell function together with immunophenotyping should provide researchers and clinicians with greater information, enabling them to better diagnose and evaluate patients. In contrast to common measurements of function, which require prolonged culturing conditions and lengthy protocols that can introduce artifacts; analysis of activated signaling pathways via protein phosphorylation is a rapid technique. By analyzing peripheral blood mononuclear cells (PBMC), which are readily obtainable and act as cellular biosensors through their role in immune surveillance, scientists and clinicians could potentially deduce information about the pathological environs that they encounter while circulating through the body. Use of a platform to analyze PBMC on a cell-by-cell basis, such as flow cytometry, rather than conventional bulk analysis methods, greatly enhances the data obtained, as PBMC are comprised of a variety of cellular subsets, each with the ability to respond differently to its environment. Because tumors and other inflammatory conditions alter the milieu of cytokines and other factors in the serum, it is likely that PBMC will display abnormal signaling or be defective in their ability to respond to stimuli. In this regard, a flow cytometric assay to detect phosphorylation of signal transduction pathways within PBMC should be a valuable tool for the diagnosis and/or monitoring of patients with cancer and other clinical states.

### 3.1 SPECIFIC AIM 1

Our first specific aim is to characterize the phosphorylation of STAT1, STAT3, STAT5b, STAT6, p38 MAPK, and ERK1/2 in total PBMC via flow cytometry following in-vitro cytokine treatment in a time and dose-dependent manner. Taking advantage of their differences in size and granularity, responses of lymphocytes and monocytes will be analyzed separately, gating on each population based on their forward and side-scatter properties. Additionally, results will be compared to those obtained by Western blotting. These experiments will be used to determine conditions that induce maximal phosphorylation within PBMC.

**Hypothesis 1a:** Phosphorylation of these signaling molecules will increase as the concentration of stimulus increases and phosphorylation will occur rapidly followed by a reduction over time.

**Hypothesis 1b:** Differences will be detectable between lymphocytes and monocytes regarding phosphorylation of a given protein with a given stimulus.

**Hypothesis 1c:** Protein phosphorylation data obtained by flow cytometry will correlate with results obtained by Western blot.

### 3.2 SPECIFIC AIM 2

Specific aim 2 is to develop flow cytometric methodology enabling the simultaneous detection of cell surface proteins used to immunophenotype PBMC subsets and intracellular phosphorylated proteins: STAT1, STAT3, STAT5b, STAT6, p38 MAPK and ERK1/2. A panel of permeabilizing agents with varying concentrations will be used to determine a suitable condition for dual staining. These experiments will use stimulation conditions obtained in aim 1 to characterize protein phosphorylation pathways within major subsets of PBMC: CD4<sup>+</sup> and CD8<sup>+</sup> T cells, CD19<sup>+</sup> B cells, CD56<sup>+</sup> NK cells, and CD14<sup>+</sup> monocytes. Additionally, experiments will be performed to assess variability when using this assay to analyze signaling within multiple draws from the same individual and in several different individuals.

**Hypothesis 2a:** Using a milder permeabilization/denaturing agent, such as diluted alcohols, will preserve cell surface epitopes while retaining the ability to stain intracellular phospho-epitopes.

**Hypothesis 2b:** Because NK cells and monocytes are associated more with rapid, innate immune responses, these cells will become phosphorylated to a greater degree than T and B lymphocytes following cytokine stimulation.

**Hypothesis 2c:** Variability in phosphorylation following stimulation within a single, normal donor or between multiple, normal donors will be minimal.

## **4.0 FLOW CYTOMETRIC CHARACTERIZATION OF PROTEIN PHOSPHORYLATION PATHWAYS IN HUMAN PBMC**

### **4.1 ABSTRACT**

Current strategies designed to assess cells in the peripheral blood are limited to evaluation of phenotype or delayed measurement [ $>6$ hours] of function, usually quantifying cytokine production, cytolytic activity, or response to antigens. We reasoned that measurable abnormalities in signaling pathways could reflect pathological environs that cells experience in the setting of inflammatory states/cancer and could be represented in the peripheral blood. Two major pathways regulating the immune response are the JAK/STAT and MAPK/ERK pathways. These pathways are initiated by ligand-receptor binding, and are rapidly propagated by subsequent protein phosphorylation cascades. We evaluated the brief application of cytokines *in-vitro* to interrogate the early phosphorylation events of these signaling pathways in normal peripheral blood mononuclear cells (PBMC). Individual cytokine doses and time intervals of treatment were assessed to identify conditions useful in a clinical laboratory and as an initial goal, to induce maximal phosphorylation. Surprisingly, all of the STAT proteins assessed and ERK1/2 are maximally phosphorylated within 15 minutes in human PBMC simply following addition of cytokines without preactivation of the cells. At two hours, cells typically return to their basal phosphorylation states. For most of the cytokines tested, increased phosphorylation

directly correlated with increased concentrations of the individual cytokines. These strategies will enable robust development of simple blood analyses to identify normal levels as well as impairments in STAT and MAPK/ERK signaling pathways associated with various human disease states including acute and chronic inflammatory conditions throughout clinical immunology.

## **4.2 INTRODUCTION**

The development of novel strategies for measurement of disease, so-called biomarkers and surrogates, has most recently focused primarily on serum proteomics and microarray assays [117]. Although leukocytes are readily separated and analyzed in the peripheral blood, most assessments have been limited to simple phenotyping and more extensive evaluations have been performed solely in research or specialty laboratories given the requirements for prolonged periods of incubation, sterile environments, and sophisticated measurement tools. Simultaneous evaluation of phenotype and function of peripheral blood lymphocytes has provided important insights for clinicians and scientists in the areas of infectious disease [1-4], autoimmunity [5, 6], and cancer [7-11]. Pure immunophenotyping, however, is of limited value in the assessment of clinical states. Most functional assays, which could be utilized in conjunction with phenotyping, are tedious or require extensive culturing periods. One simple, yet information-dense, approach is to examine signaling pathways within individual peripheral blood cells following cytokine or mitogenic stimulation. Abnormalities in signaling pathways can provide clues to disorders



related to pathological environments that cells experience while emigrating from the bone marrow and recirculating from tissues and lymph nodes or emergent from altered serum cytokines [118].

Traditionally, cell signaling analysis has been performed using Western blots on large populations of homogeneous cells. The data obtained is an average of all of the cells analyzed. If performed on a complex mixture of cells, such as peripheral blood mononuclear cells (PBMC), such a technique would not yield signaling information of individual cellular subsets within the total population. The advent of flow cytometry allowed us to perform cell signaling analysis on individual cells, thus resolving signaling events within previously obscure subsets of cells [119, 120]. Additionally, signaling analysis using flow cytometric methods correlates very well with other established techniques [69, 116].

Most signaling pathways are initiated by ligand-receptor binding and are propagated by subsequent protein phosphorylation cascades. These phosphorylation events occur very rapidly following receptor engagement. With the introduction of antibodies having specificity for phosphorylated epitopes of proteins and intracellular staining techniques, very proximal signaling events can be captured that were previously inaccessible. One important pathway in the regulation of immune responses is the JAK/STAT pathway. This pathway is important in host defense, growth control, and apoptosis [21, 26, 121]. Within cancer cells, signaling through many STAT proteins is dysfunctional [33, 35, 122, 123]. Another major pathway driven by protein phosphorylation is the MAPK/ERK pathway. It regulates cell cycle progression, apoptosis, cytokine production, RNA splicing, and cell differentiation in response to stress, inflammation, and other stimuli [24, 86, 87]. The MAPK pathway is activated within many cancers, promoting it as either a cause or consequence of tumor progression [32, 34, 124, 125].

We evaluated the brief application of cytokines and mitogens *in-vitro* to interrogate the signaling pathways of normal PBMC and analyzed the early phosphorylation events of important, available signaling proteins within the JAK/STAT, and MAPK/ERK pathways: STAT1, STAT3, STAT4, STAT5, STAT6, ERK1/2, and p38 MAPK. The individual cytokine doses and time intervals of treatment were assessed to identify conditions for maximal phosphorylation. Additionally, due to the differences in light scatter between monocytes and lymphocytes, we were able to evaluate their responses separately without the use of additional reagents. It should be noted that the phosphorylation events assessed in these studies were obtained on two different cytometers. Where appropriate, we have indicated which cytometer was used to obtain the data. We provide qualitative data concerning dose responses and kinetics of phosphorylation for many proteins within the JAK/STAT and p38 MAPK families, as well as differential responses to stimuli in distinct PBMC populations. Although the results are not quantitatively comparable between cytometers, the observation that most of the proteins qualitatively follow robust and similar kinetics of phosphorylation serves to verify the assay's reproducibility. Furthermore, our data indicate that this assay is extremely reproducible within a single experiment. The techniques developed offer a rapid approach for evaluating protein phosphorylation within normal PBMC and will have broad applicability in assessing patients with cancer [117] and other inflammatory states [126-128].

## 4.3 MATERIALS AND METHODS

### 4.3.1 Reagents

PBMC were isolated from normal, volunteer donor whole blood at the University of Pittsburgh using Ficoll-Paque Plus (Amersham Biosciences, Uppsala, Sweden) in accordance with an approved IRB protocol (IRB #960279, UPCI #86-22.) ACK buffer (0.15M NH<sub>4</sub>Cl, 10mM KHCO<sub>3</sub>, 0.1mM NaEDTA; pH 7.2-7.4) was used to lyse remaining red blood cells (RBC). PBMC were stored in freeze medium (90% FBS, 10% DMSO) in liquid nitrogen. IFN $\gamma$ , IL-2, IL-3, IL-6, IL-10 (R&D systems, Minneapolis, Minnesota), IFN $\alpha$ A, IL-4 (Biosource, Camarillo, California), IL-7 (Biodesign International, Saco, Maine), phorbol 12-myristate 13-acetate (PMA) (Sigma, Saint Louis, Missouri) and IL-13 (IDM, Paris, France) were used to stimulate cell signaling pathways. IMDM (Mediatech, Herndon, Virginia) was the medium used during cytokine treatment. 2% paraformaldehyde (Fisher Scientific, Pittsburgh, Pennsylvania) was prepared in Dulbecco's PBS (Mediatech, Herndon, Virginia). 90% methanol (Fisher Scientific, Pittsburgh, Pennsylvania) in PBS at -20°C was used to permeabilize the PBMC. Primary antibodies: pSTAT1(Y701):PE, pSTAT3(Y705): PE, pSTAT5(Y694):PE, pSTAT5(Y694), pSTAT6(Y641):Alexa488, pSTAT6(Y641):A647, pERK1/2(T202/Y204):PE, p-p38 MAPK(T180/Y182):PE (Becton Dickinson, Franklin Lakes, New Jersey) were used to label phosphorylated proteins. Rabbit anti-STAT5 used to label total protein for Western blotting was obtained from (Santa Cruz Biotechnology, Santa Cruz, CA.) The PBMC were analyzed on a FACScan flow cytometer or FACSArray (Becton Dickinson) in FACS buffer (PBS, 10% FBS, 0.1% azide, 0.1% glucose). Sphero rainbow fluorescent particles (Becton Dickinson) were used to calibrate the flow cytometer before analysis where indicated. CellQuest software (Becton

Dickinson) was used during acquisition of the samples on the FACScan and FACSDiva software (Becton Dickinson) was used for acquisition on the FACSArray. Off-line analysis was performed using FACSDiva software.

#### **4.3.2 Isolation of PBMC**

10mL of Ficoll-Paque Plus was pipetted into the bottom of a centrifuge tube containing 20 mL of whole blood and 20 mL of PBS to set up a density gradient. The blood was spun at 400Xg for 30 minutes. PBMC were pipetted off into a new centrifuge tube. The cells were spun into a pellet at 400Xg for 10 minutes. 5 mL of ACK buffer was added to the cells for 15 minutes at RT to lyse remaining RBC. The cells were pelleted and resuspended in IMDM. Cells were counted, spun, and resuspended in freeze medium at a concentration of  $10^7$  cells/mL.  $10^7$  PBMC were placed into individual cryogenic vials (Corning, Corning, New York). The PBMC were kept at -80°C for one day and were then transferred to a liquid nitrogen freezer until needed.

#### **4.3.3 Preparation of PBMC for flow cytometry**

PBMC were removed from liquid nitrogen and were thawed in a 37°C water bath. Freeze medium was removed and the cells were resuspended in IMDM.  $5 \times 10^5$  PBMC in 50µl of media were pipetted into separate centrifuge tubes for FACScan analysis or wells of a 96-well polypropylene plate for FACSArray analysis. For dose response experiments, cells were treated with increasing doses of various cytokines. The PBMC were left to incubate with the cytokines at 37°C for 15 minutes. For time course experiments, the PBMC were treated with the dose of cytokine found to cause maximal phosphorylation in the dose response experiments. The treatment was left at 37°C for 5, 10, 15, 30, 60 and 120 minutes. At the end of the treatment, the

PBMC were spun and the supernatant was discarded. 2 % paraformaldehyde was added to achieve a final concentration of 1% and was left at RT for 10 minutes to fix the PBMC. The fixative was removed by centrifugation. PBS was used to wash out residual fixative. 90% methanol was added to permeabilize the cells at -20°C for 10 minutes. PBS was used again to wash out residual methanol. The cells were blocked with isotype IgG at 10 µg/ml in FACS buffer for 15 minutes at RT. After centrifugation, the cells were resuspended in 50 µL of FACS buffer. For experiments using fluorophore-conjugated primary antibodies, 7 µL of antibody was added to 50 µL of PBMC and was left in the dark at RT for 30 minutes. After incubation with antibody, cells were washed with PBS + 0.2% Tween-20 for 10 minutes to eliminate non-specific binding. Labeled cells were pelleted and resuspended in 300 µL of FACS buffer for flow cytometric analysis.

#### **4.3.4 Western blotting of total and phospho-STAT**

PBMC are first magnetically separated into lymphocytes and monocytes using MACS CD14 positive selection (Miltenyi Biotec, Auburn, CA.) according to the manufacturer's suggestion. Monocytes and lymphocytes were either left untreated in IMDM or were treated with IL-2 at 10, 100, or 1000 IU/ml for 15 min at 37°C for dose response experiments. For time course experiments, monocytes and lymphocytes were left untreated as before or were treated with IL-2 at 1000 IU/ml for 15, 30, 60, or 120 min at 37°C. Whole cell lysates were prepared by incubating the cells in lysis buffer (100 mM NaCl, 10 mM Tris (pH 8.4), 1% NP-40, phosphatase inhibitor cocktail I and II (Sigma, St. Louis, MO)) for 15 minutes. Following lysis, a BCA assay (Pierce Biotechnology, Rockford, IL) was performed to analyze total protein concentration within each of the lysates. Lysates were boiled for 5 minutes in XT buffer (Bio-

Rad Laboratories, Hercules, CA) containing 10%  $\beta$ -mercaptoethanol. The samples were loaded into Criterion XT precast gels (Bio-Rad Laboratories, Hercules, CA) at 10 $\mu$ g per lane. Proteins were separated by gel electrophoresis at 100V for 1.5 hours. The proteins were then transferred to nitrocellulose membranes (Bio-Rad Laboratories, Hercules, CA) at 100V for 45 minutes. After blocking the membranes in TBS containing 1% BSA overnight at room temperature, the membranes were probed with mouse anti-pSTAT5 at a 1:500 dilution or rabbit anti-STAT5 at a 1:200 dilution for 1 hour at room temperature under constant agitation. After three 10 minutes washes with TBS containing 0.2% Tween-20, the blots were probed with HRP-conjugated donkey-anti-mouse IgG at 10 ng/ml for 1 hour at room temperature under constant agitation. The blots were washed three times with TBS containing 0.2% Tween-20. Supersignal West Pico Chemiluminescence Substrate (Pierce Biotechnology, Rockford, IL) was added to the blots according to the manufacturer's instructions. After exposing the pSTAT5 blot to x-ray film for 10 min and the STAT5 blot for 30 seconds, the film was developed using a Kodak X-OMAT 2000A processor.

#### **4.3.5 Flow cytometric analysis of phospho-proteins**

The samples were analyzed on a FACScan or FACSArray flow cytometer. CellQuest software was used for the acquisition of events on the FACScan and FACSDiva software was used for acquisition on the FACSArray. 10,000 gated events were collected for each sample. Off-line analysis was performed using FACSDiva software. Within FACSDiva, a monocyte and lymphocyte gate was created based on forward and side scatter properties. For each of these gated populations, the geometric mean fluorescence intensity was analyzed.

## 4.4 RESULTS

### 4.4.1 Dose and time-dependent responsiveness of STAT1 phosphorylation in cytokine stimulated PBMC

PBMC ( $5 \times 10^5$  in 50  $\mu$ l) were treated with IFN $\gamma$  or IFN $\alpha$  at concentrations of 10, 100, or 1000 IU/mL or were left untreated in IMDM alone. During cytokine treatment, the PBMC were incubated at 37°C for 15 minutes. Panel A of Figure 7 displays the level of STAT1 phosphorylation represented as geometric mean fluorescence intensity (GMFI) as measured by flow cytometry on a BD FACScan. The responsiveness of PBMC to IFN $\gamma$ , even at low concentrations (10 IU/mL), is primarily within the monocyte gate, with very little phosphorylation of STAT1 in the lymphocyte population. The entire monocyte population increased expression of pSTAT1 following treatment, as shown in panel C, whereas the lymphocyte population was unresponsive. The necessary concentration of IFN $\gamma$  as a stimulus for maximal STAT1 phosphorylation is 100 IU/mL. IFN $\alpha$  exhibits a dose-dependent effect on STAT1 phosphorylation within PBMC, also primarily within the monocyte gate, with the necessary concentration for maximal STAT1 phosphorylation being 1000 IU/mL. Once again, the entire monocyte population increased pSTAT1, whereas the lymphocytes produced a bimodal peak, as shown in panel D. At low concentrations (10 IU/mL), IFN $\alpha$  is not as effective as IFN $\gamma$  at eliciting STAT1 activation. To analyze the kinetics of STAT1 phosphorylation, PBMC were treated with 100 IU/ml and 1000 IU/ml of IFN $\gamma$  and IFN $\alpha$  respectively for 5, 10, 15, -30, 60, and 120 minutes at 37°C and were analyzed on a BD FACScan in separate experiments. Panel B of Figure 7 illustrates the time-course experiment depicting STAT1 phosphorylation as GMFI in PBMC following treatment with IFN $\gamma$  and IFN $\alpha$ . Once again, IFN $\gamma$  exerted its effects

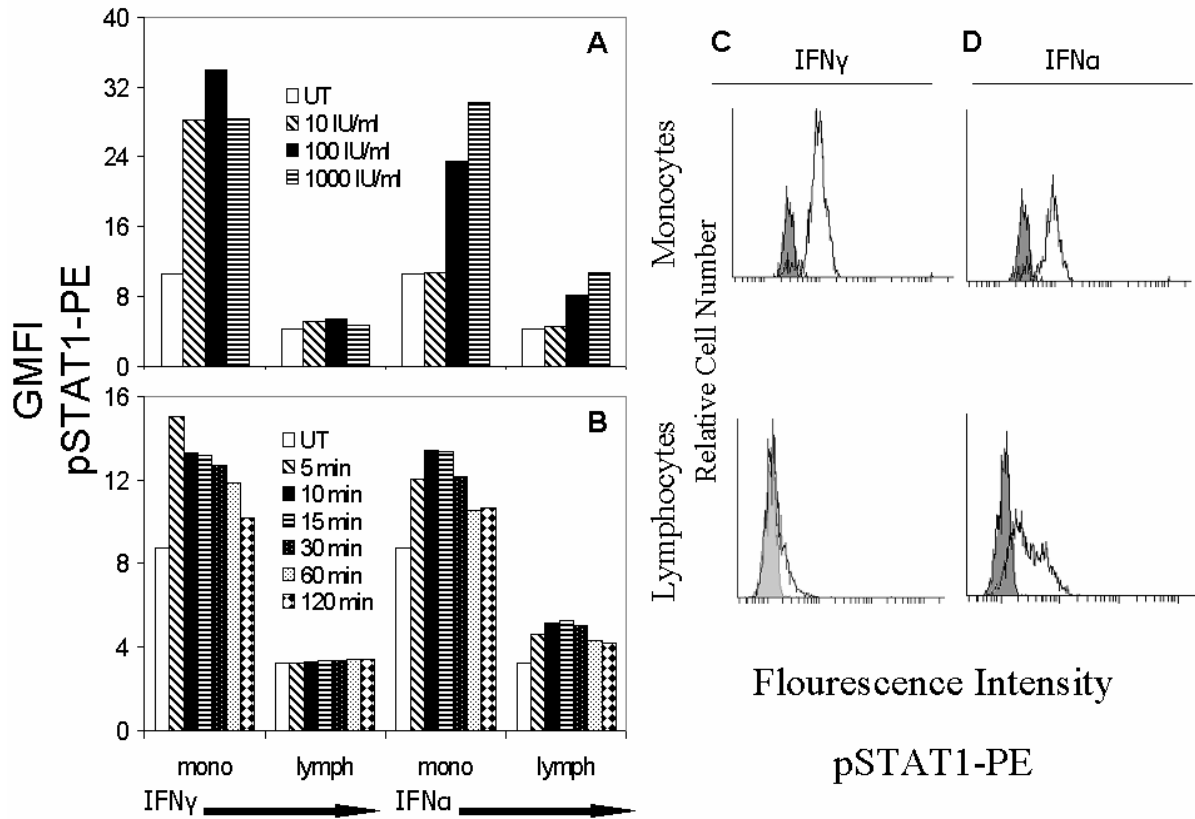


**Figure 7. Interferons ( $\alpha$  and  $\gamma$ ) induce rapid phosphorylation of STAT1 in PBMC, primarily in monocytes, in a dose-dependent manner.** PBMC were stimulated with varying concentrations of IFN $\gamma$  or IFN $\alpha$  for 15 min at 37°C (panel A) and with 100 IU/ml of IFN $\gamma$  or 1000 IU/ml of IFN $\alpha$  for the indicated time intervals (panel B). STAT1 phosphorylation is expressed as the geometric mean fluorescence intensity of pSTAT1-PE within gated [by size and granularity] monocyte and lymphocyte populations as measured by flow cytometry. Panels C and D indicate STAT1 phosphorylation in untreated cells (filled histograms) and cells treated for 15 min with 100 IU/ml of IFN $\gamma$  or 1000 IU/ml of IFN $\alpha$  (unfilled histograms) respectively. Note the rapid phosphorylation following stimulation and subsequent loss of phosphorylation at late time points, as well as the differential activation of monocytes and lymphocytes. Each experiment was performed on a separate day on a BD FACScan with cells from different draws.



on the monocyte population alone, with maximal phosphorylation occurring very rapidly ( $\leq 5$  minutes). The level of STAT1 phosphorylation decreased steadily, approaching baseline levels over the two-hour time frame. Stimulation with IFN $\alpha$  caused activation of STAT1 within both cell populations, but primarily in monocytes. Following IFN $\alpha$  treatment, maximal phosphorylation of STAT1 occurred at 10 to 15 minutes. At later time points, levels of phosphorylation decreased to baseline. The actual magnitude of response is not the same in panels A and B even though both experiments were analyzed on the same cytometer, but we attribute this difference to performing the experiments without prior voltage calibration of the instruments. It is also likely that there will be some variability in the cellular response between normal donors or even the same donor on different dates.

#### **4.4.2 Dose and time-dependent responsiveness of STAT3 phosphorylation in cytokine stimulated PBMC**

PBMC ( $5 \times 10^5$  in 50  $\mu$ l) were left untreated with IMDM or were treated with IL-10 or IL-6 at concentrations of 1, 10, and 100 ng/mL or IFN $\alpha$  at concentration of 10 IU/ml, 100 IU/ml, or 1000 IU/ml for 15 minutes at 37°C to induce STAT3 phosphorylation. Panel A of Figure 8 demonstrates the relationship between STAT3 phosphorylation and cytokine concentration in monocytes and lymphocytes as assessed by GMFI on a BD FACScan. IL-6 titration experiments were not performed in the same experiment, so the responses should not be compared to those of the other cytokines. With the cytokines evaluated, STAT3 activation appears to occur within both monocytes and lymphocytes. There is a clear dose-dependent response of pSTAT3 to IL-6, with activation occurring at concentrations as low as 1 ng/mL with maximal activation at 100 ng/mL. IFN $\alpha$  and IL-10 both activated STAT3 with maximal levels attained at concentrations of

100 IU/ml and 10 ng/mL respectively. In contrast to the STAT1 experiments, the entire monocyte and lymphocyte populations increased expression of pSTAT3 for each of the cytokines evaluated (data not shown.) To analyze the kinetics of STAT3 phosphorylation, PBMC were treated with IMDM as a control, IL-10 (10 ng/mL), IFN $\alpha$  (100 IU/mL), or IL-6 (50 ng/mL). The results are indicated in panel B of Figure 8. IL-6 treated cells were assessed in a separate experiment and were analyzed using a BD FACSAarray, whereas other samples were analyzed on a BD FACScan. Following IFN $\alpha$  and IL-10 treatment, maximal phosphorylation of STAT3 occurs rapidly by 10 minutes. STAT3 phosphorylation decreases towards baseline values as the incubation time with both cytokines approaches two hours. When PBMC are stimulated with IL-6, phosphorylation of STAT3 increases to maximal levels by 15 minutes. At later time points, pSTAT3 levels approach baseline, but appear to increase again at the two hour time point.

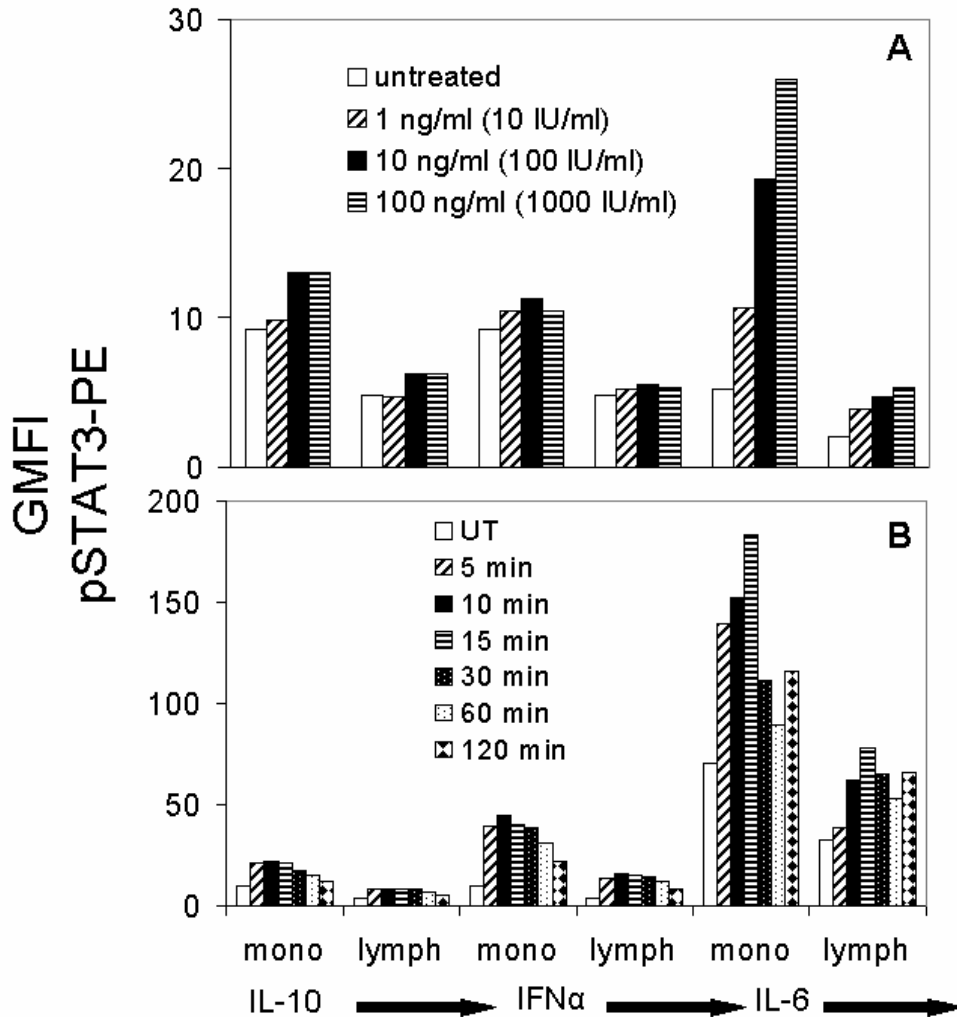


**Figure 8. Following cytokine treatment (IL-10, IFN $\alpha$ , and IL-6) phosphorylation of STAT3 is transiently induced in a dose-dependent manner.** PBMC were stimulated with varying concentrations of IL-10, IFN $\alpha$  (concentration in parentheses), or IL-6 for 15 min at 37°C (panel A) or with 10 ng/ml of IL-10, 100 IU/ml of IFN $\alpha$ , or 50 ng/ml of IL-6 for the indicated time intervals (panel B). STAT3 phosphorylation is expressed as the geometric mean fluorescence intensity of pSTAT3-PE within monocyte and lymphocyte populations as measured by flow cytometry. Responsiveness is transient and generally has returned towards baseline by two hours following stimulation. All experiments in panel A were performed on a BD FACScan, but the IL-6 experiment was performed in a separate experiment with cells from a different separation and date from the same normal donor. In panel B, all experiments were performed on a BD FACScan in the same experiment except for the IL-6 experiment, which was performed separately on a BD FACSArray (explains the difference in GMFI.)

#### **4.4.3 Dose and time-dependent responsiveness of STAT5 phosphorylation in cytokine stimulated PBMC**

IL-3 at concentrations of 1, 10, and 100 IU/mL was used to stimulate  $5 \times 10^5$  PBMC in 50  $\mu$ l for 15 minutes at 37°C. As a control, cells were incubated with IMDM. In a separate experiment, the cells were treated with IL-7 at concentrations of 1, 10, and 100 ng/mL under the same conditions. Cells were analyzed for pSTAT5 by recording GMFI on a BD FACScan for the dose response experiments. Panel A of Figure 9 illustrates the dose response relationship of pSTAT5 following stimulation. IL-3 induces dose-dependent responses in pSTAT5 within the entire monocyte population exclusively. The differential effects of IL-3 on monocytes and lymphocytes is shown in panel C of Figure 9. Of the concentrations tested, 100 IU/mL of IL-3 was sufficient for maximal pSTAT5 induction. On the other hand, monocytes were unresponsive to IL-7, but approximately 50% of lymphocytes increased pSTAT5, as shown in panel D of Figure 9. This bimodal peak is similar to that observed for STAT1 phosphorylation in lymphocytes following IFN $\alpha$  treatment. STAT5 was phosphorylated in lymphocytes even at the lowest concentration of 1 ng/mL, while increasing concentrations did not appear to have any greater effect. Time-course experiments were performed by treating PBMC with 100IU/ml of IL-3, or 50 ng/mL of IL-7 at 37°C for 5, 10, 15, 30, 60, and 120 minutes. IL-3 was assessed on the BD FACScan, while the IL-7 experiment was analyzed on the BD FACSArray. This explains the large difference in baseline GMFI. Phosphorylation kinetics following treatment are displayed in panel B of Figure 9. As expected, STAT5 phosphorylation does not increase above baseline in the monocyte population with IL-7 treatment. However, lymphocytes rapidly phosphorylate STAT5 within 5 minutes of treatment. Unlike previous data, the levels of

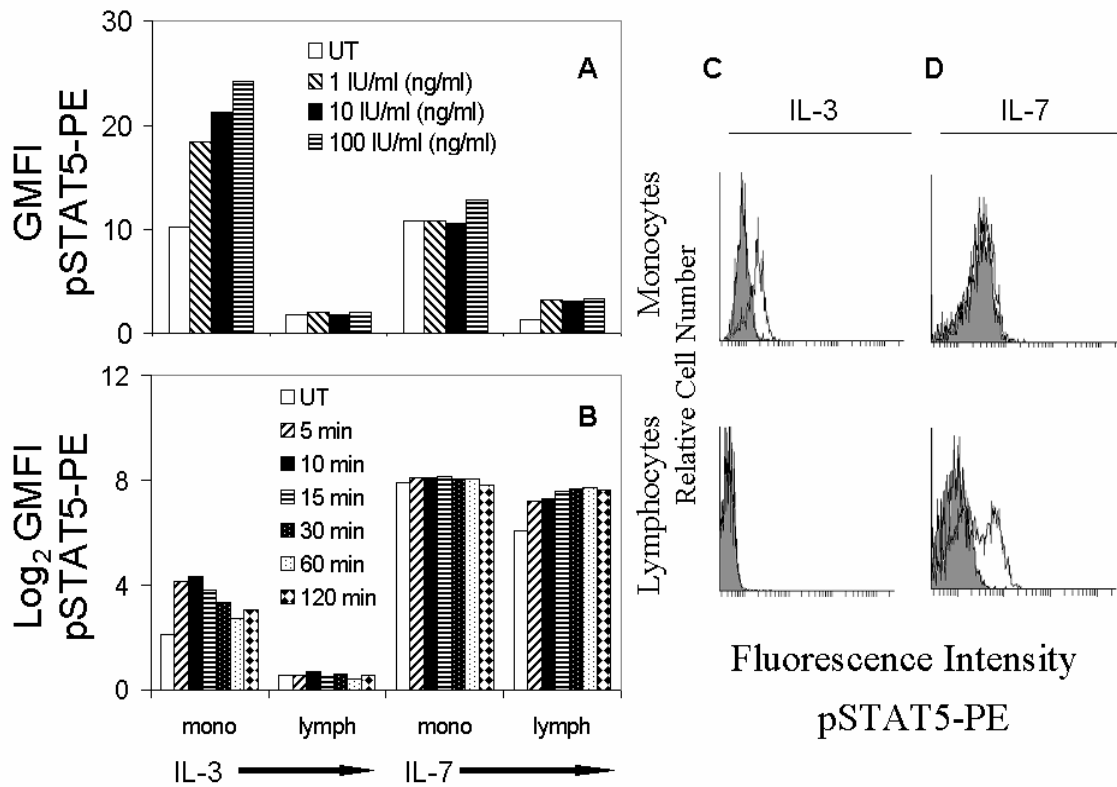


**Figure 9. IL-3 and IL-7 induce phosphorylation of STAT5 in different PBMC populations.** PBMC were stimulated with 0, 1, 10, or 100 IU/ml of IL-3, or 0, 1, 10, or 100 ng/ml of IL-7 for 15 min at 37°C (panel A) or treated with 100 IU/ml of IL-3, or 50 ng/ml of IL-7 for the indicated time intervals (panel B). STAT5 phosphorylation is expressed as GMFI or log<sub>2</sub>(GMFI) of pSTAT5-PE within monocyte and lymphocyte populations as measured by flow cytometry. Panels C and D show STAT5 phosphorylation in untreated cells (filled histograms) and cells treated for 15 min with 100 IU/ml of IL-3, or 50 ng/ml of IL-7 for 2 hours (unfilled histograms) respectively. Interestingly, IL-7 mediated prolonged activation and induced phosphorylation in lymphocytes alone, whereas that with IL-3 was only transient and exclusively in monocytes. All experiments were performed on a BD FACScan, except the time-course experiment involving IL-7, which was performed separately on a BD FACSArray (explains increased GMFI.) The dose and time course experiments were not performed in the same experiment.

phosphorylation do not quickly decay towards baseline over the two-hour treatment. Whereas lymphocytes were unresponsive to IL-3, monocytes phosphorylated STAT5 to maximal levels at 10 minutes following treatment with a subsequent decrease in pSTAT5 towards baseline at later time points. This differential responsiveness of monocytes and lymphocytes to individual cytokines/stimuli allows inferences regarding the earliest events in inflammation occurring rapidly within circulating cells.

To verify that this assay is specifically detecting phosphorylated proteins within distinct cell populations, a Western blot experiment was performed in parallel with flow cytometry. Because a Western blot is a bulk analysis method, and therefore unable to distinguish between different cell types, PBMC were magnetically separated into lymphocytes and monocytes via CD14 positive selection prior to stimulation. Cells were either left untreated or were treated with a dose response of IL-2 at 10, 100, or 1000 IU/ml for 15 min at 37°C. In a separate experiment, cells were untreated or treated with 1000 IU/ml of IL-2 for 15, 30, 60, or 120 min at 37°C. Cell lysates were blotted for either pSTAT or total STAT5. The upper panel of Figure 10A illustrates the results of the Western blot. The bands in the upper row represent pSTAT5 within lymphocytes and monocytes, while the lower band depicts total STAT5. It is clear that untreated lymphocytes and monocytes, as well as IL-2 treated monocytes do not contain any phosphorylated STAT5 or it is below the limits of detection. However, lymphocytes treated with IL-2 show an increase in phosphorylation, as indicated by the band intensities, with increasing IL-2 concentration. Unseparated PBMC were simultaneously treated for IL-2 in triplicate and were analyzed in parallel using the BD FACSArray cytometer for STAT5 phosphorylation. In the lower panel of Figure 10A, the median pSTAT5 GMFI of the triplicate wells is plotted for each concentration of IL-2 within lymphocyte and monocyte populations. The error bars

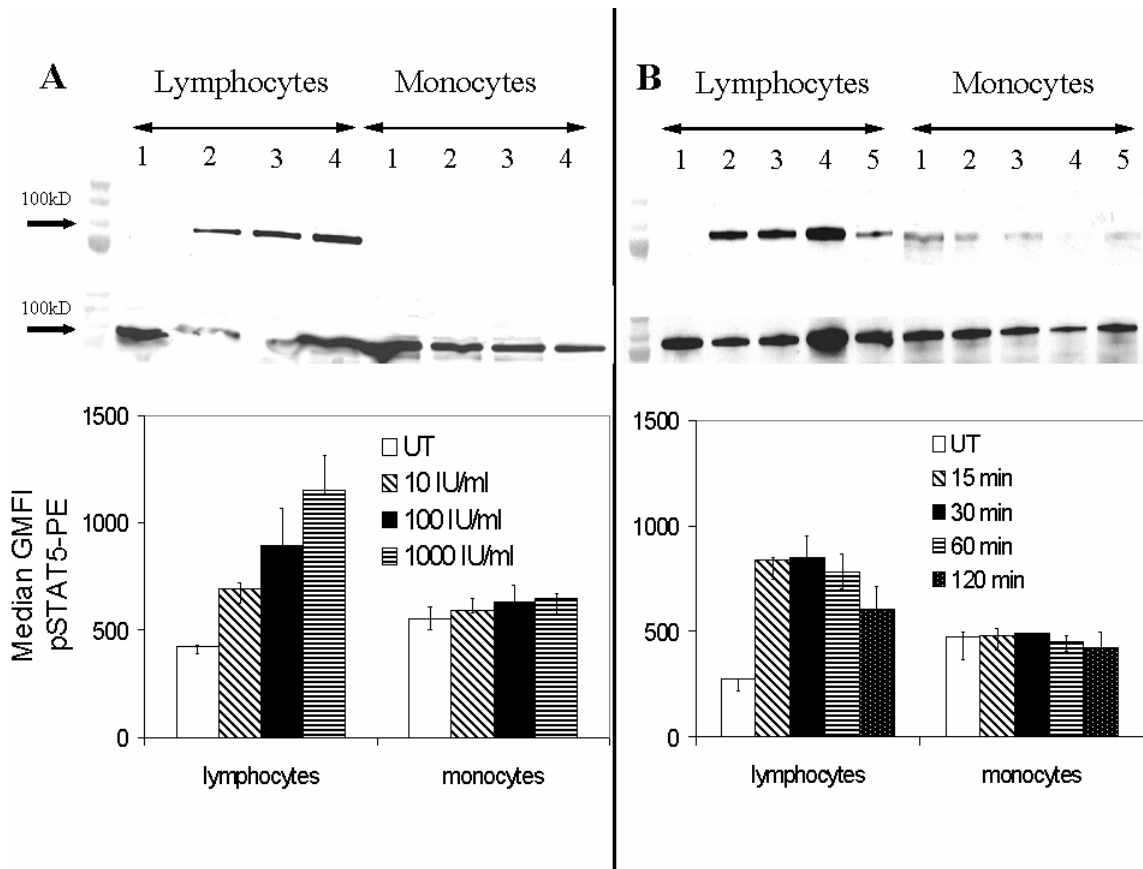


**Figure 10. Differential responsiveness of STAT5 to IL-2 in lymphocytes and monocytes is verified via Western blot and flow cytometry.** In the upper portion of panel A, PBMC were separated into lymphocytes and monocytes prior to IL-2 stimulation. PBMC were treated with (1) IMDM or IL-2 at (2) 10 IU/ml, (3) 100 IU/ml, or (4) 1000 IU/ml for 15 min. In the upper portion of panel B, separated lymphocytes and monocytes were treated with (1) IMDM or 1000 IU/ml of IL-2 at (2) 15 min, (3) 30 min, (4) 60 min, or (5) 120 min. Lysates were blotted for pSTAT5 (top row) and total STAT5 (bottom row.) The bottom portions of panels A and B, illustrate flow experiments run in parallel on the same day using triplicate wells on the BD FACSArray. The median STAT5 GMFI is plotted and the GMFI of the remaining wells are plotted as error bars. These experiments demonstrate strong correlation between western blotting and the flow cytometric assay, as well as high intra-experimental reproducibility for the flow-based assay.

represent the GMFI of pSTAT5 from the two remaining wells. This figure shows an obvious escalation in pSTAT5 following increasing concentrations of IL-2. In the top panel of Figure 10B, Western blot results from the IL-2 time course are provided. Once again, the top row represents pSTAT5, while the bottom row represents total STAT5. It is clear that there is an absence of pSTAT5 within unstimulated lymphocytes. However, monocytes from this separation exhibited slight basal phosphorylation of STAT5. This band does not increase with IL-2 treatment. Within the lymphocyte population, there are strong bands corresponding to pSTAT5 following IL-2 stimulation. These bands decrease at the two-hour time point, which is a trend that has been exhibited with many other signaling proteins in this manuscript. The stronger band at 60 minutes is likely due to unequal protein loading, as evidenced by the thicker band for total STAT5 on the bottom row. Unseparated PBMC were simultaneously treated for IL-2 in triplicate and were analyzed in parallel on a BD FACSArray cytometer for STAT5 phosphorylation. In the lower portion of Figure 10B, the median GMFI of pSTAT5 for the triplicate wells is plotted for each time point within lymphocyte and monocyte gates. In agreement with previous data, there is no apparent increase in pSTAT5 following IL-2 within the monocyte population. However, there is roughly a 4-fold increase in pSTAT5 within lymphocytes up to about 30 minutes following treatment, whereupon pSTAT5 levels decrease towards baseline. To further highlight the validity of the flow cytometric results, the flow data from Figure 10 is included together with densitometry plots of the Western bands from Figure 10 in the Appendix. Thus, our flow cytometric assay correlates very well with results obtained by Western blot. Moreover, it does not require a priori separation of cells to analyze subsets and allows for a greatly reduced protocol time. Additionally, the coefficients of variation for the triplicate samples analyzed by flow cytometry are roughly 10% or less for all data points shown,



highlighting the intra-experimental reproducibility of this assay. It should also be noted that voltage calibration was performed prior to analysis, which decreases the variation in fluorescence intensity between experiments.

#### **4.4.4 Dose and time-dependent responsiveness of STAT6 phosphorylation in cytokine stimulated PBMC**

IL-4 and IL-13 were applied at concentrations of 1, 10, and 100 ng/mL in individual experiments on  $5 \times 10^5$  PBMC in 50  $\mu$ l for 15 minutes at 37°C to induce STAT6 phosphorylation. As a control, cells were incubated with IMDM under the same conditions. Panel A of Figure 11 demonstrates the level of pSTAT6 measured as GMFI on the BD FACScan following cytokine treatment. IL-4 and IL-13 both induced dose-dependent responses in pSTAT6 levels in the entire monocyte population following treatment even at levels as low as 1 ng/mL. The optimal concentration for stimulation tested is 100 ng/mL of either cytokine. IL-4 also caused a dose-dependent increase in pSTAT6 within the entire lymphocyte population. On the other hand, lymphocytes were completely unresponsive to IL-13, consistent with previous findings [129, 130]. Examples of the differential effects of these cytokines on STAT6 phosphorylation in lymphocytes and monocytes are shown in panels C and D of Figure 11. Kinetics of STAT6 phosphorylation were tested by treating PBMC with 100 IU/mL of IL-4 or 50 ng/mL of IL-13 in separate experiments for 5, 10, 15, 60, or 120 minutes at 37°C. IL-4 experiments were analyzed using a BD FACScan while IL-13 experiments were analyzed separately on a BD FACSArray, which once again explains the large difference in GMFI. Monocytes and lymphocytes were both rapidly phosphorylated by IL-4 with maximal phosphorylation occurring within 5 to 15 minutes, as shown in panel B of Figure 11. Levels of pSTAT6 decrease comparatively slowly towards

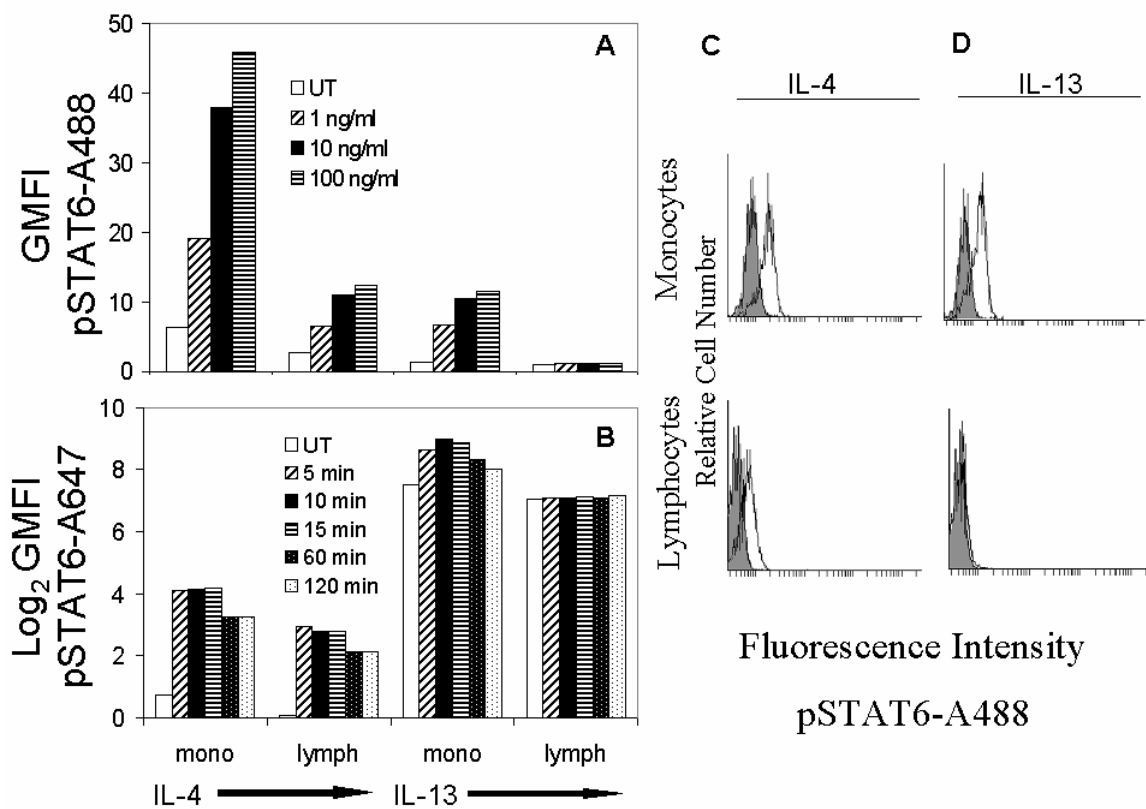


**Figure 11. TH2 cytokines IL-4 and IL-13 induce phosphorylation of STAT6 in a dose-dependent manner.** Human PBMC were stimulated with varying concentrations of IL-4 or IL-13 for 15 min at 37°C (panel A) or with 100 IU/ml of IL-4 or 50 ng/ml of IL-13 for the indicated time intervals (panel B). STAT6 phosphorylation is expressed as GMFI of pSTAT6-A488 or log<sub>2</sub>(GMFI) of pSTAT6-A647 within monocyte and lymphocyte populations as measured by flow cytometry. Panels C and D show STAT6 phosphorylation in untreated cells (filled histograms) and cells treated for 15 min with 100 IU/ml of IL-4, or 100 ng/ml of IL-13 (unfilled histograms) respectively. While IL-4 acted on both populations, IL-13 only activated the monocytes. All experiments were performed on a BD FACScan, except for the IL-13 time course experiment, which explains the difference in GMFI. Each of the dose and time-course experiments were performed on separate days.

baseline over the two-hour IL-4 treatment. Once again, IL-13 produces no effect within the lymphocyte subpopulation, but quickly induces pSTAT6 within the monocytes. Following IL-13 treatment, maximal activation of STAT6 occurred at 10 minutes and decreased toward baseline by two hours. This assay could be useful in assessing specific small molecule and antibody strategies targeting either IL-4 or IL-13.

#### **4.4.5 Dose and time-dependent responsiveness of p38 MAPK and ERK1/2 phosphorylation in cytokine stimulated PBMC**

PBMC ( $5 \times 10^5$  in 50  $\mu$ l) were either left untreated in IMDM or were treated with PMA at concentrations of 1nM, 10nM, 100nM, or 1 $\mu$ M for 15 minutes at 37°C. GMFI of pp38 MAPK-PE and pERK1/2-PE was measured with a BD FACSArray. Panel A of Figures 12 and 13 demonstrate the results of dose response experiments for p-p38 MAPK and pERK1/2 respectively. p38 MAPK phosphorylation increases steadily within the majority of the monocyte population as the concentration of PMA increases. PMA does not, however, induce phosphorylation of p38 MAPK within the lymphocyte population. These findings are illustrated in histograms in panel C of Figure 12. On the other hand, ERK1/2 phosphorylation increases uniformly within both the monocyte and lymphocyte populations, as shown in panel C of Figure 13. Of the concentrations tested, maximal phosphorylation occurs at a PMA concentration of 1 $\mu$ M. The kinetics of p38 MAPK and ERK1/2 phosphorylation were examined by treating PBMC with 100 nM of PMA at 37°C for 5, 10, 15, 30, 60, or 120 minutes. GMFIs of p-p38 MAPK-PE and ERK1/2-PE were measured with a BD FACSArray and were plotted in panel B of Figures 12 and 13 respectively. Once again, p38 MAPK was not phosphorylated within the lymphocyte population throughout the entire time course, confirming the previous results.

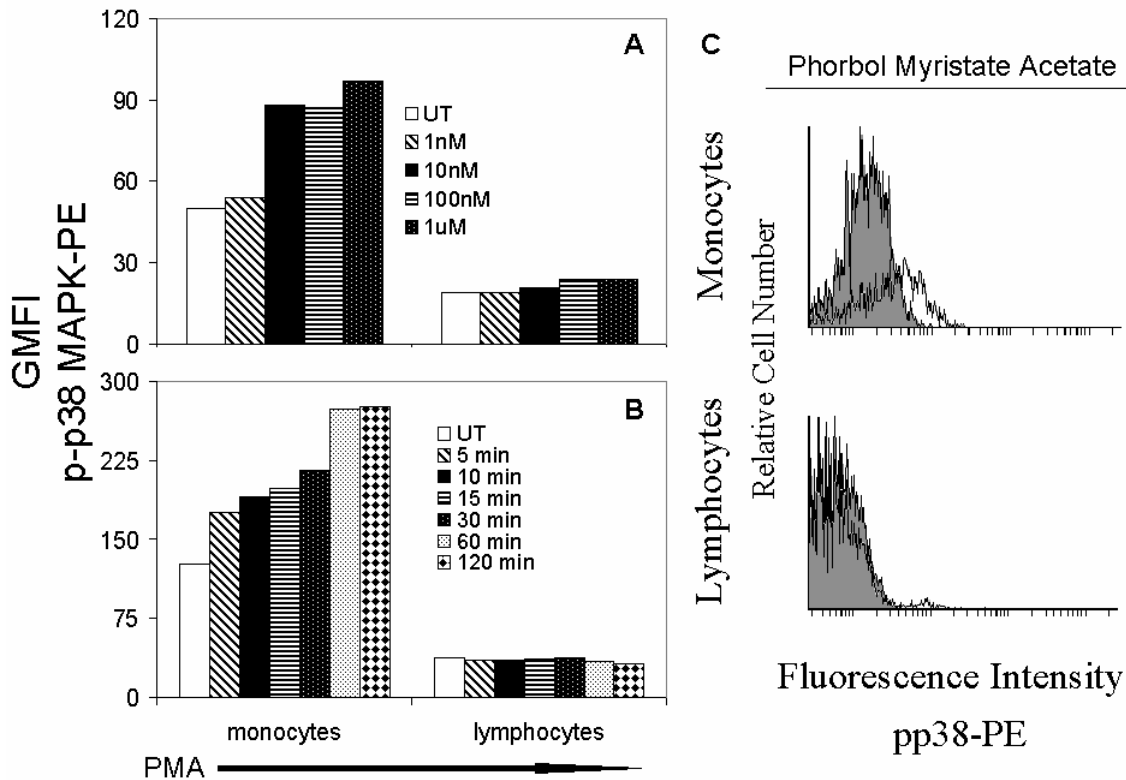


**Figure 12. Prolonged phosphorylation of p38 MAPK by PMA within monocytes.** PBMC were stimulated with varying concentrations of PMA for 15 min at 37°C (panel A) or treated with 100 nM PMA for the indicated time intervals (panel B). p38 MAPK phosphorylation is expressed as GMFI of pp38-PE within the monocyte and lymphocyte populations as measured by flow cytometry on a BD FACSArray. Panel C shows p38 phosphorylation in untreated cells (filled histograms) and cells treated for two hours with 100nM PMA (unfilled histograms.) Only gated monocytes responded to PMA stimulation under these conditions. The dose and time course experiments were performed on separate days.

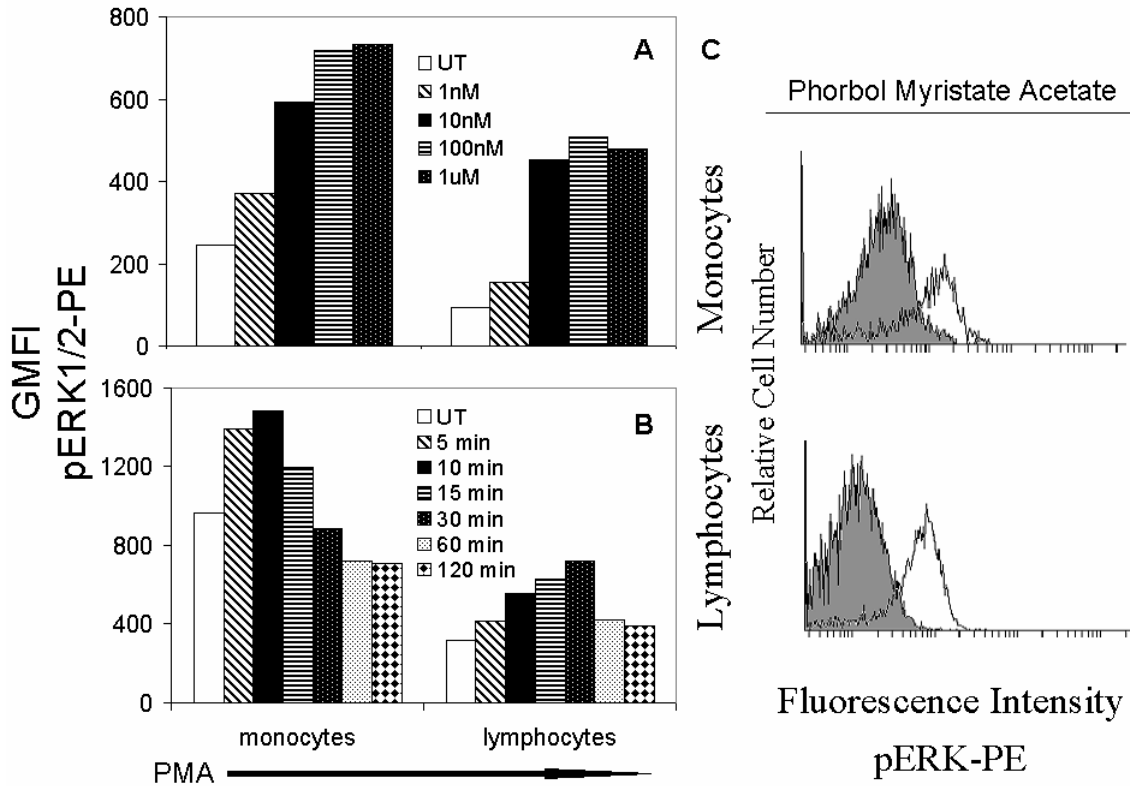


**Figure 13. Global phosphorylation of ERK1/2 in both monocytes and lymphocytes.** PBMC were stimulated with varying concentrations of PMA for 15 min at 37°C (panel A) or treated with 100 nM PMA for the indicated time intervals (panel B). pERK1/2 phosphorylation is expressed as GMFI of pERK1/2-PE within monocyte and lymphocyte populations as measured by flow cytometry on a BD FACSArray. Panel C shows ERK phosphorylation in untreated cells (filled histograms) and cells treated for 15 min with 100nM PMA (unfilled histograms.) Substantial increases in phosphorylation were observed in both populations. The dose and time course experiments were performed on different days.

Unlike most signaling proteins examined in this study, p38 MAPK was increasingly phosphorylated over the entire two hour incubation period. Conversely, maximum ERK1/2 phosphorylation occurred within 10 minutes in the monocyte population and decreased to levels lower than baseline at later time points. The kinetics within the lymphocyte population differed as maximum phosphorylation was reached at 30 minutes, followed by decay towards baseline at 1 and 2 hours.

#### **4.5 DISCUSSION**

We have applied flow cytometric-based techniques to evaluate the cytokine-induced phosphorylation pathways [CIPP] of STAT1, STAT3, STAT5, STAT6, p38 MAPK, and ERK1/2 in response to various concentrations and time-course treatments with a panel of cytokines. STAT proteins and ERK1/2 are rapidly phosphorylated within human PBMC, maximal activation normally occurring within 15 minutes. Increased phosphorylation correlated with higher concentrations of the cytokines tested. At two hours, cells typically approached their basal phosphorylation states with the exception of pp38 in monocytes following PMA treatment and pSTAT5 in lymphocytes following IL-7 treatment. Using human monocytes, Fleisher et. al found similar results with comparable concentrations of IFN $\gamma$  to induce STAT1 phosphorylation [15]. That study was limited, however, to monocytes and analysis of pSTAT1. Our results confirm these findings and extend them to further demonstrate that individual cytokines induce phosphorylation in specific cell types and cause differential activation kinetics. For example, we show that IL-3, IL-13, and IFN $\gamma$  exclusively activate monocytes in short-term culture, while IL-2 and IL-7 solely activate lymphocytes using assessment of STAT5 signaling pathways.

By using a cytometric approach, the analysis time is significantly reduced when compared to Western blotting, fewer cells are required, and use of PBMC allows visualization of both monocytes and lymphocytes without the need for additional separation steps or reagents, enabling ready application in a clinical laboratory. Western blotting and flow cytometry provide similar results when applied to phospho-protein analysis [19, 69, 116], as we have also demonstrated by examining STAT5 phosphorylation following IL-2 dose and time-course experiments in Figure 10. However, compared to Western blotting, flow cytometry allows for less manipulation of cells and can allow one to identify cells with differences in responsiveness, rather than a mean value for the total cell population. Additionally, flow-based techniques allow one to examine rare populations of cells, such as plasmacytoid dendritic cells (PDCs) and myeloid dendritic cells (MDCs) [131].

We validated this strategy using two individual cytometers: the Becton Dickinson FACScan and FACSArray. As the GMFIs differed greatly depending on the instrument used, comparison between experiments is difficult, but the consistent patterns of activation for many of the signaling proteins examined, i.e. maximal phosphorylation within 15 minutes followed by a decrease at later time points, as well as verification of the results with Western blotting serve to illustrate the robustness of this strategy. Additionally, the differential effects of cytokines on distinct cell populations were reproducible between different experiments, as well as on different cytometers. The cytometers were not voltage calibrated before the early experiments, causing increased inter-experimental variability, and we thus now recommend this procedure as an important and necessary step before each experiment. We have provided qualitative data comparing two different cytometers, demonstrating similar relative quantitative dose responses and kinetics of phosphorylation for many proteins within the JAK/STAT and p38 MAPK

families, as well as differential responses to stimuli in distinct PBMC populations. Additionally, we show that the sample-to-sample variability within a single experiment is extremely low, as evidenced by the triplicate samples provided in Figure 10 with CVs approximately 10% or less for all data points. Due to the large number of cells analyzed for each sample (approximately 20,000), verification of the data by Western blot, reproducible patterns of phosphorylation kinetics observed with various stimuli, and the non-trivial increases in phosphorylation illustrated in the raw histograms following stimulation, we did not include any tests of statistical significance. From the histograms that we have recently included, one can observe that the shift in fluorescence intensity (phosphorylation) is not trivial. In most cases, the entire population can be seen to shift. This taken with the observation that many of the proteins follow the same kinetics of phosphorylation, as well as verification of the data by Western blot, suggest that this flow-based technique represents a reproducible and meaningful way of analyzing phosphorylation events within complex cell populations. Using a single cytometer for acquisition and calibrating it regularly before analysis can increase quantitative, inter-experimental reproducibility. The results obtained in these experiments suggest interesting strategies for titrating immunosuppressive or immunostimulatory reagents such as FK506, cyclosporine, rapamycin, IL-2, CTLA4 antibody, and possibly pathogen or damage associated molecular pattern molecules [PAMPs/DAMPs] including HMGB1[132] or CpG molecules.

Acute and chronic inflammation can set up altered microenvironments encountered by circulating PBMC. Abnormal cytokine profiles within these microenvironments could indeed alter signaling pathways. Studies suggest that PBMC are disordered in number and function in the setting of cancer, suggesting that global immune function is compromised beyond the immediate tumor microenvironment. These defects include a higher proportion of PBMC



undergoing spontaneous apoptosis and decreased zeta-chain expression [133, 134]. There are a number of ways in which aberrant signaling may occur specifically within the STAT and MAPK pathways. For example, there could be an increased/decreased level of phosphorylation in the basal state or increased/decreased activation in response to cytokines. Recently a similar technique examined STAT1 phosphorylation in PBMC of melanoma patients following IFN $\alpha$  stimulation. Unstimulated PBMC from melanoma patients had significantly less pSTAT1 than healthy controls, whereas pSTAT1 levels in IFN $\alpha$  stimulated cells were comparable [116]. Even though the magnitudes of cytokine-induced responses are normal, it is possible that the kinetics of phosphorylation are altered.

As we have detected bimodal lymphocyte responses to various stimuli (e.g. IFN $\alpha$ , IL-7), we plan to assess discrete cell populations within PBMC by using antibodies against surface proteins, cell-specific markers, which will allow identification of signaling responses in subsets. In preliminary experiments, using the current permeabilization strategy, 90% methanol, many surface epitopes are compromised, thus unable to be stained. Another manuscript is in the works to address these problems with permeabilization and detrimental effects on surface staining. Coupling cell surface or other intracellular markers can enable more sophisticated analysis of rare populations including PDCs and MDCs, as well as cells poorly able to be cryopreserved such as neutrophils and eosinophils. Once the normal responses to individual cytokines have been identified within specific PBMC subpopulations, similar techniques can be used to analyze cells from patients with a variety of inflammatory states. Before this can be done however, methods must be optimized to standardize quantitative flow cytometry. Due to the technical simplicity, low number of cells required, and the ability to use banked, frozen PBMC, this flow-cytometric technique is promising for use in the clinic as a diagnostic tool or to monitor immune-

directed therapies. The combination of immunophenotyping with a rapid, cytometric assay to detect the integrity of signaling pathways will prove a valuable tool in dissecting out discrete cell populations within complex mixtures to assess individuals in the setting of both acute and chronic diseases [135] or following immunotherapy [136-138].

## **5.0 SIMULTANEOUS MEASUREMENT OF CELL SURFACE AND INTRACELLULAR PHOSPHORYLATED PROTEINS IN HUMAN PBMC**

### **5.1 ABSTRACT**

Phenotyping and simple enumeration of peripheral blood mononuclear cells (PBMC) is of limited value for the assessment of many clinical states. As a preferred alternative, cell surface phenotyping may be combined with functional assays for enhanced assessment of altered cells circulating in patients. One simple, yet informative and rapid approach is to examine signaling within individual cells following brief periods of stimulation via flow cytometry. Although monocytes and lymphoid cells can be distinguished based on size, current permeabilization strategies necessary for identifying intracellular phosphorylated signaling molecules largely compromise the labeling of cell surface proteins used to distinguish individual cellular subsets. We have successfully developed conditions that allow for simultaneous detection of cell surface proteins and intracellular phosphorylated proteins in human PBMC following rapid *in vitro* cytokine stimulation. We analyzed permeabilized CD4, CD8, CD14, CD19, and CD56 expressing cells together with intracellular pSTAT1, pSTAT3, pSTAT5, pSTAT6, pp38 MAPK, or pERK1/2 within total PBMC. Of the permeabilizing conditions tested, 75% methanol enabled superior simultaneous detection of both cell surface and intracellular epitopes. This method

enables the rapid functional analysis of subsets within complex cell mixtures and provides an opportunity for assessing abnormalities arising in the setting of acute or chronic inflammatory states.

## 5.2 INTRODUCTION

When compared with other functional assays, analysis of signaling pathways using antibodies directed against phospho-specific proteins provides a more rapid assessment of the functional state of immune cells [Montag DT, Lotze MT; submitted; [117]]. Western blotting has been typically used for cell signaling analysis, but this technique requires the use of large, homogenous populations of cells and is impractical for analysis of rare subpopulations, particularly within PBMC. Additionally, this technique does not yield information at the single-cell level. Flow cytometry can be utilized for the detection of phosphorylated proteins, which is quantitative, more rapid, and allows single cell analysis as a technique preferable to Western blotting. Complex or rare populations of cells can be assessed without the need for additional cell separation [119, 120]. Qualitatively, flow cytometry and Western blotting provide similar results for phospho-protein analysis [69, 116].

Protein phosphorylation is critical for the propagation of signals delivered by responses to pathogen [PAMP] or damage [DAMP] associated molecular pattern recognition as well as cytokine receptor ligation through pathways that ultimately mediate immunity. These pathways are initiated by ligand-binding to specific receptors, which result in an almost immediate cascade of protein phosphorylation events. The JAK/STAT and MAPK/ERK are two important families of signaling proteins that regulate immune responses, which are themselves propagated by

protein phosphorylation. Host defense, growth control, and apoptosis are regulated through signals amplified by the JAK/STAT pathway [21, 26, 121]. In the setting of cancer, abnormalities in STAT signaling are commonly observed [33, 35, 122, 123]. Stress, inflammation, and other stimuli, initiate the MAPK/ERK pathway to regulate cell cycle progression, apoptosis, cytokine production, RNA splicing, and cell differentiation [24, 86, 87]. Like the JAK/STAT family, MAPK/ERK signaling is dysfunctional in both stromal/immune cells as well as the epithelial components in many types of cancer [32, 34, 124, 125].

The currently established means to analyze phospho-proteins by flow cytometry compromises antibody binding to several cell surface epitopes [69]. We adapted the current procedure to examine the normal signaling events within subsets of PBMC by simultaneously detecting cell-specific surface proteins and phosphorylated intracellular signaling proteins following a cytokine stimulus that has previously been determined to provide maximal phosphorylation. Important members of the JAK/STAT and MAPK/ERK pathways including pSTAT1, pSTAT3, pSTAT5, pSTAT6, p-p38 MAPK, and pERK1/2 were evaluated within CD4, CD8, CD14, CD19, and CD56 expressing cells. Additionally, the technique was assessed for its reproducibility within a healthy individual at different time points and in several healthy individuals simultaneously. This strategy allows for rapid, reproducible detection of phosphorylated proteins within distinct cell populations within a complex mixture, which could be used to interrogate the signaling pathways of PBMC in patients. This technique also enabled us to examine proximal signaling events and differential effects of cytokine treatment on major subpopulations of cells within the blood. The reproducibility of this assay was favorable with substantial consistency from study to study, enabling it to serve now as a robust measure of individual cell types and immediate cytokine responsiveness/function.

## 5.3 MATERIALS AND METHODS

### 5.3.1 Antibodies, cytokines, and fixation and permeabilization reagents

Primary fluorophore-conjugated and unconjugated antibodies specific to phosphorylated proteins: pSTAT1(Y701):Alexa 647, pSTAT1(Y701):PE, pSTAT3(Y705):Alexa 647, pSTAT5(Y694):Alexa 647, pSTAT5(Y694), pSTAT6(Y641):Alexa 647, pERK(T202/Y204):Alexa 647, and p-p38 MAPK(T180/Y182):Alexa 647, were purchased from BD PharMingen (San Diego, CA.) Likewise, primary fluorophore-conjugated antibodies against cell-specific surface proteins: CD4:APC, CD4:PE, CD8:APC, CD8:PE, CD14:APC, CD19:PE, CD56:APC, and CD56:PE, were purchased from BD PharMingen (San Diego, CA.) Antibodies to total STAT5 were purchased from Santa Cruz Biotechnology (Santa Cruz, CA.) Interferon (IFN)- $\alpha$ , IL-4 (Biosource, Camarillo, CA), interferon (IFN)- $\gamma$ , IL-2, IL-10 (R&D Systems Inc, Minneapolis, MN), and phorbol 12-myristate 13-acetate (PMA) (Sigma, St. Louis, MO) were used to induce phosphorylation in PBMC. Cells were fixed using 2% paraformaldehyde (Fisher Scientific, Pittsburgh, PA.) BSA (Spectrum Chemical, Gardena, CA), sodium azide, and saponin (Sigma, St. Louis, MO) were used to make 0.5% BSA/0.1% sodium azide/0.1% saponin in PBS (Fisher Scientific, Pittsburgh, PA) for cell permeabilization. Alternatively, cells were permeabilized in varying concentrations of methanol (Fisher Scientific, Pittsburgh, PA), ethanol (Pharmco, Brookfield, CT), isopropanol (Acros Organics, Geel, Belgium) or acetone (Sigma, St. Louis, MO.)

### **5.3.2 Isolation of PBMC**

10mL of Ficoll-Paque Plus (Amersham Biosciences, Uppsala, Sweden) was pipetted into the bottom of a centrifuge tube containing 20 mL of whole blood and 20 mL of PBS. The blood was spun at 400xG for 30 minutes. PBMC were pipetted off into a new centrifuge tube. The cells were spun into a pellet at 400xG for 10 minutes. 5 mL of ACK buffer (0.15M NH<sub>4</sub>Cl, 10mM KHCO<sub>3</sub>, 0.1mM NaEDTA; pH 7.2-7.4) was added to the cells for 15 minutes at RT to lyse remaining RBC. The cells were pelleted and resuspended in IMDM (Mediatech, Herndon, VA). Cells were counted, spun, and resuspended in freeze medium at a concentration of 10<sup>7</sup> cells/mL. Freeze medium used to store PBMC consisted of 90% heat denatured FBS (Mediatech, Herndon, VA) and 10% DMSO (Fisher Scientific, Pittsburgh, PA). 10<sup>7</sup> PBMC were put into separate cryogenic vials (Corning, Corning, New York). The PBMC were kept at -80°C for one day and were then transferred to a liquid nitrogen freezer.

### **5.3.3 PBMC stimulation and phospho-protein staining**

PBMC were removed from liquid nitrogen and were thawed in a 37°C water bath. The cells were washed in IMDM to remove the freeze medium. 5x10<sup>5</sup> cells in 50 µl were pipetted into separate wells of a 96-well polypropylene plate (Corning, Corning, NY.) 7 µl of primary-conjugated antibody against cell surface proteins was incubated with the cells for 30 minutes at room temperature. The cells were washed and resuspended in 50 µl of IMDM containing cytokines for stimulation for 15 minutes at 37°C. We have previously determined the concentrations needed to achieve maximum phosphorylation in dose response experiments. The concentrations of the cytokines used were as follows: IFN $\alpha$  (100 IU/ml), IFN $\gamma$  (1000 IU/ml), IL-2 (1000 IU/ml), IL-4 (100 ng/ml), IL-10 (100 ng/ml), PMA (100 nM). 50 µl of 2%

paraformaldehyde was added to give a final concentration of 1% and was left at room temperature for 10 minutes to fix the cells. The PBMC were washed in PBS to remove the fixative. For permeabilization, several different strategies were employed. Cells were either incubated with 200  $\mu$ l of varying concentrations of methanol, ethanol, isopropanol, or acetone at -20°C for 10 minutes. Alternatively, cells were permeabilized using 200  $\mu$ l of 0.5% BSA/0.1% sodium azide/0.1% saponin in PBS at room temperature for 10 minutes. Saponin-treated cells were washed in PBS/0.5% BSA/0.1% saponin, while the other treatment groups were washed in PBS. The cells were resuspended in 50  $\mu$ l of FACS buffer (10% FBS/0.1% sodium azide in PBS.) 7  $\mu$ l of phospho-specific primary-conjugated antibody was added to each well and was left at room temperature for 30 minutes. After incubation with antibody, the cells were washed in PBS + 0.2% Tween-20 for 10 minutes to eliminate non-specific binding. Labeled cells were resuspended in 250  $\mu$ l of FACS buffer in preparation for flow cytometry analysis.

#### **5.3.4 Western blotting of total and phospho-STAT**

PBMC are first magnetically separated into lymphocytes and monocytes using MACS CD14 positive selection (Miltenyi Biotec, Auburn, CA.) according to the manufacturer's suggestion. Monocytes and lymphocytes were either left untreated in IMDM or were treated with IL-2 at 1000 IU/ml for 15 minutes. Whole cell lysates were prepared by incubating the cells in lysis buffer (100 mM NaCl, 10 mM Tris (pH 8.4), 1% NP-40, phosphatase inhibitor cocktail I and II (Sigma, St. Louis, MO)) for 15 minutes. Following lysis, a BCA assay (Pierce Biotechnology, Rockford, IL) was performed to analysis total protein concentration within each of the lysates. Lysates were boiled for 5 minutes in XT buffer (Bio-Rad Laboratories, Hercules, CA) containing 10%  $\beta$ -mercaptoethanol. The samples were loaded into Criterion XT precast gels (Bio-Rad



Laboratories, Hercules, CA) at 10 $\mu$ g per lane. Proteins were separated by gel electrophoresis at 100V for 1.5 hours. The proteins were then transferred to nitrocellulose membranes (Bio-Rad Laboratories, Hercules, CA) at 100V for 45 minutes. After blocking the membrane in TBS containing 1% BSA overnight at room temperature, the membrane was probed with mouse anti-pSTAT5 at a 1:500 dilution for 1 hour at room temperature under constant agitation. After three 10 minutes washes with TBS containing 0.2% Tween-20, the blot was probed with HRP-conjugated donkey-anti-mouse IgG at 10 ng/ml for 1 hour at room temperature under constant agitation. The blot was washed three times with TBS containing 0.2% Tween-20. Supersignal West Pico Chemiluminescence Substrate (Pierce Biotechnology, Rockford, IL) was added to the blot according to the manufacturer's suggestion. After the blot was exposed to x-ray film for 10 minutes, the film was developed using a Kodak X-OMAT 2000A processor. Following developing, the blot was incubated in stripping solution (2.5 pH, 0.2M glycine, 0.05% Tween-20) at 80°C for 30 minutes. To ensure that stripping was complete, the blot was washed in TBS three times, then re-incubated in chemiluminescence substrate and re-exposed to x-ray film. The blot was re-probed for total STAT5 by first blocking the membrane at room temperature for one hour, then incubated rabbit anti-STAT5 at 1 $\mu$ g/ml at room temperature for one hour under constant agitation. Then blot was washed three times with TBS containing 0.2% Tween-20. HRP-conjugated goat-anti-rabbit IgG at a concentration of 10ng/ml was incubated with the blot for one hour at room temperature under constant agitation. The blot was washed three times with TBS containing 0.2% Tween-20. Chemiluminescence substrate was added to the blot according to the manufacturer's suggestions. After the blot was exposed to x-ray film for 30 seconds, it was developed.

### **5.3.5 Flow cytometric analysis of phospho-proteins**

A FACSAArray (BD Bioscience, Franklin Lakes, NJ) was used for flow cytometric analysis. The FACSAArray was first calibrated using Sphero Rainbow fluorescent particles (BD Bioscience, Franklin Lakes, NJ). After calibration, the 96-well plate containing the samples was placed into the instrument. The instrument automatically compensated for optical spillover using three set-up wells: one unlabeled, and two containing cells labeled with one of each of the fluorophores used. A gate was created around populations that stained positive for labeled cell surface proteins. Gates were also created around total lymphocyte and monocyte populations based on forward and side scatter intensities. 10,000 cells within the lymphocyte/monocyte gates were collected for each sample. FACSDiva software (BD Bioscience, Franklin Lakes, NJ) was used for data acquisition and off-line analysis. For each of the gated populations, the geometric mean fluorescence intensity was analyzed.

## **5.4 RESULTS**

### **5.4.1 Effects of saponin and 90% methanol permeabilization on intracellular and cell surface labeling**

PBMC were either left untreated in IMDM or were treated with 100 IU/ml of IFN $\alpha$  for 15 minutes at 37°C. Following fixation, cells were either permeabilized with 0.1% saponin or 90% methanol as described in the materials and methods section. All of the PBMC were labeled with anti-pSTAT1-PE. Additionally, anti-CD4-APC, anti-CD8-APC, anti-CD14-APC, and anti-CD56-APC were used to label untreated and treated cells in each permeabilization group. Figure

14 shows the dot plots of pSTAT1-PE fluorescence intensity versus that of the cell surface proteins. Quadrants have been set to gate on positive and negative populations. The top two rows represent untreated cells permeabilized with either saponin or methanol. It is readily apparent that saponin allows for better labeling of extracellular proteins than methanol, especially CD56 and CD14, but not for pSTAT1, as the upper quadrants are basically devoid of cells. Methanol allows one to visualize cells that presumably have basally phosphorylated STAT1 in the untreated group, where approximately 30% are positive in the CD14 population. Following IFN $\alpha$  stimulation, a large increase in STAT1 phosphorylation is evident only in methanol permeabilized cells, as indicated in the bottom row of Figure 14. With saponin permeabilization, there is no detectable change in activated STAT1. Thus, we have concluded that methanol permeabilization is necessary for the detection of phosphorylated STAT1, but this technique is not optimal for staining of cell surface proteins.

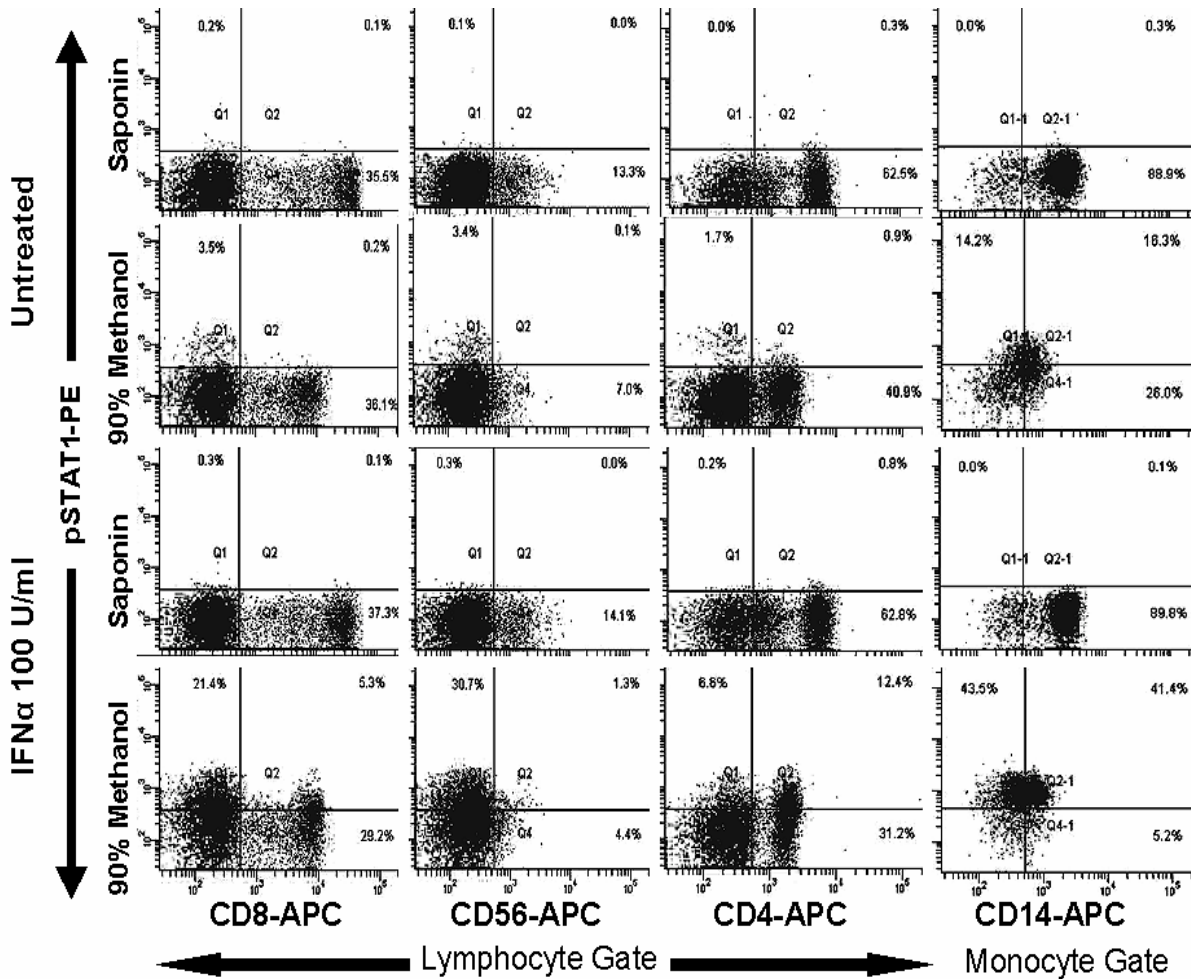


**Figure 14. Methanol is superior to saponin permeabilization for simultaneous staining of intracellular and cell surface proteins.** PBMC were untreated (upper two rows) or treated with 100 IU/ml of IFN $\alpha$  (bottom two rows) for 15 minutes at 37°C. Permeabilization was performed in 0.1% saponin or 90% methanol. Cells were labeled with APC-conjugated antibodies against CD8, CD56, CD4, or CD14 and with a PE-conjugated antibody to pSTAT1. CD14 labeled cells were collected in a monocyte gate, but all other cells were collected in a lymphocyte gate based on scatter. Intracellular labeling is best accomplished with methanol, while saponin is superior for cell surface labeling

#### **5.4.2 Use of a panel of different permeabilizing agents to enhance concurrent intracellular and cell surface detection**

Following 15 minutes of stimulation with 100 ng/ml of IL-4 or IMDM alone at 37° C, PBMC were fixed. Cells were then permeabilized in varying concentrations of methanol, ethanol, isopropanol, or acetone for 10 minutes at -20°C. Cells were labeled with both anti-pSTAT6-Alexa 647 and anti-CD56-PE. During flow cytometric acquisition, cells were divided into three gates: monocytes, lymphocytes, and CD56<sup>+</sup>, based on forward scatter, side scatter, and fluorescence intensity of CD56-PE. As expected, the upper panel of Figure 15 indicates that the GMFI of CD56 within the CD56<sup>-</sup> populations (monocytes and lymphocytes) is low. However, in the CD56<sup>+</sup> population, as shown, there is a large amount of variation in the GMFI of CD56-PE for each individual permeabilizing agent applied. Based on the upper figure, 70% methanol, 50% ethanol, all isopropanol concentrations, and all concentrations of acetone except 100%, allow for suitable identification and resolution of CD56<sup>+</sup> cells from negative cells. Additionally, the effectiveness of pSTAT6 labeling was examined by plotting the relative difference in GMFI of pSTAT6 (GMFI of IL-4 stimulated cells minus GMFI of untreated cells) versus the three gated cell populations. As shown in the lower panel of Figure 15, of the permeabilizing agents tested that enabled superior CD56 labeling, 70% methanol allows for maximal detection of pSTAT6. In fact, the GMFI of pSTAT6 is comparable to the group permeabilized with 90% methanol in the monocyte population, which is the current method utilized for detecting phospho-proteins [69]. The asterisks in the CD56<sup>+</sup> group indicate that insufficient cells were present to meaningfully assess the GMFI.

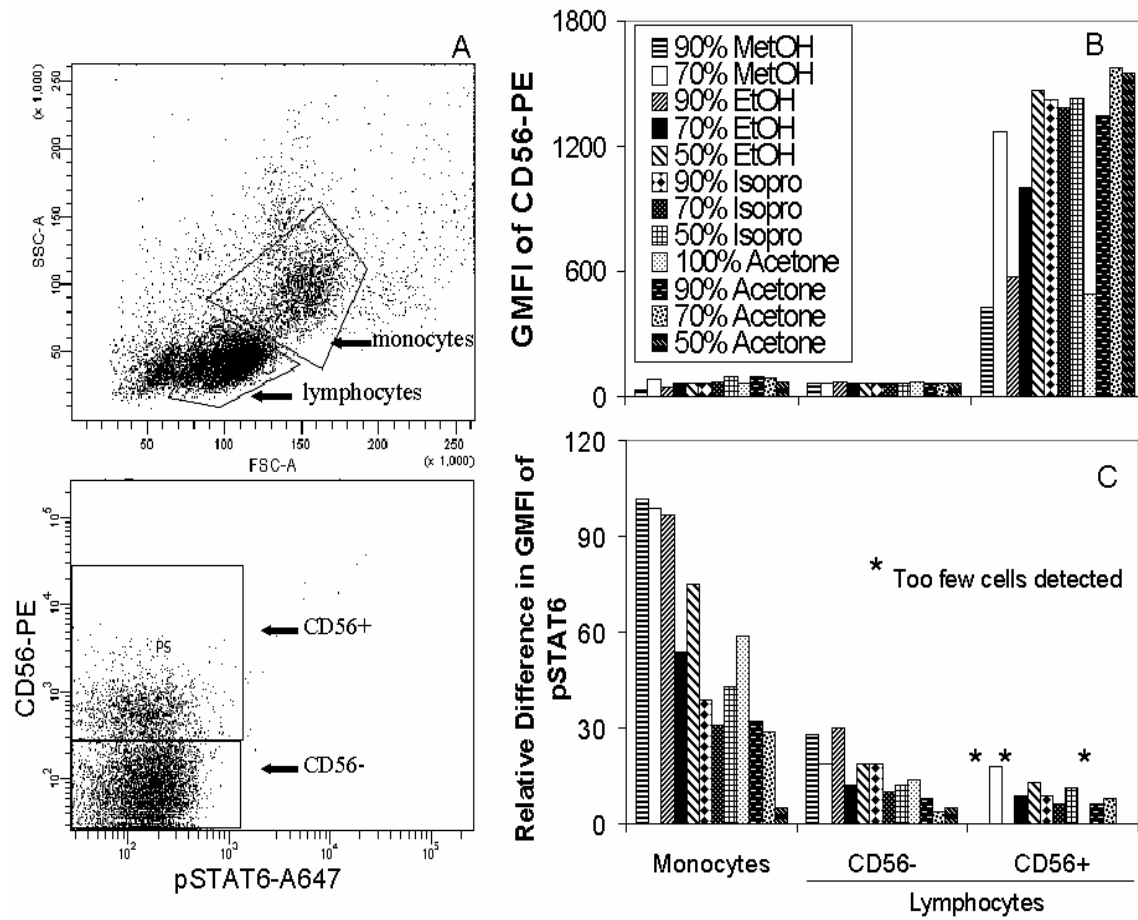


**Figure 15. Marked differences in intracellular and cell surface staining of proteins are noted using a panel of permeabilizing agents.** PBMC were either untreated or treated with 100 ng/ml of IL-4 for 15 minutes at 37°C. Cells were labeled with anti-CD56-PE and anti-pSTAT6-Alexa 647. The gating used to identify CD56<sup>+</sup> lymphocytes is indicated in panel A. The lymphocyte gate in the upper panel is used to create the CD56 gates in the lower panel. Cell surface labeling efficiency is shown as GMFI of anti-CD56-PE versus a gated cell population (monocytes, CD56<sup>-</sup>, or CD56<sup>+</sup> lymphocytes) for each permeabilization condition (panel B.) Intracellular labeling efficiency is represented as the relative difference in GMFI (IL-4 treated minus untreated) of anti-pSTAT6 (panel C.) Of the conditions tested, 70% methanol allowed for maximal simultaneous staining.

### **5.4.3 Varying methanol concentrations to improve simultaneous cell surface and intracellular labeling**

PBMC were treated identically as in the previous experiment, except the cells were permeabilized with a broader range of methanol concentrations alone at  $-20^{\circ}\text{C}$ . The upper panel of Figure 16 illustrates the effect that different methanol concentrations had on the GMFI of CD56-PE in the same three gated populations. As was expected, the GMFI was very low in both CD56<sup>-</sup> populations. There was a negative correlation between the GMFI of CD56-PE and methanol concentration in the CD56<sup>+</sup> gate. A distinct population of CD56<sup>+</sup> cells was first identifiable at a concentration of 75% methanol and further dilutions. In the lower panel of Figure 16, intracellular labeling is examined once again by plotting the relative difference in GMFI of pSTAT6 versus the three gated populations. In a few cases, mainly with 0% methanol (PBS), i.e. not permeabilized, there were negative values for the relative difference in GMFI. This likely occurred because the auto-fluorescence of the untreated cells was greater than that of the IL-4 treated cells. Within the monocyte gate, 90% methanol seemed to give a lower GMFI for pSTAT6 compared to slightly lower concentrations, but this is also likely due to untreated cells having higher autofluorescence. At methanol concentrations of 70% or less, there is a decrease in the GMFI of pSTAT6 in both CD56<sup>-</sup> populations. 80-85% methanol allows for superior detection of pSTAT6, but these concentrations did not enable satisfactory labeling of CD56. The asterisks in the lower panel indicate that these concentrations did not generate enough identifiable CD56<sup>+</sup> cells to calculate a meaningful GMFI. The next greatest GMFI in pSTAT6 occurs when 75% methanol was used, which also permitted a CD56<sup>+</sup> population to be gated. Considering these results, 75% methanol is the permeabilization condition of choice, enabling superior detection of both cell surface and intracellular proteins simultaneously.

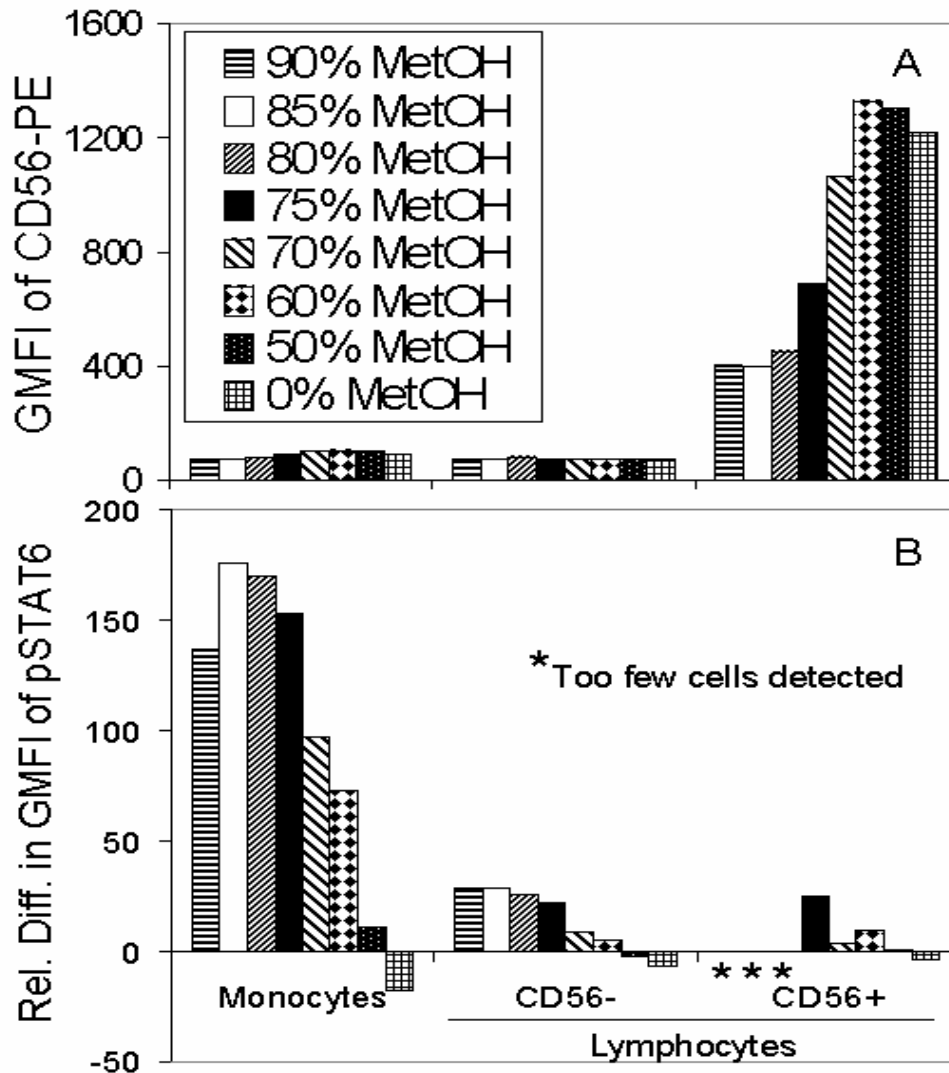


**Figure 16. 75% methanol enables simultaneous intracellular and cell surface labeling.** PBMC were either untreated or treated with 100 ng/ml of IL-4 for 15 minutes at 37°C. Following permeabilization with varying concentrations of methanol, cells were labeled with anti-CD56-PE and anti-pSTAT6-A647. GMFI of anti-CD56-PE versus a gated cell population (monocytes, CD56<sup>-</sup>, or CD56<sup>+</sup> lymphocytes) is plotted for each permeabilization condition (upper panel.) Intracellular labeling efficiency is represented as the relative difference in GMFI (IL-4 treated minus untreated) of anti-pSTAT6 (lower panel.) To maximize both intracellular and cell surface labeling, 75% methanol appeared to give the best results.



#### **5.4.4 Characterization of differential responses in protein phosphorylation in PBMC subtypes following cytokine stimulation**

In this set of experiments, PBMC were either left untreated in IMDM or were treated with IFN $\gamma$  (1000 IU/ml), IL-10 (100 ng/ml), IL-2 (1000 IU/ml), IL-4 (100 ng/ml), or PMA (100 nM) for 15 minutes at 37°C. All of the cells were fixed, washed, and then permeabilized in 75% methanol for 10 minutes at -20°C. Both untreated and cytokine stimulated cells were labeled with antibodies against anti-CD4-PE, anti-CD8-PE, anti-CD19-PE, or anti-CD56-PE. Depending on which cytokine was used to treat the cells, untreated and treated PBMC were labeled with Alexa 647-conjugated antibodies to STAT1, pSTAT3, pSTAT5, pSTAT6, pp38 MAPK, or pERK1/2. During analysis of individual phospho-proteins, there were four sets of untreated and cytokine-treated cells except for pSTAT1 labeled cells due to low cells counts in the CD56 labeled group. Because monocytes were gated in each of these groups based on scatter properties alone, their results are represented as the mean of four comparable conditions including standard error bars. Figure 17 shows the mean GMFI of all the labeled phospho-proteins in both unstimulated and stimulated monocytes. Treatment of PBMC with IL-2 or PMA did not appear to significantly increase the phosphorylation of STAT5 or p38 MAPK in monocytes. The absence of STAT5 phosphorylation in monocytes following IL-2 stimulation is confirmed by Western blot as well (Figure 19a.) On the other hand, IFN $\gamma$ , IL-10, IL-4, and PMA induced phosphorylation of STAT1, STAT3, STAT6, and ERK1/2 respectively in monocytes. The error bar is large on the IFN $\gamma$  treated cells, which is due to the mean being calculated from three rather than four samples and one outlier in the data.

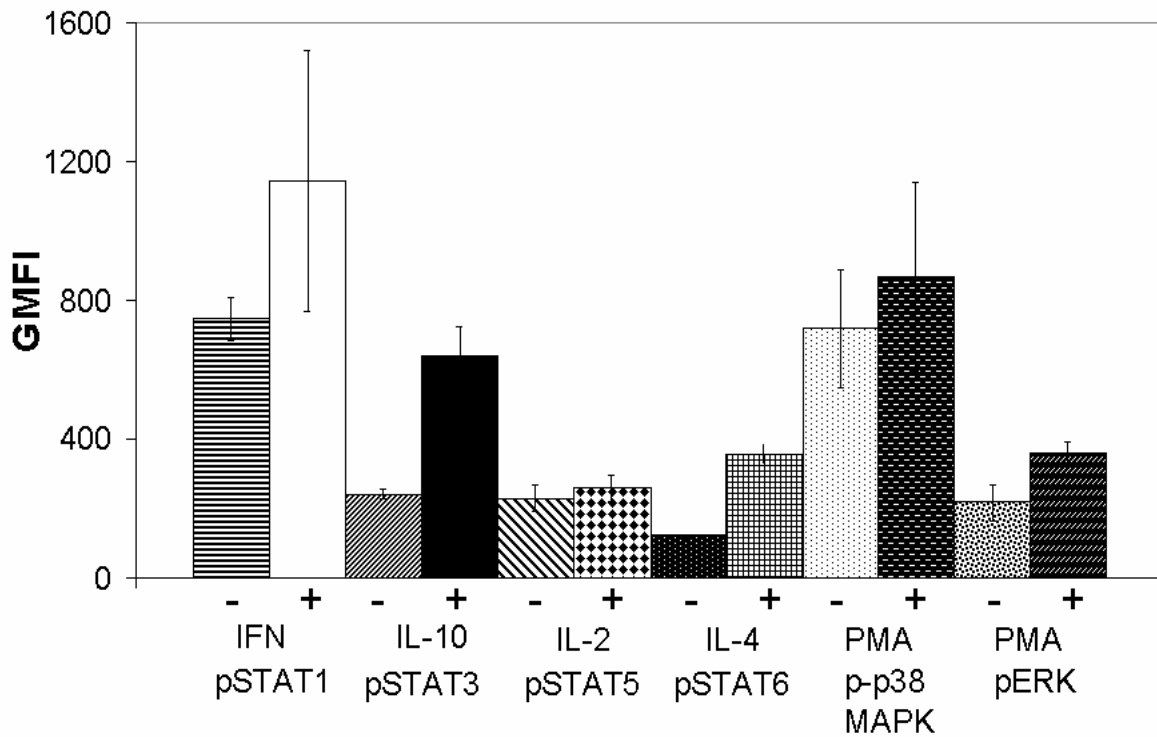


**Figure 17. Remarkable differences in individual phospho-proteins are detected in monocytes.** PBMC were untreated or treated with IFN $\gamma$  (1000 IU/ml), IL-10 (100ng/ml), IL-2 (1000 IU/ml), IL-4 (100 ng/ml), or PMA (100nM) for 15 minutes at 37°C. All cells were permeabilized in 75% methanol. Monocytes were gated based on scatter properties. Cells were labeled with Alexa 647-conjugated antibodies against pSTAT1, pSTAT3, pSTAT5, pSTAT6, p38 MAPK, or ERK1/2. GMFI of monocytes was measured in four samples per condition and the standard deviation is included as error bars.

In Figure 18, lymphocytes are grouped into panels based on the phospho-protein being analyzed. Within each panel the GMFI of the labeled phospho-protein is plotted against cells positive for CD19, CD4, CD8, or CD56. IFN $\gamma$  appears to have modest effects on STAT1 phosphorylation in lymphocytes, CD4<sup>+</sup> cells being the most responsive of the subsets examined. All PBMC subsets phosphorylated STAT3 in response to IL-10, CD19<sup>+</sup> cells being the least responsive. STAT5 was phosphorylated to the greatest degree in CD4<sup>+</sup> cells, followed by CD8<sup>+</sup> and CD56<sup>+</sup> cells after IL-2 treatment. In contrast, CD19<sup>+</sup> cells appeared to be unresponsive to IL-2. To confirm that STAT5 is indeed phosphorylated in lymphocytes following IL-2 stimulation, a Western blot was performed. Figure 19b clearly verifies that phosphorylated STAT5 is present only in IL-2 stimulated lymphocytes. Following incubation with IL-4, all PBMC subsets increased STAT6 phosphorylation relatively equally. Likewise, all groups of cells examined induced phosphorylation of ERK1/2 similarly following PMA treatment. PMA stimulation also resulted in phosphorylation of p38 MAPK within all subsets tested, but only modestly within CD4<sup>+</sup> cells. Another observation taken from Figures 17 and 18 is that fluorescence in untreated cells labeled for pSTAT1 is higher than that of other phospho-proteins. This could be due to increased basal phosphorylation levels in STAT1 compared to other family members, suggesting some possible chronic release and exposure to interferon family members. At least for STAT5, Western blot confirms that there is basically no phosphorylation present in the unstimulated cells. Additionally, fluorescence intensity is higher in untreated monocytes labeled for pp38 MAPK, likely due to increased basal activity as well.

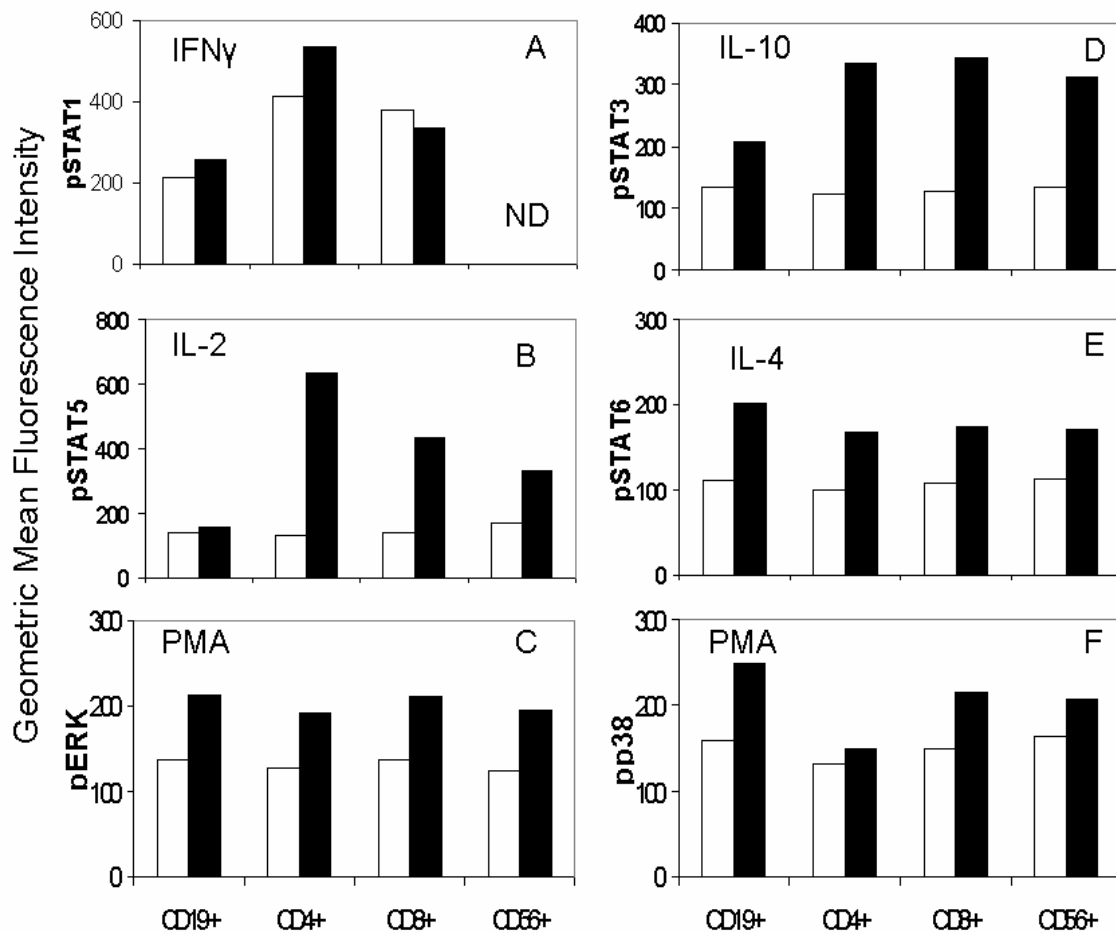


**Figure 18. Phospho-protein analysis reveals differential responsiveness of CD19<sup>+</sup>, CD4<sup>+</sup>, CD8<sup>+</sup>, and CD56<sup>+</sup> cells to individual cytokines.** PBMC were untreated (unfilled bars) or treated with IFN $\gamma$  (1000 IU/ml), IL-10 (100ng/ml), IL-2 (1000 IU/ml), IL-4 (100 ng/ml), or PMA (100nM) (filled bars) for 15 minutes at 37°C. The treatment that each group of cells received is in the upper left corner. All cells were permeabilized in 75% methanol. Cells were labeled with PE-conjugated antibodies to CD19, CD4, CD8, or CD56 and Alexa 647-conjugated antibodies to pSTAT1 (panel A), pSTAT5 (panel B), pERK (panel C), pSTAT3 (panel D), pSTAT6 (panel E), or pp38 (panel F.) The GMFI of each labeled phospho-protein was plotted against cells gated positive for the labeled cell surface protein. (ND) indicates not determined due to low cell counts.

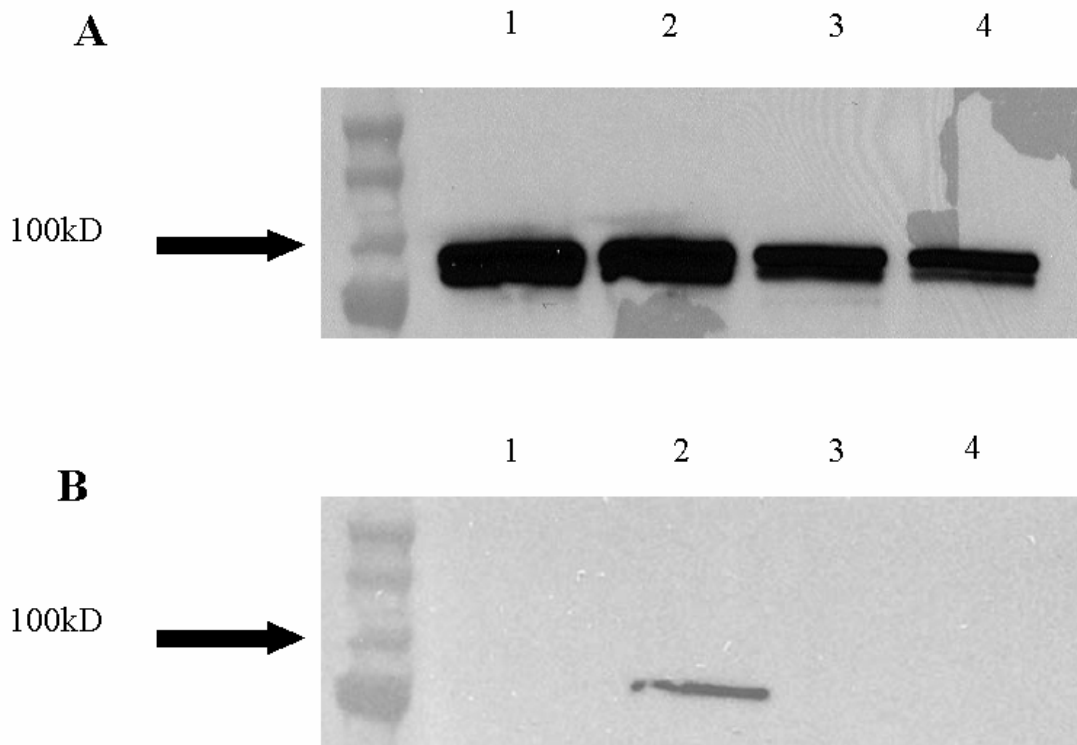


**Figure 19. Western blot confirms differential protein phosphorylation in distinct cell types.** PBMC were separated into monocytes and lymphocytes and were either treated with IL-2 or left untreated. The amount of total STAT5 is comparable between monocytes/lymphocytes and does not change following IL-2 stimulation (panel A.) There is no basal phosphorylation of STAT5 within lymphocytes/monocytes and STAT5 is phosphorylated in lymphocytes alone following IL-2 stimulation (panel B), confirming previous results in figures 4 and 5 obtained by flow cytometry. 1: unstimulated lymphocytes; 2: IL-2 (1000 IU/ml) stimulated lymphocytes; 3: unstimulated monocytes; 4: IL-2 (1000 IU/ml) stimulated monocytes.

#### 5.4.5 Inter- and intra-individual variability in STAT phosphorylation

For inter-individual variability experiments, PBMC were isolated from three different individuals on the same day. For intra-individual variability experiments, PBMC were isolated from one individual three times over a course of ten months. All cells were frozen, thawed on the same day, and used in the same experiment to evaluate STAT phosphorylation. PBMC were either treated with IL-10 (100 ng/ml), IL-2 (1000 IU/ml), IFN $\alpha$  (1000 IU/ml) or left untreated in IMDM for 15 minutes at 37°C. Following cytokine stimulation and fixation, cells were permeabilized in 75% methanol as noted above. Untreated and treated cells were labeled with Alexa 647-conjugated antibodies to pSTAT1, pSTAT3, or pSTAT5. Additionally, cells were labeled with PE-conjugated antibodies against CD4, CD8, CD19, or CD56.

In Figure 20, inter-individual variability is represented by plotting the GMFI of each labeled phospho-STAT for each individual within a positive-gated subset of cells. Monocytes were gated based on scatter properties. In agreement with previously shown data, following IL-2 treatment, STAT5 is not phosphorylated in the monocyte or CD19<sup>+</sup> populations of all individuals. Also in agreement with previous data, STAT5 is phosphorylated primarily within the CD4<sup>+</sup> population, followed by CD8<sup>+</sup> and CD56<sup>+</sup> populations. After treatment with IL-10, STAT3 is phosphorylated in all cell types examined, but predominantly within the monocytes. There is some variability in individual responses, but referring to Table 2, the CVs are less than 20 for most of the treatment conditions. It is interesting to note that one healthy individual consistently had lower levels of phosphorylation in both STAT proteins in all PBMC subsets tested.

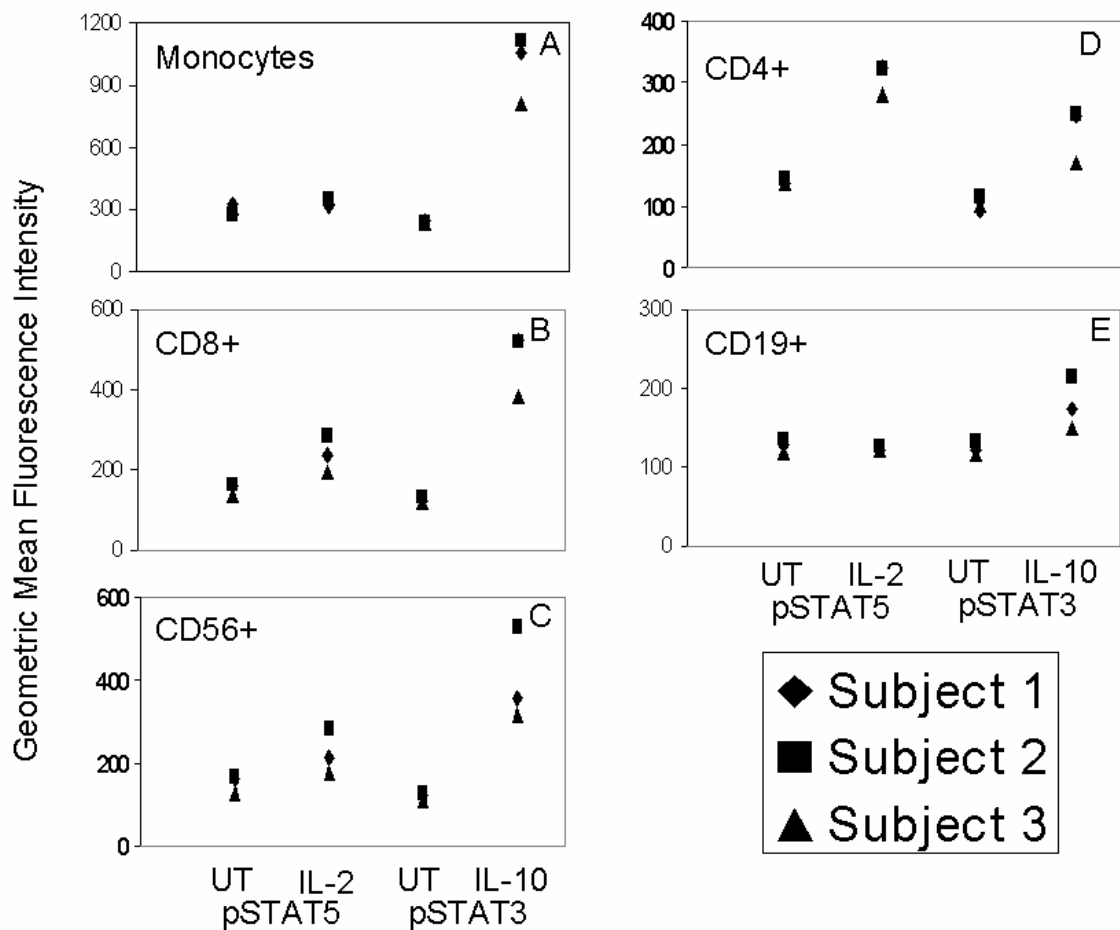


**Figure 20. Modest inter-individual variability in protein phosphorylation.**

PBMC were isolated from three different individuals on the same day. The cells were untreated or treated with IL-2 (1000 IU/ml) or IL-10 (100 ng/ml) for 15 minutes at 37°C. Gates were set on monocytes (panel A) based on scatter properties and cells positively labeled for CD8 (panel B), CD56 (panel C), CD4 (panel D), and CD19 (panel E.) Within these gates, GMFIs of labeled pSTAT5 and pSTAT3 were measured. Different shapes encoded in the legend represent the three subjects.

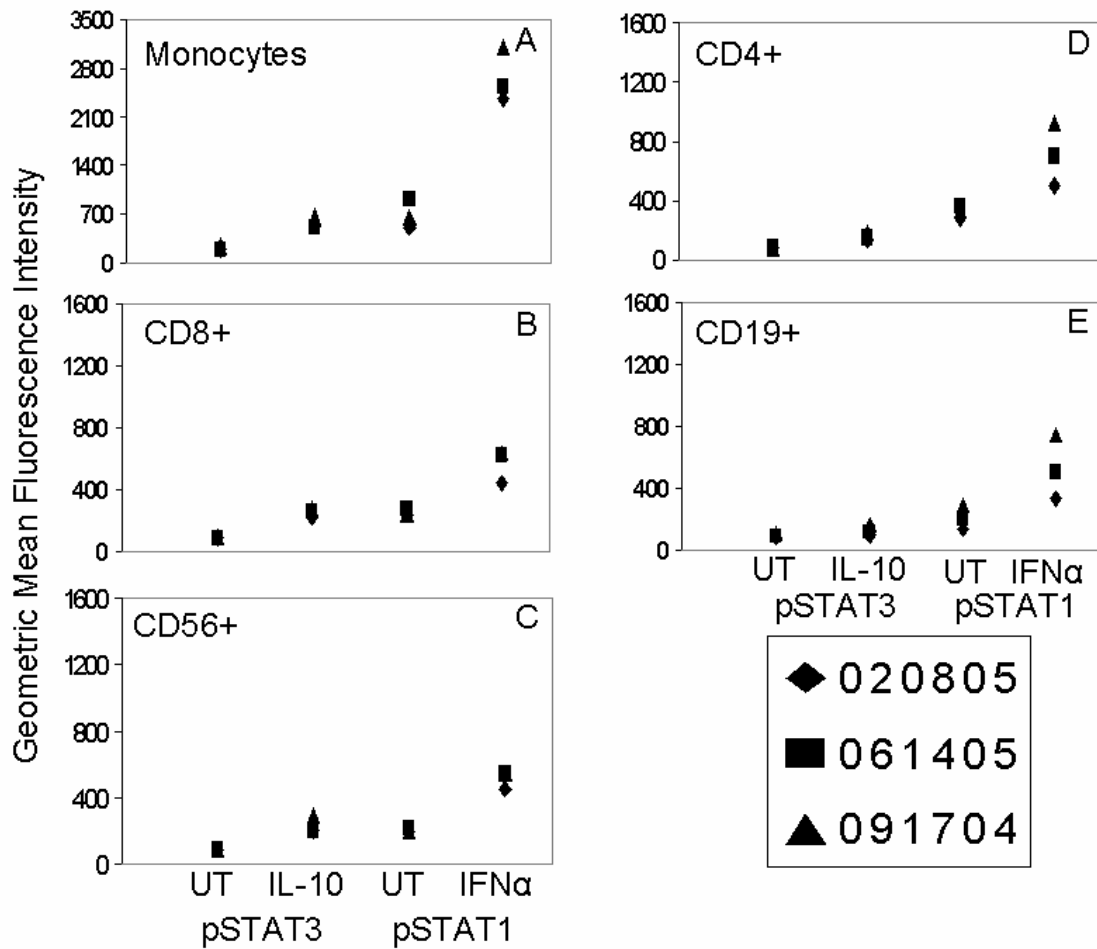
**Table 2. Multiple donor variability in STAT phosphorylation.** This table summarizes the results in Figure 20. The GMFI was averaged for labeled pSTAT5 and pSTAT3 in unstimulated and stimulated cells from all three donors and the coefficient of variance was calculated.

Table 2. Multiple Donor Variability in STAT Phosphorylation

Gated Population	pSTAT5				pSTAT3			
	UT		IL-2		UT		IL-10	
	Avg. GMFI	CV (%)	Avg. GMFI	CV (%)	Avg. GMFI	CV (%)	Avg. GMFI	CV (%)
Monocytes	303.3	8.1	339.0	5.6	238.3	2.7	993.7	16.3
CD4+	139.7	2.7	309.0	9.8	103.0	10.8	221.7	20.2
CD8+	154.0	10.2	238.3	19.3	125.7	4.8	475.7	16.7
CD19+	127.3	6.3	123.3	2.6	123.7	7.0	179.7	18.3
CD56+	153.3	14.4	225.3	23.0	121.7	7.2	400.0	27.9



The results of the intra-individual variability experiment are shown in Figure 21 with the dates of each draw included in the legend. The amount of time that cells spent frozen did not seem to correlate with responsiveness, as cells frozen the longest were usually most responsive and cells frozen the shortest amount of time had intermediate responsiveness. Once again, the relative responsiveness of the cells appeared to be consistent within each cell type and for each STAT protein. When compared to STAT3, STAT1 phosphorylation levels appear to be higher in untreated cells, which were observed in previous experiments as well. Similar to the inter-individual variability, the CVs for STAT phosphorylation within a single individual were mostly less than 20, as indicated in Table 3. There were large CVs in STAT1 phosphorylation in untreated monocytes and CD19 cells and IFN $\alpha$ -treated cells within CD4 and CD19 subsets, suggesting some heterogeneity of responsiveness. Likewise, CVs were also somewhat high for pSTAT3 in IL-10 treated CD19 and CD56 cells. These differences could be of modest importance if larger sample sizes [which we are now examining in patients with melanoma on immunotherapy regimens] were obtained.



**Figure 21. Limited intra-individual variability in protein phosphorylation.** PBMC were isolated three times from a single individual over ten months. The cells were untreated or treated with IL-10 (100 ng/ml) or IFN $\alpha$  (1000 IU/ml) for 15 minutes at 37°C. Gates were set on monocytes (panel A) based on scatter properties and cells positively labeled for CD8 (panel B), CD56 (panel C), CD4 (panel D), and CD19 (panel E.) Within these gates GMFIs of labeled pSTAT3 and pSTAT1 were measured. The dates of the blood draws are included next to the shapes in the legend.

**Table 3. Single donor variability in STAT phosphorylation.** This table summarizes the results in Figure 21. The GMFI was averaged for labeled pSTAT3 and pSTAT1 in unstimulated and stimulated cells from each of the three blood draws and the coefficient of variance was calculated.

Table 3. Single Donor Variability in STAT Phosphorylation

Gated Population	pSTAT3				pSTAT1			
	UT		IL-10		UT		IFN $\alpha$	
	Avg. GMFI	CV (%)	Avg. GMFI	CV (%)	Avg. GMFI	CV (%)	Avg. GMFI	CV (%)
Monocytes	207.7	11.6	567.3	14.9	691.7	30.6	2663.0	14.6
CD4+	84.7	0.7	154.3	14.7	327.0	12.9	708.3	29.7
CD8+	87.3	6.7	248.0	10.8	247.0	10.2	562.3	19.4
CD19+	91.0	15.5	123.7	27.6	209.3	37.1	524.7	39.7
CD56+	87.0	3.0	230.3	22.4	205.3	4.9	516.0	10.7

## 5.5 DISCUSSION

Our objective was to develop a robust methodology to detect activated signaling pathways within all major PBMC subpopulations by simultaneously staining cell-specific surface epitopes and intracellular phosphorylated proteins for flow cytometry. By using a flow cytometric strategy, evaluation and set-up time is greatly reduced and fewer cells are required when compared with alternative techniques including Western blotting. Western blotting and flow cytometry provide similar qualitative results for phospho-protein analysis [19, 69, 116], as we have also demonstrated in this report. Flow cytometry, however, offers greater sensitivity and allows one to identify individual cells with differences in responsiveness, rather than a mean value for the total cell population without separating cells prior to stimulation and analysis.

We began by comparing saponin permeabilization, which is a standard technique for labeling many intracellular proteins [17, 139], to 90% methanol, which was recently established for staining of phosphorylated proteins [69]. In saponin treated cells, detection of phosphorylated proteins was severely impaired, however labeling of surface proteins improved. With 90% methanol treatment, CD14 and CD56 positive cells were virtually undetectable. Thus, it appears that methanol compromises the labeling of surface epitopes given currently available commercial antibodies, some more than others, while saponin is unable to allow staining antibodies access to intracellular phosphorylated epitopes.

When permeabilized with acetone and a panel of alcohols at varying concentrations, the phospho-protein signal was greatest at higher concentrations, whereas surface protein staining decreased. Of the permeabilizing conditions tested, methanol provided maximal detection of phosphorylated proteins. Based on this, we permeabilized cells with a broader range of methanol concentrations to maximize both intracellular and cell surface labeling. 75% methanol provided

an increase in the detection of surface protein, CD56, and staining of phospho-protein equivalent to 90% methanol. This concentration seems to be sufficient to expose the phosphorylated epitope within cells while limiting detrimental effects to surface epitopes. In addition, phosphorylation patterns were consistent with previous studies of dose and timing of responsiveness of individual populations as we have previously reported.

This technique resulted in low variability when applied to a single, healthy donor at different time points or several, healthy donors at a single time point. The CV for the level of activated signaling protein was less than 20% in most cases for both treated and untreated cells. The relatively low levels of variability associated with this method hold promise that differences in cellular responsiveness will be detected between healthy individuals and those with abnormal signaling pathways in various disorders.

The conditions that we developed enabled us to visualize the differential effects of cytokines on signaling proteins within major subpopulations of PBMC, which were gratifying and quite substantial. One can imagine that this technique may also be readily applied to rare populations of cells, such as mDCs and pDCs. In acute and chronic inflammation and cancer, our studies and others suggest that PBMC are disordered in both their number and function [133, 134, 140, 141]. Dysfunctional signaling could result from persistent cytokine release, homeostatic inhibition mediated by suppressor of cytokine signaling [SOCS] proteins, other proteins elicited within pathological environments, or by pathogens interfering with normal signaling. Because of the ease with which this technique is performed and the availability of blood samples from patients, this technique holds promise to enumerate specific cell populations from patients while evaluating their functional integrity in a clinical laboratory. By detecting

abnormal cell populations and some of the changes in responsiveness to cytokine signals, this method can also be used potentially to enable and monitor pharmacologic intervention and treatment, as well as monitor response to treatment.

We have described here a simple and easily applied technique to simultaneously detect surface epitopes and intracellular phosphorylated signaling proteins within PBMC by flow cytometry. The ability to use banked, frozen PBMC enables this flow-cytometric technique to be readily applied in the clinic as a diagnostic tool or to monitor effects of immunosuppressive or immunostimulatory reagents such as FK506, cyclosporine, rapamycin, IL-2, CTLA4 antibody, and possibly pathogen or damage associated molecular pattern molecules [PAMPs/DAMPs] including HMGB1[132] or CpG molecules. Furthermore, this technique is clinically applicable due to its technical simplicity and the low number of cells required for analysis. We conclude that combining immunophenotyping with a rapid, cytometric assay to detect the integrity of signaling pathways is a remarkably valuable tool in assessing discrete cell populations within complex mixtures in the setting of both acute and chronic diseases including autoimmunity and cancer.

## 6.0 SUMMARY AND FUTURE DIRECTIONS

As demonstrated here, a flow cytometric-based assay is a rapid and robust platform for measuring activated signaling pathways within a complex mixture of cells. We were able to identify cytokines, as well as their most effective concentrations and duration of application that elicit maximal phosphorylation of a number of target signaling proteins within the JAK/STAT and MAP kinase pathways including STAT1, STAT3, STAT5b, STAT6, ERK1/2, and p38 MAPK. By manipulating the permeabilization conditions, we were able to successfully stain for intracellular phosphorylated proteins in combination with cell surface proteins used to identify subpopulations of PBMC, such as CD4, CD8, CD14, CD19, and CD56, which we have published [142]. Furthermore, this technique afforded the ability to examine differential phosphorylation within distinct cell types following application of identical stimuli, even without dual cell surface/intracellular staining, but by gating on lymphocytes and monocytes based on their intrinsic forward and side scatter properties. Lastly, the technique developed herein resulted in a relatively low degree of variability when applied to PBMC from multiple individuals, as well as PBMC acquired from a single individual at different time points. These findings strengthen our belief that this approach will be useful for identifying differences between healthy individuals and those with disease.

Taken together, these results illustrate that flow cytometric measurement of activated signaling pathways is a powerful technique to rapidly analyze function within subsets of cells

comprising complex populations without excessive manipulation and separation. Additionally, the results obtained by flow cytometry are qualitatively comparable to those acquired by the more time-consuming bulk analysis method, Western blotting. Because our technique uses PBMC, which is a readily attainable source of cells, and the protocol is extremely rapid, it is very likely that this method will be of utility to scientists to define abnormalities in signaling within the setting of various inflammatory conditions, including cancer, rheumatoid arthritis [143, 144], inflammatory bowel disease [140, 145, 146], systemic lupus erythematosus [147], and infectious diseases. Furthermore, once these disease-specific differences have been established, it may even be used as a diagnostic tool, where certain disorders are associated with an activation signature, meaning a defined group of proteins are abnormally phosphorylated in the context of a particular disorder. To increase the likelihood of finding differences in activation between normal and disease states, protein microarrays using PSSAs could be utilized prior to the flow cytometric analysis. In this way, the array could be used to rapidly screen a large number of phosphorylated proteins to identify potential targets. Thereafter, the assay developed in this thesis could be used to pinpoint the aberrant cell type and its frequency. Without much further development, flow cytometric analysis of phosphorylated proteins could be applied to therapeutic monitoring, such as administration of IL-2 and subsequent analysis of STAT5 phosphorylation or blood could be drawn over the course of treatment to see if abnormal activation has subsided.

At this point, little is known about the effects of factors such as age, obesity, smoking, or gender on phosphorylation events in signaling pathways. Before utilizing this technique to analyze clinical samples, it should be applied to a much larger, diverse population of disease-free individuals to first define normal phosphorylation levels and their variability, both in basal and



cytokine-perturbed states. This should illuminate any differences in signaling due to environmental, gender, or age-related factors. Alternatively, phospho-signaling pathways could be analyzed directly between different groups of individuals to determine if the aforementioned factors indeed alter phosphorylation events. Another option to avoid any environmental influences is to use samples taken from the same individual before and after therapy, which is what we have done in the following initial study.

As a preliminary study to apply our developed methodology to a clinical disorder, we evaluated STAT1, STAT3, STAT5b, STAT6, p38 MAPK, and ERK phosphorylation, pre- and post *in vitro* stimulation with cytokines, within total PBMC isolated from stage IV melanoma patients before and after combined anti-CTLA4/IL-2 therapy. We received cells from 13 patients at points before and after therapy with roughly an equal number of patients either not responding, partially responding, or completely responding to therapy. Of these patients, some also developed autoimmunity. Our analysis objectives were to determine if combined anti-CTLA4/IL-2 therapy, or the presence of tumor or autoimmunity affects the baseline activation state of PBMC and/or the ability of PBMC to respond to stimuli. To negate the influence of cell viability on differences in phosphorylation, we measured cell viability by annexin V and Sytox orange staining prior to fixation. We analyzed responses within lymphocytes and monocytes by gating on forward and side scatter, as well as within CD4<sup>+</sup> lymphocytes, by including a fluorophore-conjugated antibody to CD4. Many of the samples were analyzed in triplicate to improve statistical analysis. Since there were roughly 72 samples for each phospho-protein target, giving a total of approximately 432 samples, we required the assistance of statisticians for analysis. Based on data obtained from literature, we would expect to observe differences in phosphorylation in the presence of melanoma or in autoimmunity, as abnormal levels of

cytokines, growth factors, and endogenous danger signals are commonly detected in the serum. We have had a preliminary meeting to go over the results of the statistical analysis, which are premature to include in this thesis. There are some provocative early notions that should be noted: All patients demonstrated greater IL-10 responsiveness following therapy, but this was especially noteworthy in the patients with autoimmunity. Indeed the pSTAT3 response to IL-10 was substantially less in those with complete responses to clinical therapy when comparing pretreatment and late responses. IL-2, one of the agents that they were clinically treated with, promotes STAT5 responses and there appeared to be enhanced responsiveness following therapy in those with autoimmunity, as did phospho-p38 in response to phorbol ester stimulation in CD4+ cells. Given the relatively small patient numbers these results will need to be confirmed in a greater number of patients.

In our studies, the number of parameters was limited to two, a cell surface protein to identify a subset of cells, and an intracellular phosphorylated protein. Since we are using a flow cytometric method, additional parameters can easily be added, such as antibodies toward negative regulators of signaling. Although these studies were performed on peripheral blood cells, the methodology should be applicable to many other cell types, especially those within complex mixtures including aspirates from solid tumors. Furthermore, due to the evolution of robotics, this technique could possibly become fully automated in the future. Through the use of automated liquid handling systems, such as the Biomek FX, it would be possible to perform all of the upfront sample preparation, including cytokine stimulation, fixation, permeabilization, and labeling without manual involvement. Additionally, robotics could also load barcoded culture plates containing samples into already automated flow cytometers. By including robotics and automation, it should be possible to increase the high-throughput nature of the technology, as

well as possibly limit sample variability caused by inaccuracies associated with manual pipetting and sample preparation. In summary, the methods developed in this thesis provide an excellent stepping-stone for more in-depth studies regarding cell activation and its involvement in disease.

## APPENDIX

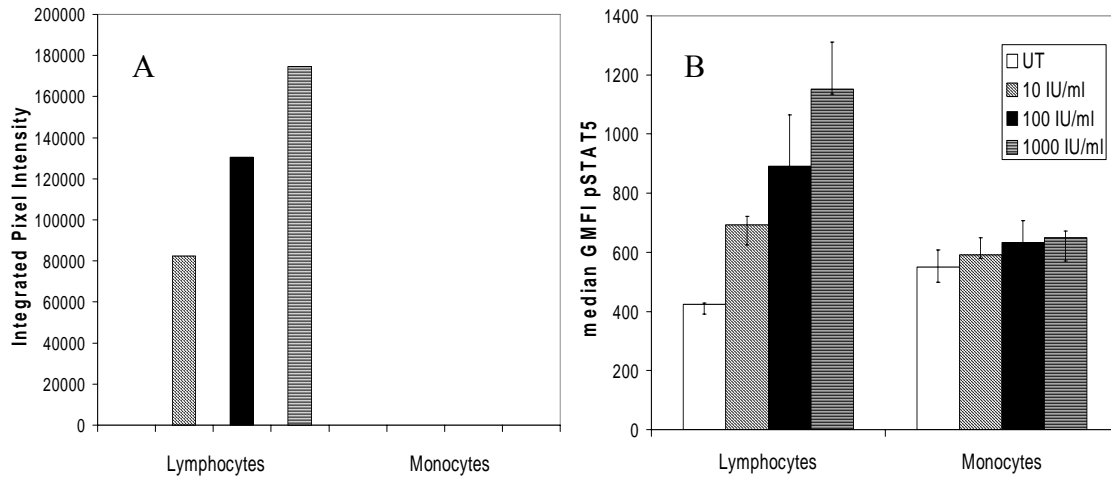


**Figure 22. Flow cytometry and Western blot provide similar results for IL-2 dose-dependent STAT5 phosphorylation.** Lymphocytes and monocytes were left untreated or were treated with increasing concentrations of IL-2 as indicated. In panel A, bands from figure 10A were analyzed by ImageJ densitometry software and the integrated pixel intensities were plotted. In panel B, median GMFIs of pSTAT5-A647 from figure 10A are plotted. There is a contribution of autofluorescence when obtaining data by flow cytometry, as indicated in the monocytes and untreated lymphocytes. Both flow and Western blotting provide qualitative results.

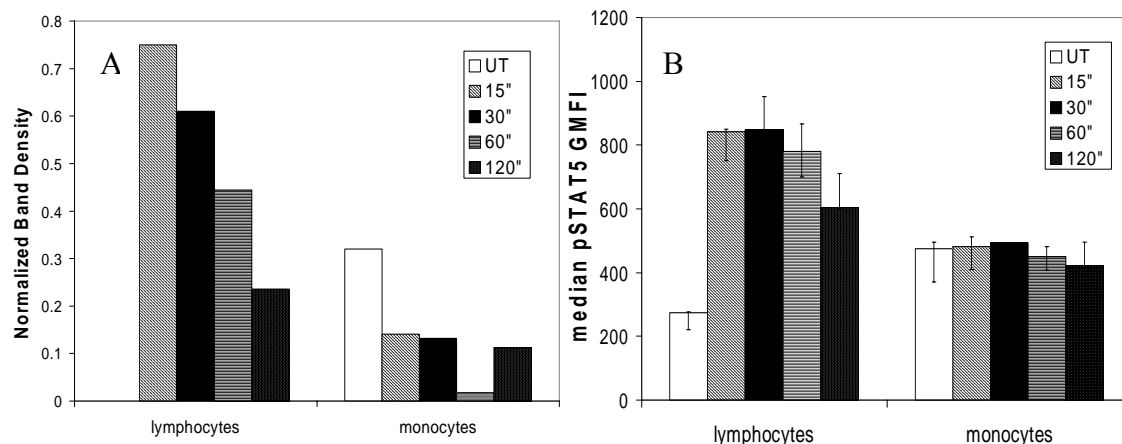


**Figure 23. Flow cytometry and Western blot provide similar results for IL-2 time-dependent STAT5 phosphorylation.**

Lymphocytes and monocytes were left untreated or were treated with 1000 IU/ml of IL-2 for the indicated time intervals. In panel A, bands from figure 10B were analyzed by ImageJ densitometry software and the integrated pixel intensities were normalized to total STAT5 and plotted. In panel B, median GMFIs of pSTAT5-A647 from figure 10B are plotted. There is a contribution of autofluorescence when obtaining data by flow cytometry, as indicated in the monocytes and untreated lymphocytes. Furthermore, it appears that there is artifactually increased phosphorylation in untreated monocytes, presumably due to increased manipulation in Western blotting. Upon IL-2 treatment, there is no increase in pSTAT5 in monocytes, but only in lymphocytes. Both flow and Western blotting provide qualitative results.

## BIBLIOGRAPHY

1. Maecker, H.T., et al., *Standardization of cytokine flow cytometry assays*. *BMC Immunol*, 2005. 6(1): p. 13.
2. Zhang, M., et al., *Lymphocyte subsets in hemophilic patients with hepatitis C virus infection with or without human immunodeficiency virus co-infection: a nested cross-sectional study*. *BMC Blood Disord*, 2005. 5(1): p. 2.
3. Tsunemi, S., et al., *Relationship of CD4+CD25+ regulatory T cells to immune status in HIV-infected patients*. *Aids*, 2005. 19(9): p. 879-886.
4. Rouzioux, C., et al., *Early Levels of HIV-1 DNA in Peripheral Blood Mononuclear Cells Are Predictive of Disease Progression Independently of HIV-1 RNA Levels and CD4+ T Cell Counts*. *J Infect Dis*, 2005. 192(1): p. 46-55.
5. Manzi, S., et al., *Measurement of erythrocyte C4d and complement receptor 1 in systemic lupus erythematosus*. *Arthritis Rheum*, 2004. 50(11): p. 3596-604.
6. Liu, C.C., J.M. Ahearn, and S. Manzi, *Complement as a source of biomarkers in systemic lupus erythematosus: past, present, and future*. *Curr Rheumatol Rep*, 2004. 6(2): p. 85-8.
7. Ormandy, L.A., et al., *Increased populations of regulatory T cells in peripheral blood of patients with hepatocellular carcinoma*. *Cancer Res*, 2005. 65(6): p. 2457-64.
8. Zea, A.H., et al., *Arginase-producing myeloid suppressor cells in renal cell carcinoma patients: a mechanism of tumor evasion*. *Cancer Res*, 2005. 65(8): p. 3044-8.
9. Zimmermann, S.Y., et al., *A novel four-colour flow cytometric assay to determine natural killer cell or T-cell-mediated cellular cytotoxicity against leukaemic cells in peripheral or bone marrow specimens containing greater than 20% of normal cells*. *J Immunol Methods*, 2005. 296(1-2): p. 63-76.
10. Hsueh, E.C., et al., *Peripheral blood CD4+ T-cell response before postoperative active immunotherapy correlates with clinical outcome in metastatic melanoma*. *Ann Surg Oncol*, 2004. 11(10): p. 892-9.

11. Maki, A., et al., *Decreased expression of CD28 coincides with the down-modulation of CD3zeta and augmentation of caspase-3 activity in T cells from hepatocellular carcinoma-bearing patients and hepatitis C virus-infected patients.* J Gastroenterol Hepatol, 2004. 19(12): p. 1348-56.
12. Rozell, M.D., R.A. Erger, and T.B. Casale, *Isolation technique alters eosinophil migration response to IL-8.* J Immunol Methods, 1996. 197(1-2): p. 97-107.
13. Tchou, I., et al., *Technique for obtaining highly enriched, quiescent immature Langerhans cells suitable for ex vivo assays.* Immunol Lett, 2003. 86(1): p. 7-14.
14. Suni, M.A., V.C. Maino, and H.T. Maecker, *Ex vivo analysis of T-cell function.* Curr Opin Immunol, 2005. 17(4): p. 434-40.
15. Fleisher, T.A., et al., *Detection of intracellular phosphorylated STAT-1 by flow cytometry.* Clin Immunol, 1999. 90(3): p. 425-30.
16. Anderson, K., et al., *Protein expression changes in spinal muscular atrophy revealed with a novel antibody array technology.* Brain, 2003. 126(Pt 9): p. 2052-64.
17. Desplat, V., et al., *Rapid detection of phosphotyrosine proteins by flow cytometric analysis in Bcr-Abl-positive cells.* Cytometry A, 2004. 62(1): p. 35-45.
18. Krutzik, P.O., et al., *Analysis of protein phosphorylation and cellular signaling events by flow cytometry: techniques and clinical applications.* Clin Immunol, 2004. 110(3): p. 206-21.
19. Uzel, G., et al., *Detection of intracellular phosphorylated STAT-4 by flow cytometry.* Clin Immunol, 2001. 100(3): p. 270-6.
20. Chow, S., H. Patel, and D.W. Hedley, *Measurement of MAP kinase activation by flow cytometry using phospho-specific antibodies to MEK and ERK: potential for pharmacodynamic monitoring of signal transduction inhibitors.* Cytometry, 2001. 46(2): p. 72-8.
21. Bromberg, J. and J.E. Darnell, Jr., *The role of STATs in transcriptional control and their impact on cellular function.* Oncogene, 2000. 19(21): p. 2468-73.
22. Aaronson, D.S. and C.M. Horvath, *A road map for those who don't know JAK-STAT.* Science, 2002. 296(5573): p. 1653-5.
23. Chang, L. and M. Karin, *Mammalian MAP kinase signalling cascades.* Nature, 2001. 410(6824): p. 37-40.
24. Dong, C., R.J. Davis, and R.A. Flavell, *MAP kinases in the immune response.* Annu Rev Immunol, 2002. 20: p. 55-72.

25. Ivashkiv, L.B. and X. Hu, *Signaling by STATs*. *Arthritis Res Ther*, 2004. 6(4): p. 159-68.
26. Levy, D.E. and J.E. Darnell, Jr., *Stats: transcriptional control and biological impact*. *Nat Rev Mol Cell Biol*, 2002. 3(9): p. 651-62.
27. Mirmohammadsadegh, A., et al., *STAT5 Phosphorylation in Malignant Melanoma Is Important for Survival and Is Mediated Through SRC and JAK1 Kinases*. *J Invest Dermatol*, 2006.
28. Hanada, T., et al., *IFN{gamma}-dependent, spontaneous development of colorectal carcinomas in SOCS1-deficient mice*. *J Exp Med*, 2006.
29. Benekli, M., et al., *Signal transducer and activator of transcription proteins in leukemias*. *Blood*, 2003. 101(8): p. 2940-54.
30. Coffey, P.J., L. Koenderman, and R.P. de Groot, *The role of STATs in myeloid differentiation and leukemia*. *Oncogene*, 2000. 19(21): p. 2511-22.
31. Kamiguti, A.S., et al., *Regulation of hairy-cell survival through constitutive activation of mitogen-activated protein kinase pathways*. *Oncogene*, 2003. 22(15): p. 2272-84.
32. Kim, S.C., et al., *Constitutive activation of extracellular signal-regulated kinase in human acute leukemias: combined role of activation of MEK, hyperexpression of extracellular signal-regulated kinase, and downregulation of a phosphatase, PAC1*. *Blood*, 1999. 93(11): p. 3893-9.
33. Mora, L.B., et al., *Constitutive activation of Stat3 in human prostate tumors and cell lines: direct inhibition of Stat3 signaling induces apoptosis of prostate cancer cells*. *Cancer Res*, 2002. 62(22): p. 6659-66.
34. Oka, H., et al., *Constitutive activation of mitogen-activated protein (MAP) kinases in human renal cell carcinoma*. *Cancer Res*, 1995. 55(18): p. 4182-7.
35. Skinnider, B.F., et al., *Signal transducer and activator of transcription 6 is frequently activated in Hodgkin and Reed-Sternberg cells of Hodgkin lymphoma*. *Blood*, 2002. 99(2): p. 618-26.
36. Ueda, T., E. Shimada, and T. Urakawa, *Serum levels of cytokines in patients with colorectal cancer: possible involvement of interleukin-6 and interleukin-8 in hematogenous metastasis*. *J Gastroenterol*, 1994. 29(4): p. 423-9.
37. Smith, P.C., et al., *Interleukin-6 and prostate cancer progression*. *Cytokine Growth Factor Rev*, 2001. 12(1): p. 33-40.



38. Scheibenbogen, C., et al., *Serum interleukin-8 (IL-8) is elevated in patients with metastatic melanoma and correlates with tumour load*. *Melanoma Res*, 1995. 5(3): p. 179-81.
39. Sakamoto, K., et al., *Interleukin-8 is constitutively and commonly produced by various human carcinoma cell lines*. *Int J Clin Lab Res*, 1992. 22(4): p. 216-9.
40. Chopra, V., T.V. Dinh, and E.V. Hannigan, *Serum levels of interleukins, growth factors and angiogenin in patients with endometrial cancer*. *J Cancer Res Clin Oncol*, 1997. 123(3): p. 167-72.
41. Chopra, V., T.V. Dinh, and E.V. Hannigan, *Circulating serum levels of cytokines and angiogenic factors in patients with cervical cancer*. *Cancer Invest*, 1998. 16(3): p. 152-9.
42. Blay, J.Y., et al., *Role of interleukin-6 in the paraneoplastic inflammatory syndrome associated with renal-cell carcinoma*. *Int J Cancer*, 1997. 72(3): p. 424-30.
43. Berek, J.S., et al., *Serum interleukin-6 levels correlate with disease status in patients with epithelial ovarian cancer*. *Am J Obstet Gynecol*, 1991. 164(4): p. 1038-42; discussion 1042-3.
44. Cram, L.S., *Flow cytometry, an overview*. *Methods Cell Sci*, 2002. 24(1-3): p. 1-9.
45. Rieseberg, M., et al., *Flow cytometry in biotechnology*. *Appl Microbiol Biotechnol*, 2001. 56(3-4): p. 350-60.
46. Perfetto, S.P., P.K. Chattopadhyay, and M. Roederer, *Seventeen-colour flow cytometry: unravelling the immune system*. *Nat Rev Immunol*, 2004. 4(8): p. 648-55.
47. Baumgarth, N. and M. Roederer, *A practical approach to multicolor flow cytometry for immunophenotyping*. *J Immunol Methods*, 2000. 243(1-2): p. 77-97.
48. Donnenberg, V.S. and A.D. Donnenberg, *Identification, rare-event detection and analysis of dendritic cell subsets in broncho-alveolar lavage fluid and peripheral blood by flow cytometry*. *Front Biosci*, 2003. 8: p. s1175-80.
49. Perez, O.D. and G.P. Nolan, *Simultaneous measurement of multiple active kinase states using polychromatic flow cytometry*. *Nat Biotechnol*, 2002. 20(2): p. 155-62.
50. Hasbold, J., et al., *Quantitative analysis of lymphocyte differentiation and proliferation in vitro using carboxyfluorescein diacetate succinimidyl ester*. *Immunol Cell Biol*, 1999. 77(6): p. 516-22.

51. Hoppner, M., et al., *A flow-cytometry based cytotoxicity assay using stained effector cells in combination with native target cells*. J Immunol Methods, 2002. 267(2): p. 157-63.
52. Lehmann, A.K., S. Sornes, and A. Halstensen, *Phagocytosis: measurement by flow cytometry*. J Immunol Methods, 2000. 243(1-2): p. 229-42.
53. Maino, V.C. and L.J. Picker, *Identification of functional subsets by flow cytometry: intracellular detection of cytokine expression*. Cytometry, 1998. 34(5): p. 207-15.
54. Herzenberg, L.A., et al., *The history and future of the fluorescence activated cell sorter and flow cytometry: a view from Stanford*. Clin Chem, 2002. 48(10): p. 1819-27.
55. Steinkamp, J., *Flow Cytometry*. Rev. Sci. Instrum., 1984. 55(9): p. 1375-1400.
56. Shoemaker, D.D. and P.S. Linsley, *Recent developments in DNA microarrays*. Curr Opin Microbiol, 2002. 5(3): p. 334-7.
57. Anderson, L. and J. Seilhamer, *A comparison of selected mRNA and protein abundances in human liver*. Electrophoresis, 1997. 18(3-4): p. 533-7.
58. Cohen, P., *The origins of protein phosphorylation*. Nat Cell Biol, 2002. 4(5): p. E127-30.
59. Mandell, J.W., *Phosphorylation state-specific antibodies: applications in investigative and diagnostic pathology*. Am J Pathol, 2003. 163(5): p. 1687-98.
60. Towbin, H., T. Staehelin, and J. Gordon, *Electrophoretic transfer of proteins from polyacrylamide gels to nitrocellulose sheets: procedure and some applications*. Proc Natl Acad Sci U S A, 1979. 76(9): p. 4350-4.
61. Lodish, H.B., Arnold; Zipursky, S. Lawrence; Matsudaira, Paul; Baltimore, David; Darnell, James E., *Molecular Cell Biology*. 4 ed. 1999, New York: W.H. Freeman & Co.
62. Westermeier, R. and R. Marouga, *Protein detection methods in proteomics research*. Biosci Rep, 2005. 25(1-2): p. 19-32.
63. Espina, V., et al., *Protein microarray detection strategies: focus on direct detection technologies*. J Immunol Methods, 2004. 290(1-2): p. 121-33.
64. Hudelist, G., et al., *Use of high-throughput protein array for profiling of differentially expressed proteins in normal and malignant breast tissue*. Breast Cancer Res Treat, 2004. 86(3): p. 281-91.

65. Grubb, R.L., et al., *Signal pathway profiling of prostate cancer using reverse phase protein arrays*. *Proteomics*, 2003. 3(11): p. 2142-6.
66. Sedlmayr, P., et al., *Species-Specific Blocking of Fc Receptors in Indirect Immunofluorescence Assays*. *Laboratory Hematology*, 2001. 7: p. 81-84.
67. Openshaw, P., et al., *Heterogeneity of intracellular cytokine synthesis at the single-cell level in polarized T helper 1 and T helper 2 populations*. *J Exp Med*, 1995. 182(5): p. 1357-67.
68. Ilangumaran, S., D. Finan, and R. Rottapel, *Flow cytometric analysis of cytokine receptor signal transduction*. *J Immunol Methods*, 2003. 278(1-2): p. 221-34.
69. Krutzik, P.O. and G.P. Nolan, *Intracellular phospho-protein staining techniques for flow cytometry: monitoring single cell signaling events*. *Cytometry A*, 2003. 55(2): p. 61-70.
70. Ecker, R.C. and A. Tarnok, *Cytomics goes 3D: toward tissomics*. *Cytometry A*, 2005. 65(1): p. 1-3.
71. Ghosh, R.N., L. Grove, and O. Lapets, *A quantitative cell-based high-content screening assay for the epidermal growth factor receptor-specific activation of mitogen-activated protein kinase*. *Assay Drug Dev Technol*, 2004. 2(5): p. 473-81.
72. Bertelsen, M. and A. Sanfridson, *Inflammatory pathway analysis using a high content screening platform*. *Assay Drug Dev Technol*, 2005. 3(3): p. 261-71.
73. Shapiro, H.M., *"Cellular astronomy"--a foreseeable future in cytometry*. *Cytometry A*, 2004. 60(2): p. 115-24.
74. Vakkila, J., R.A. DeMarco, and M.T. Lotze, *Imaging analysis of STAT1 and NF-kappaB translocation in dendritic cells at the single cell level*. *J Immunol Methods*, 2004. 294(1-2): p. 123-34.
75. Pozarowski, P., E. Holden, and Z. Darzynkiewicz, *Laser scanning cytometry: principles and applications*. *Methods Mol Biol*, 2006. 319: p. 165-92.
76. Shuai, K. and B. Liu, *Regulation of JAK-STAT signalling in the immune system*. *Nat Rev Immunol*, 2003. 3(11): p. 900-11.
77. Rawlings, J.S., K.M. Rosler, and D.A. Harrison, *The JAK/STAT signaling pathway*. *J Cell Sci*, 2004. 117(Pt 8): p. 1281-3.
78. Shah, M., et al., *Membrane-associated STAT3 and PY-STAT3 in the cytoplasm*. *J Biol Chem*, 2006. 281(11): p. 7302-8.

79. Zhong, M., et al., *Implications of an antiparallel dimeric structure of nonphosphorylated STAT1 for the activation-inactivation cycle*. Proc Natl Acad Sci U S A, 2005. 102(11): p. 3966-71.
80. Yuan, Z.L., et al., *Stat3 dimerization regulated by reversible acetylation of a single lysine residue*. Science, 2005. 307(5707): p. 269-73.
81. Wormald, S. and D.J. Hilton, *Inhibitors of cytokine signal transduction*. J Biol Chem, 2004. 279(2): p. 821-4.
82. Chen, Z., et al., *Selective regulatory function of Socs3 in the formation of IL-17-secreting T cells*. Proc Natl Acad Sci U S A, 2006. 103(21): p. 8137-8142.
83. Schindler, C.W., *Series introduction. JAK-STAT signaling in human disease*. J Clin Invest, 2002. 109(9): p. 1133-7.
84. Roux, P.P. and J. Blenis, *ERK and p38 MAPK-activated protein kinases: a family of protein kinases with diverse biological functions*. Microbiol Mol Biol Rev, 2004. 68(2): p. 320-44.
85. Johnson, G.L. and R. Lapadat, *Mitogen-activated protein kinase pathways mediated by ERK, JNK, and p38 protein kinases*. Science, 2002. 298(5600): p. 1911-2.
86. Martin-Blanco, E., *p38 MAPK signalling cascades: ancient roles and new functions*. Bioessays, 2000. 22(7): p. 637-45.
87. Ono, K. and J. Han, *The p38 signal transduction pathway: activation and function*. Cell Signal, 2000. 12(1): p. 1-13.
88. Rincon, M., R.A. Flavell, and R.A. Davis, *The JNK and P38 MAP kinase signaling pathways in T cell-mediated immune responses*. Free Radic Biol Med, 2000. 28(9): p. 1328-37.
89. Tibbles, L.A. and J.R. Woodgett, *The stress-activated protein kinase pathways*. Cell Mol Life Sci, 1999. 55(10): p. 1230-54.
90. Torii, S., et al., *Regulatory mechanisms and function of ERK MAP kinases*. J Biochem (Tokyo), 2004. 136(5): p. 557-61.
91. Tamura, S., et al., *Regulation of stress-activated protein kinase signaling pathways by protein phosphatases*. Eur J Biochem, 2002. 269(4): p. 1060-6.
92. Camps, M., A. Nichols, and S. Arkininstall, *Dual specificity phosphatases: a gene family for control of MAP kinase function*. Faseb J, 2000. 14(1): p. 6-16.

93. Plataniias, L.C., *The p38 mitogen-activated protein kinase pathway and its role in interferon signaling*. *Pharmacol Ther*, 2003. 98(2): p. 129-42.
94. Lin, T.S., S. Mahajan, and D.A. Frank, *STAT signaling in the pathogenesis and treatment of leukemias*. *Oncogene*, 2000. 19(21): p. 2496-504.
95. Sternberg, D.W. and D.G. Gilliland, *The role of signal transducer and activator of transcription factors in leukemogenesis*. *J Clin Oncol*, 2004. 22(2): p. 361-71.
96. Steelman, L.S., et al., *JAK/STAT, Raf/MEK/ERK, PI3K/Akt and BCR-ABL in cell cycle progression and leukemogenesis*. *Leukemia*, 2004. 18(2): p. 189-218.
97. Plataniias, L.C., *Map kinase signaling pathways and hematologic malignancies*. *Blood*, 2003. 101(12): p. 4667-79.
98. Ogasawara, T., M. Yasuyama, and K. Kawauchi, *Constitutive activation of extracellular signal-regulated kinase and p38 mitogen-activated protein kinase in B-cell lymphoproliferative disorders*. *Int J Hematol*, 2003. 77(4): p. 364-70.
99. Ben-Baruch, A., *Host microenvironment in breast cancer development: inflammatory cells, cytokines and chemokines in breast cancer progression: reciprocal tumor-microenvironment interactions*. *Breast Cancer Res*, 2003. 5(1): p. 31-6.
100. Boudreau, N. and C. Myers, *Breast cancer-induced angiogenesis: multiple mechanisms and the role of the microenvironment*. *Breast Cancer Res*, 2003. 5(3): p. 140-6.
101. Chen, Z., et al., *Expression of proinflammatory and proangiogenic cytokines in patients with head and neck cancer*. *Clin Cancer Res*, 1999. 5(6): p. 1369-79.
102. Oka, M., et al., *Relationship between serum levels of soluble interleukin-2 receptor and various disease parameters in patients with squamous cell carcinoma of the esophagus*. *Hepatogastroenterology*, 1999. 46(28): p. 2254-9.
103. Aldinucci, D., et al., *Interactions between tissue fibroblasts in lymph nodes and Hodgkin/Reed-Sternberg cells*. *Leuk Lymphoma*, 2004. 45(9): p. 1731-9.
104. Zeh, H.J., 3rd and M.T. Lotze, *Addicted to death: invasive cancer and the immune response to unscheduled cell death*. *J Immunother*, 2005. 28(1): p. 1-9.
105. Baniyash, M., *TCR zeta-chain downregulation: curtailing an excessive inflammatory immune response*. *Nat Rev Immunol*, 2004. 4(9): p. 675-87.
106. Kuss, I., et al., *Clinical significance of decreased zeta chain expression in peripheral blood lymphocytes of patients with head and neck cancer*. *Clin Cancer Res*, 1999. 5(2): p. 329-34.

107. Reichert, T.E., et al., *Signaling abnormalities, apoptosis, and reduced proliferation of circulating and tumor-infiltrating lymphocytes in patients with oral carcinoma*. Clin Cancer Res, 2002. 8(10): p. 3137-45.
108. Rabinowich, H., et al., *Expression and activity of signaling molecules in T lymphocytes obtained from patients with metastatic melanoma before and after interleukin 2 therapy*. Clin Cancer Res, 1996. 2(8): p. 1263-74.
109. Takahashi, A., et al., *Elevated caspase-3 activity in peripheral blood T cells coexists with increased degree of T-cell apoptosis and down-regulation of TCR zeta molecules in patients with gastric cancer*. Clin Cancer Res, 2001. 7(1): p. 74-80.
110. Kurt, R.A., et al., *Peripheral T lymphocytes from women with breast cancer exhibit abnormal protein expression of several signaling molecules*. Int J Cancer, 1998. 78(1): p. 16-20.
111. Healy, C.G., et al., *Impaired expression and function of signal-transducing zeta chains in peripheral T cells and natural killer cells in patients with prostate cancer*. Cytometry, 1998. 32(2): p. 109-19.
112. Schmielau, J. and O.J. Finn, *Activated granulocytes and granulocyte-derived hydrogen peroxide are the underlying mechanism of suppression of t-cell function in advanced cancer patients*. Cancer Res, 2001. 61(12): p. 4756-60.
113. Marie-Cardine, A. and B. Schraven, *Coupling the TCR to downstream signalling pathways: the role of cytoplasmic and transmembrane adaptor proteins*. Cell Signal, 1999. 11(10): p. 705-12.
114. Bukowski, R.M., et al., *Signal transduction abnormalities in T lymphocytes from patients with advanced renal carcinoma: clinical relevance and effects of cytokine therapy*. Clin Cancer Res, 1998. 4(10): p. 2337-47.
115. Pericle, F., et al., *Immunocompromised tumor-bearing mice show a selective loss of STAT5a/b expression in T and B lymphocytes*. J Immunol, 1997. 159(6): p. 2580-5.
116. Lesinski, G.B., et al., *Multiparametric flow cytometric analysis of inter-patient variation in STAT1 phosphorylation following interferon Alfa immunotherapy*. J Natl Cancer Inst, 2004. 96(17): p. 1331-42.
117. Lotze, M.T., et al., *Workshop on cancer biometrics: identifying biomarkers and surrogates of cancer in patients: a meeting held at the Masur Auditorium, National Institutes of Health*. J Immunother, 2005. 28(2): p. 79-119.

118. Lotze, M.T. and R.C. Rees, *Identifying biomarkers and surrogates of tumors (cancer biometrics): correlation with immunotherapies and immune cells*. *Cancer Immunol Immunother*, 2004. 53(3): p. 256-61.
119. Donnenberg, V.S., et al., *Rare-event analysis of circulating human dendritic cell subsets and their presumptive mouse counterparts*. *Transplantation*, 2001. 72(12): p. 1946-51.
120. Campana, D., et al., *Detection of minimal residual disease in acute lymphoblastic leukemia: the St Jude experience*. *Leukemia*, 2001. 15(2): p. 278-9.
121. Smithgall, T.E., et al., *Control of myeloid differentiation and survival by Stats*. *Oncogene*, 2000. 19(21): p. 2612-8.
122. Gouilleux-Gruart, V., et al., *STAT-related transcription factors are constitutively activated in peripheral blood cells from acute leukemia patients*. *Blood*, 1996. 87(5): p. 1692-7.
123. Watson, C.J. and W.R. Miller, *Elevated levels of members of the STAT family of transcription factors in breast carcinoma nuclear extracts*. *Br J Cancer*, 1995. 71(4): p. 840-4.
124. Sivaraman, V.S., et al., *Hyperexpression of mitogen-activated protein kinase in human breast cancer*. *J Clin Invest*, 1997. 99(7): p. 1478-83.
125. Towatari, M., et al., *Constitutive activation of mitogen-activated protein kinase pathway in acute leukemia cells*. *Leukemia*, 1997. 11(4): p. 479-84.
126. Maeda, S., et al., *Nod2 mutation in Crohn's disease potentiates NF-kappaB activity and IL-1beta processing*. *Science*, 2005. 307(5710): p. 734-8.
127. Rice, L., et al., *CpG oligodeoxynucleotide protection in polymicrobial sepsis is dependent on interleukin-17*. *J Infect Dis*, 2005. 191(8): p. 1368-76.
128. Tsung, A., et al., *The nuclear factor HMGB1 mediates hepatic injury after murine liver ischemia-reperfusion*. *J Exp Med*, 2005. 201(7): p. 1135-43.
129. La Grutta, S., et al., *CD4(+)IL-13(+) cells in peripheral blood well correlates with the severity of atopic dermatitis in children*. *Allergy*, 2005. 60(3): p. 391-5.
130. Krug, N., et al., *Frequencies of T cells expressing interleukin-4 and interleukin-5 in atopic asthmatic children. Comparison with atopic asthmatic adults*. *Am J Respir Crit Care Med*, 1998. 158(3): p. 754-9.

131. Ida, J.A., et al., *A whole blood assay to assess peripheral blood dendritic cell function in response to Toll-like receptor stimulation*. J Immunol Methods, 2006. 310(1-2): p. 86-99.
132. Lotze, M.T. and R.A. DeMarco, *Dealing with death: HMGB1 as a novel target for cancer therapy*. Curr Opin Investig Drugs, 2003. 4(12): p. 1405-9.
133. Hoffmann, T.K., et al., *Spontaneous apoptosis of circulating T lymphocytes in patients with head and neck cancer and its clinical importance*. Clin Cancer Res, 2002. 8(8): p. 2553-62.
134. Whiteside, T.L., *Down-regulation of zeta-chain expression in T cells: a biomarker of prognosis in cancer?* Cancer Immunol Immunother, 2004. 53(10): p. 865-78.
135. Lotze, M.T.a.T., A.W., ed. *Measuring Immunity: Basic Science and Clinical Practice*. 2004, Elsevier Academic Press: London, U.K. 722.
136. Sanderson, K., et al., *Autoimmunity in a phase I trial of a fully human anti-cytotoxic T-lymphocyte antigen-4 monoclonal antibody with multiple melanoma peptides and Montanide ISA 51 for patients with resected stages III and IV melanoma*. J Clin Oncol, 2005. 23(4): p. 741-50.
137. Phan, G.Q., et al., *Cancer regression and autoimmunity induced by cytotoxic T lymphocyte-associated antigen 4 blockade in patients with metastatic melanoma*. Proc Natl Acad Sci U S A, 2003. 100(14): p. 8372-7.
138. Hodi, F.S., et al., *Biologic activity of cytotoxic T lymphocyte-associated antigen 4 antibody blockade in previously vaccinated metastatic melanoma and ovarian carcinoma patients*. Proc Natl Acad Sci U S A, 2003. 100(8): p. 4712-7.
139. Mascher, B., P. Schlenke, and M. Seyfarth, *Expression and kinetics of cytokines determined by intracellular staining using flow cytometry*. J Immunol Methods, 1999. 223(1): p. 115-21.
140. Mudter, J., et al., *Activation pattern of signal transducers and activators of transcription (STAT) factors in inflammatory bowel diseases*. Am J Gastroenterol, 2005. 100(1): p. 64-72.
141. Halary, F., et al., *Shared reactivity of V $\delta$ 2(neg)  $\gamma\delta$  T cells against cytomegalovirus-infected cells and tumor intestinal epithelial cells*. J Exp Med, 2005. 201(10): p. 1567-78.
142. Montag, D.T. and M.T. Lotze, *Successful simultaneous measurement of cell membrane and cytokine induced phosphorylation pathways [CIPP] in human peripheral blood mononuclear cells*. J Immunol Methods, 2006.



143. Walker, J.G., et al., *Changes in synovial tissue Jak-STAT expression in rheumatoid arthritis in response to successful DMARD therapy*. *Ann Rheum Dis*, 2006.
144. Sawa, S.I., et al., *Autoimmune arthritis associated with mutated interleukin (IL)-6 receptor gp130 is driven by STAT3/IL-7-dependent homeostatic proliferation of CD4+ T cells*. *J Exp Med*, 2006.
145. Plevy, S., *A STAT need for human immunologic studies to understand inflammatory bowel disease*. *Am J Gastroenterol*, 2005. 100(1): p. 73-4.
146. Musso, A., et al., *Signal transducers and activators of transcription 3 signaling pathway: an essential mediator of inflammatory bowel disease and other forms of intestinal inflammation*. *Inflamm Bowel Dis*, 2005. 11(2): p. 91-8.
147. Li, Z., et al., *Expression of interleukin-12 and its signaling molecules in peripheral blood mononuclear cells in systemic lupus erythematosus patients*. *Chin Med J (Engl)*, 2002. 115(6): p. 846-50.